Dynamic mapping of the immunological synapse in T cell homeostasis and activation

Dissertation zur Erlangung des

naturwissenschaftlichen Doktorgrades

der Julius-Maximilians-Universität Würzburg

vorgelegt von

Julian Storim

aus

Datteln

Würzburg, 2011

Eingereicht am: .....

Mitglieder der Promotionskommission:

Vorsitzender: .....

Gutachter: Prof. Dr. Dr. Peter Friedl

Gutachter: Prof. Dr. Ricardo Benavente

Tag des Promotionskolloquiums: .....

Doktorurkunde ausgehändigt am: .....

Table of contents

1 Abbreviations

AP-1	Activator protein-1
APC	Antigen-presenting cell
Arp2/3	Actin-related protein 2/3
BMDC	Bone-marrow derived dendritic cell
CAMs	Cell adhesion molecules
CD	Cluster of differentiation
Cdc42	Cell-division cycle 42
CFSE	Carboxyfluorescein-diacetate-succinimidyl-ester
CMTMR	Chloromethyl-benzoyl-amino-tetramethylrhodamine
CTx b	B subunit of cholera toxin
DAG	Diacylglycerol
DC	Dendritic cell
ECM	Extracellular matrix
EGFP	Enhanced green fluorescent protein
ER	Endoplasmatic reticulum
ERM	Ezrin, radixin and moesin proteins

F-actin	Filamentous actin
FITC	Fluorescein isothiocyanate
GEF	Guanine-nucleotide exchange factor
GFP	Green fluorescent protein
GM-CSF	Granulocyte-macrophage colony stimulation factor
ICAM-1	Intercellular adhesion molecule-1
IL	Interleukin
IL-7R	IL-7-receptor
IP_3	Inositol trisphosphate
IS	Immunological synapse
ITAM	Immunoreceptor tyrosine-based activation motifs
ITK	IL-2-inducible T cell kinase
Jak	Janus kinase
LAT	Linker for activation of T cells
LFA-1	Leukocyte function-associated antigen-1
LPS	Lipopolysaccharides
mAb	Monoclonal antibody

MHC	Major histocompatibility complex
MMLV	Moloney Murine Leukemia Virus
MTOC	Microtubule organization center
NFAT	Nuclear factor of activated T cells
NF-κB	Nuclear factor κ B
PBS	Phosphate buffered saline
PH	Pleckstrin homology
PIP3	Phosphatidylinositol(3,4,5)trisphosphate
PKCΘ	Proteins kinase C Θ
PLCγ1	Phospholipase C γ 1
$pMCC_{88-103}$	Peptide from moth cytochrome c, residues 88-103
PTEN	Phosphatase and tensin homologue deleted on chromosome ten
PTK	Protein tyrosine kinase
$pOVA_{323-339}$	Peptide from ovalbumine, residues 323-339
pY	Phosphotyrosine (phosphorylated tyrosine residues)
SD	Standard deviation

SH	Src homology
SLP-76	SH2 domain-containing leukocyte phosphoprotein of 76 kDa
TCR	T cell receptor
TGF-β	Transforming growth factor β
TLR	Toll-like receptor
WASP	Wiskott-Aldrich syndrome protein
WAVE	WASP family verprolin-homologous protein 2
ZAP-70	ζ-associated protein of 70 kDa

2 Introduction

2.1 $CD4^+$ T lymphocytes – migrating conductors of the immune system

The mammalian immune system consists of the innate and the adaptive immune system, both of which contain an array of non-resident leukocytes that respond to pathogens, including bacteria and viruses, cell and tissue damage, and tumors. Cells of the innate immune system (e.g. neutrophilic granulocytes and macrophages) recognize unspecific danger signals that are present in a wide range of diseases, e.g. lipopolysaccharides (LPS) of the bacterial cell wall during a bacterial infection or the loss of major histocompatibility complexes (MHC) on the surface of neoplastic and/or virally infected cells. These cells are ready to function when they exit the bone marrow and therefore act quickly after the onset of a threat.

The adaptive immune system is composed of B and T lymphocytes. The outstanding feature of these cells is their ability to specifically recognize one specific target molecule, a so-called antigen. For this aim, every single B cell expresses a unique surface immunoglobulin that develops during a process called somatic recombination where the genes encoding this receptor are reorganized and mutated yielding a highly variable region in every immunoglobulin, the antigen binding site (Jung and Alt, 2004). This gene rearrangement happens randomly, producing a huge array of different B cells. As every B cell recognizes a different antigen, only an extremely small percentage out of the entire B cell pool recognizes one pathogen, e.g. a bacterium, and is able to produce specific antibodies (soluble forms of the immunoglobulin receptor) that may neutralize the pathogen. On the other hand, there are B cells with specificity against virtually every conceivable antigen. Thus, even entirely new

pathogens that do not display common pathogenic patterns like LPS are likely to face a B cell that is able to produce antibodies against it.

The equivalent to the immunoglobulin receptor in B cells is the T cell receptor (TCR) in T cells which also develops through somatic gene rearrangement during the maturation of T cell precursors in the thymus. Unlike immunoglobulins, TCR recognize their specific antigen (usually polypeptides) only when it is presented by another cell-surface receptor on a so-called antigen-presenting cell (APC), the major histocompatibility complex (MHC) (Davis and Bjorkman, 1988). There are two main subsets of T lymphocytes that can be distinguished by their expression of the TCR co-receptors CD4 and CD8: While CD8 facilitates the recognition of antigen in the context of MHC class I molecules in cytotoxic T lymphocytes, CD4 co-engages MHC class II molecules together with the TCR in so called helper T cells (Rudolph et al., 2006). The main function of $CD8^+$ cytotoxic T cells is the killing of (virally) infected or neoplastic cells by inducing apoptosis. The effector functions of $CD4^+$ helper T cells on the other hand are diverse: via direct cell-cell contacts and/or the production of cytokines they control the immune response to a pathogen. Helper T cells are required for the maturation of B cells to antibody-producing plasma cells (MacLennan, 1994), they prime dendritic cells (DC) to more effectively stimulate cytotoxic T cells(Zhang et al., 2009), and they may shift the entire immune response toward a so-called Th-1 response (a mainly "humoral" immune response dominated by the production of (IgE)-antibodies) or a Th-2 response (a mainly cellular immune response dominated by cytotoxic T cells)(Glimcher and Murphy, 2000). Therefore, $CD4^+$ helper T cells may be regarded as the conductor of an immune response.

As (B and T) lymphocytes only recognize one specific antigen (their cognate antigen) and finding this antigen is a rare event, every antigen-inexperienced (or naïve) lymphocyte is inactive. After antigen recognition, lymphocytes get activated, proliferate, and either become effector cells that carry out the immune response or develop into memory cells that build up immunity against known pathogens. To this aim, naïve T cells need to get in direct contact with professional APC that not only present their cognate antigenic peptide in an MHC-dependent manner (signal 1) but also provide additional co-stimulatory signals (like CD80/CD86 or cell-adhesion molecules (CAMs like ICAM-1); signal 2). The most potent APC is a mature dendritic cell (DC; Banchereau and Steinman, 1998). TCR and co-receptor triggering initiate a signaling cascade that involves the phosphorylation of signaling and adaptor proteins, the activation of GTPases, Ca^{++}-influx, and eventually leads to the clonal expansion of the stimulated T cell and the transcription of an array of genes that control effector and/or memory functions (Smith-Garvin et al., 2009).

In order to find their cognate antigen, T cells constantly patrol the body and scan DC. While the bloodstream enables fast and passive transport through the organism, within secondary lymphoid organs or at sites of inflammation T cells leave the blood vessels and start to actively migrate in order to get in contact with DC (Friedl and Weigelin, 2008). Thus, the ability to migrate is one of the fundamental functions of a T cell. However, the scanning of DC does not only facilitate the search for the cognate antigen; contacts with low-affinity, non-cognate (self-) antigens presented by MHC molecules on the DC surface also deliver signals that help to control the size and function of the peripheral T cell pool (T cell homeostasis; Surh and Sprent, 2008).

The following work describes homeostatic and activating $CD4^+$ T cell/DC interactions under an *in vivo*-like situation, i.e., cells have to migrate in a 3D environment to make contact with each other. The mechanisms of T cell migration, activation and homeostasis as well as the characteristics of DC will be briefly described in the next paragraphs of this introduction.

2.2 T cell migration and polarity

In contrast to fibroblasts or tumor cells that migrate at a rather low speed (less than 1 μm/min) and digest and remodel their environment (e. g. collagen fibers), T cells migrate at high speed (up to 30 μm/min) and in general do not cleave interstitial fibers while migrating (Friedl and Weigelin, 2008). Therefore, T cells have to constantly change their cell shapes while they squeeze through preexisting holes in fibrillar networks or migrate within cell-rich environments like the lymph node. This mode of migration, which is largely driven by the actin cytoskeleton and does not depend on adhesion receptors like integrins in a 3D environment, is called “amoeboid migration” as it is reminiscent of the amoeba *Dictyostelium discoideum* (Friedl et al., 1998; Friedl et al., 1995; Lämmermann et al., 2008; Lämmermann and Sixt, 2009).

For migration, T cells have to polarize by forming a leading edge and a trailing edge called “uropod” (Fig. 1). These compartments and the actual cell body (containing the nucleus) differ in actin dynamics, cell surface receptors and cellular functions.

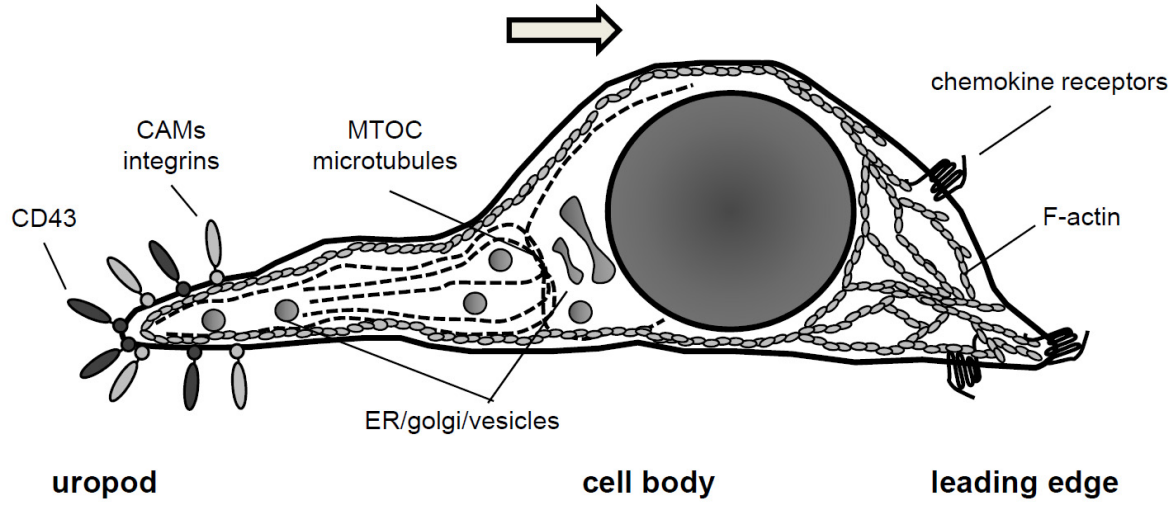

Figure 1: Morphology, cytoskeletal and molecular asymmetry of a migrating T cell.

2.2.1 The leading edge

In T lymphocytes the leading edge is a highly dynamic compartment with rapid actin turnover. The "front" signal is largely delivered by a local accumulation of the second messenger phosphatidylinositol(3,4,5)trisphosphate (PIP_3) which is produced as a the result of the ligation of chemokines to G-protein coupled receptors that in turn activate a class Ib phosphatidylinositol-3-kinase (Charest and Firtel, 2007). PIP_3 then recruits guanine-nucleotide exchange factors (GEFs) that activate Rac and Cdc42, two of the Rho-family of small GTPases, via their pleckstrin homology (PH) domains (Affolter and Weijer, 2005). In their GTP-bound state, Rac and Cdc42 activate members of the Wiskott-Aldrich syndrome protein (WASP) family, namely WASP itself and WAVE2 (WASP family verprolin-homologous protein 2), that regulate actin polymerization by controlling the actin-related protein 2/3 (Arp2/3) complex (Bompard and Caron, 2004; Insall and Machesky, 2009). Finally, the polymerization and accumulation of filamentous actin (F-actin) in the leading

edge results in the formation of sheet-like (lammelipods) and rod-like (filopods) membrane protrusions that drive forward locomotion.

Besides its contribution to locomotion, the leading edge constantly probes adjacent cells and the extracellular matrix for signals. This includes the sensing of chemokines and promigratory cytokines which induce and direct T cell migration (Friedl and Weigelin, 2008; Sanchez-Madrid and del Pozo, 1999). Furthermore, compared with rear parts of the cell, the leading edge of T cells is more sensitive for TCR-triggering which is relevant for detecting antigenic signals during migration through lymphoid and peripheral tissues (Negulescu et al., 1996). Thus, during migration, environmental signaling is particularly confined to the leading edge.

2.2.2 Cell body and uropod

The cell body harbors the nucleus and forms the central compartment of a polarized T cell. Here, activity of the phosphatase PTEN (phosphatase and tensin homologue deleted on chromosome ten) which is excluded from the leading edge counteracts the formation of PIP_3 and thereby inhibits the formation of lateral protrusions (Li et al., 2003). Together with myosin II, subcortical F-actin forms parallel bundles that mediate contraction in the area of the cell body and the trailing uropod which is essential for T cell migration (Jacobelli et al., 2004). The small GTPase RhoA controls both, PTEN activity and myosin II contraction (Li et al., 2005; Xu et al., 2003).

The trailing uropod at the rear end of a migrating T cell forms via the capping of the cytoskeletal linker proteins ezrin, radixin and moesin (ERM proteins) and CD43, a highly glycosylated transmembrane protein (Lee et al., 2004; Serrador et al., 1998). Here, RhoA also mediates actin-myosin contraction and therefore the retraction of the uropod (Heasman et al.,

2010; Jacobelli et al., 2004; Worthylake et al., 2001). Besides being typical morphological criterion for migrating leukocyte, the uropod is an adhesive structure rich in cell adhesion molecules (CAMs like ICAM-1) and integrins (del Pozo et al., 1997; Friedl et al., 1998). These cell surface receptors partly become internalized within the uropod and recycle via endosomal trafficking (Samaniego et al., 2007). Consequently, most of the intracellular membrane compartments including the endoplasmatic reticulum (ER) and the golgi apparatus are also located within the uropod in direct vicinity to the microtubule organization center (MTOC, Krummel and Macara, 2006; Ratner et al., 1997). It is unknown how the uropod contributes to the migration process mechanistically and whether the uropod, like the leading edge, is involved in cell signaling.

2.3 Dendritic cells

The main functions of DC are i) the induction of an immune response (e.g. in case of an infection) and ii) the maintenance of self tolerance (Steinman and Banchereau, 2007). Additionally, DC deliver signals that control the homeostasis and function of the peripheral T cell pool (see 2.5; Surh and Sprent, 2008).

Immature DC are found in virtually all tissues, especially lining the outer and inner body surfaces (e. g. skin and gut). Additionally, a dense DC network is found in lymph nodes taking up antigens that enter the lymph node via the afferent lymphatic vessels (Lindquist et al., 2004). In order to take up antigens, immature DC contain specialized endocytic mechanisms including phagocytosis, macropinocytosis and receptor mediated endocytosis (e.g. via lectins like CD209/DC-SIGN; Figdor et al., 2002). After endocytosis, antigens get degraded and loaded to MHC molecules. Importantly, not only MHC class II molecules are

loaded (a process that takes place solely in endocellular vesicles). In a process termed “cross-presentation” endocytosed antigens also gain access to the cytoplasm and are subsequently distributed to MHC class I molecules (Trombetta and Mellman, 2005).

In steady state, DC are “immature” and take up self-antigens and harmless environmental antigens. Most of the MHC molecules are stored in intracellular vesicles and the surface expression of co-stimulatory molecules like ICAM-1, CD80 and CD86 is low. As co-stimulation therefore is very limited, high affinity TCR binding to a (self-)peptide-MHC complex on the surface of an immature DC leads to T cell anergy and tolerance induction (Hawiger et al., 2001). Thus, under non-inflammatory conditions immature DC are professional endocytic cells that prevent auto-immunity via antigen-specific contacts to T cells.

Under inflammatory conditions, DC not only endocytose pathogenic particles but also sense so called “danger signals” like microbial products (e.g. lipopolysaccharides (LPS) from bacterial cell walls) and immune complexes via Toll-like receptors (TLRs) and Fc-receptors, respectively. This induces a cascade of changes in DC that are collectively termed maturation (Banchereau and Steinman, 1998): DC that locate in peripheral organs start to migrate along a chemotactic gradient towards the draining lymph node. During migration, DC lose their ability for endocytosis, undergo a morphological transformation with the development of numerous membrane extensions (called veils and dendrites), and upregulate MHC-molecules and important co-stimulatory receptors (e.g. CD80 and CD86) on the cell surface. Additionally, DC start to synthesize pro-inflammatory cytokines such as interleukin 12 and type I interferon. Mature DC then position themselves in the T cell zones of the lymph nodes where they are strong inducers of T cell activation.

The high density of (co-)stimulatory molecules on the surface of mature DC is central to their particularly powerful T cell activation capabilities. Additionally, the DC cytoskeleton and rho-GTPases strongly contribute to T cell activation (Al-Alwan et al., 2003) (Kobayashi et al., 2001). Finally, the delivery of MHC-peptide complexes from endosomal stocks to the site of T cell binding, so called “tubulations”, support TCR engagement and signaling (Boes et al., 2002; Jo et al., 2010). However, a necessity for DC polarization in order to coordinate T cell activation has not been shown.

2.4 T cell activation

2.4.1 TCR signal transduction

As mentioned above, recognition of the cognate antigen leads to the activation of T cells, i.e. T cells clonally expand and acquire effector functions. To this aim TCR triggering needs to induce mitosis and an altered gene expression profile by activating transcription factors. As the TCR/CD3 complex itself is catalytically inactive, the first step after the ligation of the cognate peptide-MHC complex is the recruitment of ZAP-70 (ζ-associated protein of 70 kDa;), a protein tyrosine kinase (PTK), to the TCR (Smith-Garvin et al., 2009). To this end numerous tyrosine residues within so-called immunoreceptor tyrosine-based activation motifs (ITAMs) are phosphorylated in the CD3 complex by the PTKs Lck and Fyn which are associated with the CD4/CD8 co-receptor and the TCR itself, respectively (Samelson et al., 1986; Veillette et al., 1988). ZAP-70 docks to phosphorylated tandem ITAM-motifs within the ζ-chain of CD3 via two Src homology 2 (SH2) domains which leads to unfolding and – together with tyrosine phosphorylations at several sites – activation of its kinase activity

(Wang et al., 2010). Activated ZAP-70 then transduces TCR signals to downstream signaling proteins (Fig. 2).

The most important targets of ZAP-70 are two adaptor proteins, the transmembrane protein LAT (linker for activation of T cells; Sommers et al., 2004) and the cytosolic protein SLP-76 (SH2 domain-containing leukocyte phosphoprotein of 76 kDa; Koretzky et al., 2006). LAT and SLP-76 do not have catalytic activities but serve as docking sites for numerous signaling molecules involved in TCR signaling that together form the so called proximal signaling complex (Smith-Garvin et al., 2009). One of the most important proteins within this complex is phospholipase C γ 1 (PLCγ1) that is activated by IL-2-inducible T cell kinase (ITK, a PTK of the Tec family that is also part of the proximal signaling complex) and hydrolyzes the membrane lipid phosphatidylinositol(4,5)bisphosphate into the second messengers diacylglycerol (DAG) and inositoltrisphosphate (IP_3) (Fig. 2; Qi and August, 2007).

DAG binds and activates proteins kinase C θ (PKCθ), a serine/threonine kinase that transduces TCR signaling via two pathways (Fig. 2). First, PKCθ activates NF-κB (nuclear factor κ B) by inducing the degradation of its inhibitor IκB leading to nuclear translocation of NF-κB (Vallabhapurapu and Karin, 2009). Then, PKCθ phosphorylates RasGRP, a GEF that also binds to DAG. Together with the GEF SOS, another component of the proximal signaling complex, RasGRP activates the Ras-Raf-Erk pathway that leads to activation of the activator protein-1 (AP-1) transcription complex (Genot and Cantrell, 2000). IP_3 binds to the IP_3-receptor on the endoplasmatic reticulum (ER) leading to a depletion of the ER Ca^{++}-stores that subsequently leads to the sustained influx of extracellular Ca^{++}. This in turn activates the phosphatase calcineurin that terminally dephosphorylates and activates members of the

nuclear factor of activated T cells (NFAT) family of transcription factors (Fig. 2; Im and Rao, 2004).

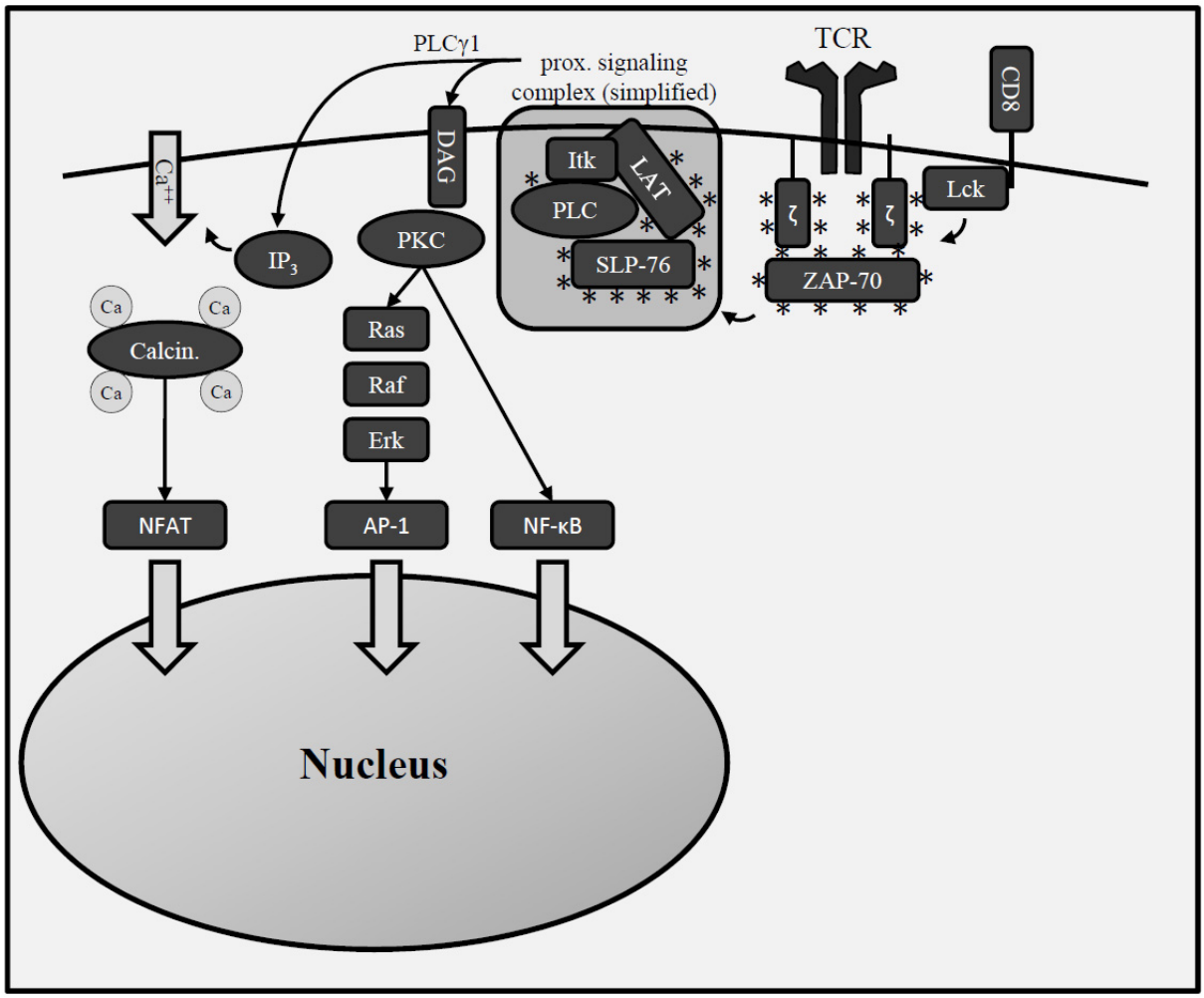

Figure 2: Main signal transduction pathways from the TCR to the nucleus. Details see text. Asterisks: tyrosine phosphorylations.

In short, TCR ligation leads to the activation of several transcription factors (NF-κB, the AP-1 complex and members of the NFAT family) via signaling pathways that involve a myriad of signaling molecules including kinases, phosphatases, small GTPases and Ca^{++}. However, the very early events after TCR ligation are almost exclusively characterized by the

phosphorylation of tyrosine residues (pY; see asterisks in Fig. 2). The detection of pY is therefore an easy-to-use tool for the detection of TCR signaling.

2.4.2 Cell biology of T cell activation

In the 1990s it was shown, that TCR triggering and signaling via the subsequent signal transduction pathways needs to be sustained for hours to initiate clonal expansion and effector functions (Valitutti et al., 1995). In line with this observation, early microscopy studies described T cell activation to be critically dependent on an antigen-dependent migratory arrest on the APC surface followed by a long-lasting and stable T cell / APC interaction (Cernuda-Morollon et al., 2010; Dustin et al., 1997). During these interactions, T cells go through considerable morphological changes (Fig. 3). They develop a roundish morphology and move their MTOC from the uropod toward the APC surface, enabling the directional delivery of cytokines and lytic granules (Kupfer et al., 1994; Stinchcombe et al., 2006). The uropod disassembles and a so called distal pole complex forms at the opposite site of the contact plane, where CD43, a known inhibitor of TCR signaling, accumulates and is therefore excluded from the interaction plane (Allenspach et al., 2001; Tong et al., 2004).

Contact stability is achieved through a mechanism termed “TCR inside-out signaling” that increases the affinity of β2 integrins via signaling pathways involving the small GTPase Ras-proximity-1 (Rap1), the cytoskeletal linker protein talin that stabilizes the high-affinity conformation of LFA-1, the actin cytoskeleton, and several adaptor proteins (e.g. ADAP and SKAP55) that link Rap1 to the proximal signaling complex (Kinashi, 2005). Activated Leukocyte-function-associated antigen 1 (LFA-1), one of the main β2 integrins of T cells,

binds ICAM-1 on the APC surface with high affinity, accumulates within the contact plane (i.e.: LFA-1 avidity increases), and stabilizes the T cell/APC conjugate (Hogg et al., 2003).

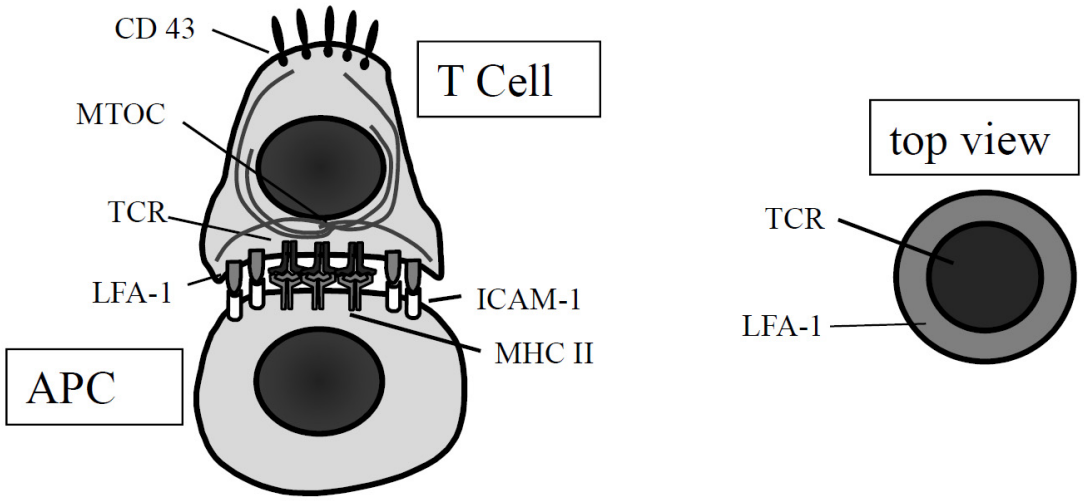

Figure 3: Reorientation of a T cell and synapse formation after recognition of the T cell's cognate antigen on a model APC in liquid culture

Using model APC in liquid cultures revealed that the TCR and LFA-1 do not diffusely accumulate within the contact plane between T cells and APC but segregate into separate areas: a ring of LFA-1 surrounds a central TCR cluster (Freiberg et al., 2002; Grakoui et al., 1999). While the distribution of talin to the outer adhesive ring suggested that LFA-1 binds its ligand ICAM-1 with high affinity, the localization of PKCθ in the central TCR-rich cluster suggested active TCR-signaling in this area (Monks et al., 1998). This large-scale segregated contact structure was thought to be mandatory for TCR signaling and was termed "immunological synapse" (IS; Fig. 3). However, TCR signaling can be detected before a mature IS is established (Lee et al., 2002). And even after the formation of an IS TCR signaling is linked to TCR microclusters that form in the periphery of the contact plane and are transported to the center of the IS in an actin-dependent manner (Campi et al., 2005;

Yokosuka et al., 2005). Newer studies suggest, that the centre of the IS is more involved in signal termination than signal transduction (Varma et al., 2006). Thus, the active signaling units within the T cell/APC contact plane are TCR microclusters in an area rich in (high-affinity) LFA-1 and the function of a highly organized IS remains unclear.

A model of T cell activation that requires large scale receptor segregation was further challenged when DC, the most potent APC (see above), were shown to activate T cells without the formation of highly organized, segregated IS (Brossard et al., 2005; Tseng et al., 2008). Using more complex *in vitro* experimental setups, particularly 3D collagen matrix models, DC were even shown to activate T cells via a sequence of short contacts (Friedl and Brocker, 2002; Gunzer et al., 2000; Gunzer et al., 2004). Using i*n vivo* setups, DC activated T cells via both migratory and adhesive interactions, depending on signal strength, DC maturation state and phase of T cell priming (Azar et al., 2010; Henrickson et al., 2008; Hugues et al., 2004; Mempel et al., 2004; Miller et al., 2004b). Consistent with the IS as a flexible, adaptive sensing device, intermittent episodes of T cell migration were associated with enhanced TCR signaling and IL-2 secretion in a lipid bilayer model (Sims et al., 2007). Thus, T cell activation does not depend upon an antigen-dependent migratory arrest or the formation of a highly organized contact plane. In fact, the spectrum of activating T cell/APC interactions is diverse and depends on the interacting APC and the activation state of the T cell, especially *in vivo (Friedl and Storim, 2004)*. However, in most experimental models of T cell activation adhesive and migratory contact phases alternate sequentially. Therefore, the specific topography of the migratory interaction plain and the exact contribution of migration to TCR signaling remain unclear.

2.5 T cell homeostasis

In contrast to clonal expansion during activation, the size of the peripheral T cell pool under non-inflammatory conditions remains constant due to a tightly controlled balance between T cell survival, death and proliferation (Surh and Sprent, 2008). Compared to the detailed information on the mechanisms of T cell activation, the knowledge about the cell biology and signaling required for T cell homeostasis is incomplete. It is well established that the homeostasis of naïve and memory T lymphocytes is mainly controlled by the availability of cytokines, mainly IL-7 (Guimond et al., 2009; Schluns et al., 2000; von Freeden-Jeffry et al., 1995), and the engagement of APC presenting low-affinity self-peptide-MHC complexes (Ernst et al., 1999; Goldrath and Bevan, 1999; Seddon et al., 2003).

IL-7 belongs to the common γ-chain family of cytokines and is produced by fibroblastic reticular cells and DC within lymph nodes (Link et al., 2007; Sorg et al., 1998). For triggering the IL-7-receptor (IL-7R), a heterodimeric receptor consisting of the common γ-chain and the IL-7-receptor α-chain (CD127), IL-7 needs to be bound to the extracellular matrix or to other cells that secure direct contact to passenger T cells (Guimond et al., 2009). IL-7 ligation then activates the Janus kinases 1 and 3 (Jak1 and Jak3) that are associated with the cytoplasmic tails of IL-7R. This results in the activation of Stat5a/b that subsequently translocates into the nucleus and facilitates the expression of the anti-apoptotic proteins Bcl-2 and Mcl-1 (Khaled and Durum, 2002) resulting in the prolonged survival of T cells. How IL-7 (together with contacts to self-peptide MHC complexes) controls T cell proliferation is less clear. However, proliferation can be substantial under lymphopenic conditions (lymphopenia induced proliferation) and IL-7 at least partly acts by facilitating T cell contacts to APC and TCR

signaling under homeostatic conditions (Park et al., 2007; Saini et al., 2009) supporting a role for "homeostatic" contacts, besides signaling through IL-7.

Low-affinity TCR signaling during homeostasis uses signal transduction pathways similar to those of T cell activation. E.g., in mice lacking the adaptor molecules Nck or Vav1, both of which are involved into TCR signaling for T cell activation, the size of the peripheral T cell pool is diminished (Fujikawa et al., 2003; Roy et al., 2010). Additionally, Lck phosphorylation, Ca^{++}-Influx and the phosphorylation of ζ-chain after low-affinity TCR ligation were demonstrated (Feuillet et al., 2005; Meraner et al., 2007; Revy et al., 2001). Thus, weak TCR triggering is required for mediating homeostatic signaling.

As in T cell activation, contacts with DC are critically important for $CD4^+$ T cell homeostasis (Kondo et al., 2001) as they deliver both an abundance of self-peptide-MHC complexes and IL-7 (Guimond et al., 2009). Thus, DC provide both, MHC-dependent and –independent signals that control homeostatic T cell survival and proliferation (Feuillet et al., 2005). Importantly, besides controlling homeostatic T cell survival and proliferation, homeostatic contacts to DC also help to maintain effective recirculation and co-receptor expression in naïve T cells (Fischer et al., 2007; Park et al., 2007), deliver signals that control TCR sensitivity (Hochweller et al., 2010; Stefanova et al., 2002) and are essential for the maintenance of T cell memory (De Riva et al., 2007; Kassiotis et al., 2002).

In contrast to activating contacts which in part depend upon a stop-signal followed by adhesive T cell arrest (Cernuda-Morollon et al., 2010; Dustin et al., 1997), homeostatic interactions between T cells and DC *in vivo* are consistently short-lived and migratory, which allows T cells to serially engage with several DC (Miller et al., 2004a). Thus, homeostatic

T cell/DC contacts allow the experimental address of signal transduction during migratory interactions. However, in contrast to the migratory, short contacts seen *in vivo* (Miller et al., 2004a), T cell / DC contacts in liquid culture are long-lived and poorly dynamic (Revy et al., 2001), possibly due to a lack of a pro-migratory environment for T cells. As the complexity of the *in vivo* situation on the other hand prevents high-resolution studies, the molecular composition of a putative dynamic, homeostatic interaction plane is so far unknown.

2.6 Purpose of the study

Migration is important for T cell recirculation, engagement with DC as well as certain phases of T cell activation. T cell migration further contributes to homeostatic contacts with APC due to ongoing T cell movement and short contact duration (Miller et al., 2004a). In order to simulate T cell kinetics in lymph nodes, we here used 3D collagen matrices to monitor T cell migration before, during and after APC binding (Friedl and Brocker, 2004). First, the homeostatic, antigen-independent condition and the influence of self-MHC recognition were analyzed to study short-lived, migratory T cell/DC contacts. Second, the interactions between T cells and cognate antigen-loaded DC leading to T cell activation were monitored.

The specific questions were:

- Does the 3D collagen matrix model deliver an *in vivo*-like experimental setup for T cell homeostasis?
- Is the amoeboid/migratory phenotype of T cells preserved during dynamic interactions?

- Is it possible to statistically analyze the complex interaction plane between T cells and DC in a three-dimensional setup?
- What is the composition of the dynamic, homeostatic interaction plane?
- What is the functional outcome/significance of a dynamic, homeostatic interaction plane?
- How do activating contacts compare to homeostatic contacts in 3D collagen?

3 Materials and methods

3.1 Mice, antibodies and reagents

Cells were isolated from DO11.10 mice (JAX mice), C5.57 mice (Seder et al., 1992), B10A mice (both kindly provided by Prof. R. Germain, NIH, USA), Balb/c mice (Charles River) and MHC class $II^{-/-}$ mice (kindly provided by Dr. M. Gunzer, Braunschweig, Germany) (Grusby et al., 1991). The following primary antibodies were used: anti-CD3 (500A2, Pharmingen), anti-CD43 (S7, Pharmingen), non-blocking anti-LFA1 (I21/7, Biozol), adhesion-blocking anti-LFA-1 antibody M17/4 (Sanchez-Madrid et al., 1983), anti-ICAM-1 (3E2, Pharmingen), anti-Tubulin (DM1A, Sigma), and anti-Phosphotyrosine (4G10, Upstate Biotechnology). Secondary antibody pairs used on the same sample were species-specific pre-absorbed Cy3-conjugated goat-anti-rat IgG, goat-anti-armenian hamster IgG, and goat-anti-mouse IgG (Dianova), Alexa Fluor 488-conjugated goat-anti-mouse IgG and Alexa Fluor 647-conjugated goat-anti-rat IgG (Invitrogen). T cell purity was assessed using Alexa Fluor 647-conjugated KJ1.26 (Caltag), R-Phycoerythrin-conjugated anti-CD4 (H129.19), R-phycoerythrin-conjugated anti-CD44 (IM7), FITC-conjugated anti-CD18 (C71/16) and FITC-conjugated anti-CD62L (MEL-14, all Pharmingen). DC maturation and purity were assessed using FITC-conjugated anti-I-A/I-E (2G9, Pharmingen), R-Phycoerythrin-conjugated CD11c (N418) and Allophycocyanin-conjugated CD86 (RMMP-2, both Caltag). Carboxyfluorescein-diacetate-succinimidyl-ester (CFSE), chloromethyl-benzoyl-amino-tetramethylrhodamine (CMTMR), 5-(and-6)-carboxy SNARF® (SNARF), Alexa Fluor 647-labeled cholera toxin subunit b and Phalloidin-Alexa Fluor 488 were obtained from Invitrogen.

3.2 T cell isolation and culture

Splenocytes were isolated from DO11.10, 5C.C7, Balb/c and B10A mice at 8 - 12 weeks of age. Spleens were removed and squeezed through a cell strainer. The obtained cell suspension was washed in PBS and erythrocytes were removed by lysis (0.15 M NH_4Cl; 1 mM $KHCO_3$; 1 mM Na_2EDTA). For generation of recently activated T cells, splenocytes from Balb/c mice and B10A mice served as APC for T cells isolated from DO11.10 mice and 5C.C7 mice, respectively. For this purpose, splenocytes from Balb/c mice and B10A mice were irradiated (30 Gy) and pulsed for two hours in medium (RPMI supplemented with 10 % fetal calf serum, 100 U/ml penicillin/streptomycin, non-essential amino acids, 1 mM sodium pyrovate, 0.5 mM β-mercaptoethanol and 10 mM HEPES) with 1 µg/ml $pOVA_{323-339}$ and $pMCC_{88-103}$, respectively. Subsequently, splenocytes from DO11.10 or 5C.C7 mice were added, co-cultures were split after 2 and 3 days of co-culture (37°C, 5 % CO_2 in humidified atmosphere), and medium was supplemented with T-stim (Becton Dickinson) at 1:10 dilution. After 9 days of culture without refreshing the medium, >95 % T cells were expressing the transgenic $pOVA_{323-339}$-specific TCR confirmed by KJ1.26 mAb. T cells were CD4+, $CD62L^{high}$, $CD18^{high}$ and $CD44^{high}$, consistent with a recently activated effector phenotype. Naïve $pOVA_{323-339}$-specific T cells were isolated from spleens from DO11.10 mice by depleting all cells positive for CD8a (Ly-2), CD45R (B220), CD49b (DX5), CD11b (Mac-1), and/or Ter-119 (Miltenyi Biotec), resulting in > 95 % CD4 and > 85 % KJ1.26 positivity.

3.3 Culture and transfection of Phoenix cells

The Phoenix cell line is a helper-free retrovirus producer cell line based on 293T cells that is stably transfected with gag, pol and env of Moloney Murine Leukemia Virus (MMLV)

(Kinsella and Nolan, 1996). Phoenix cells that stably produced replication deficient MMLV encoding for the following peptide-MHC class II-EGFP fusion proteins (kindly provided by Dr. R. Germain, NIH, Bethesda):

- the β-chain of the I-E^k MHC class II molecule tagged to EGFP at the carboxy-terminus and to the residues 88-103 of moth cytochrome c ($pMCC_{88-103}$) to the NH2-terminus via a flexible polypeptide linker (Fremont et al., 1996); together with the α-chain of the I-E^k MHC class II molecule this fusion protein forms a peptide-MHC class II complex presenting the cognate antigen of 5C.C7 T cells (pMCC-MHC-GFP)(Seder et al., 1992; Wulfing et al., 2002).

- a control β-chain fusion protein covalently linked to a non-activating variant of the $pMCC_{88-103}$ ($MCC^{D93E,K99T,T102A}$; null-MHC-GFP; (Reay et al., 1994).

For virus production and isolation cells were seeded into 10 cm culture dishes at approximately 70% confluence and cultured in complete medium for 48 h. Subsequently, the supernatant was collected and filtered using a 0.45 mm syringe filter

3.4 DC culture and infection with MMLV containing EGFP tagged peptide-MHC class II complexes

For preparation of bone marrow-derived DC Balb/c and B10A mice were sacrificed and femurs and tibiae were prepared. After clipping of the epiphyses bone marrow was flushed out with PBS, cells were separated by aspiration several times and subsequently washed with PBS.

Cells derived from Balb/c mice were cultured in medium supplemented with recombinant GM-CSF and IL-4 at a concentration of 5 x 10^6 cells / 10 ml in a 10 cm diameter cell culture dish. Half of the medium was refreshed on day 3, and cultures were split on day 6. On day 7, 1 µg/ml LPS was added for the last 24 h in order to induce final termination before the DC were used on day 8.

Cells derived from B10A mice were cultured in medium supplemented with recombinant GM-CSF and IL-4 at a concentration of 1 x 10^6 cells / 3 ml in a 6-well plate. At day 1, day 2 and day 3 of culture cells were infected with MMLV containing peptide-MHC II-GFP fusion proteins as follows: Filtered viral supernatant was supplemented with 8 µg/ml polybrene and added to the BMDC culture (6 ml / well after removing 2 ml of the BMDC culture supernatant). Subsequently, the 6-well plates were centrifuged at 2600 rpm for 90 min at 30°C and incubated for another 60 min at 37°C. Finally, the supernatant was replaced by fresh GMCSF/IL-4 containing medium. At day 5 medium was replaced. At day 7 LPS was added at a concentration of 1 µg/ml for 24 h before BMDC were used on day 8.

3.5 T cell-DC cocultures in 3D collagen lattices

3D collagen lattices consisting of type I bovine or rat tail collagen at final concentrations of 1.8 mg/ml (Nutacon and Becton Dickinson, respectively) were generated as described (Friedl and Brocker, 2004). To preselect for mobile T cells and exclude non-moving T cells from the DC-containing compartment, an immigration assay of DC-containing collagen matrices (150,000 / 100 µl collagen) overlaid with DO11.10 T cells was used (Fig. 2). After 3 h of incubation, immigration cultures were used for life-cell imaging or fixed (buffered paraformaldehyde, 2% final concentration) and stained for confocal analysis.

3.6 Live-cell imaging and cell tracking

Time-lapse bright-field microscopy was performed as described (Friedl et al., 1998) with 20 sec/frame. For fluorescence microscopy, DO11.10 CD4+ cells were labeled with CFSE in PBS (2.5 µM, 3 min, 37°C), suspended in medium (1:10 dilution) and washed with PBS. For some experiments, cells were additionally stained with Alexa Fluor647-labeled cholera toxin subunit b (10 µM) in RPMI (10 min, 4°C). DC were labeled with CMTMR in RPMI (10 µM; 30 min, 37°C), washed with PBS, suspended in RPMI (30 min, 37°C), washed again, and used for co-cultures with T cells (37°C, 5% CO_2). 3D confocal image stacks were acquired with a Leica SP2 confocal scanner (40 x, NA=1.25) at 4 µm step and 30 sec stack interval. 4D rendering and tracking of migration velocity as well as contact duration were performed using the Volocity 4.0 software (Improvision).

For some experiments, CD4+ T cells from 5C.C7 mice were stained with SNARF in PBS (2,5 µM, 5 min, 37°C), suspended in medium (1:10 dilution), washed with PBS and co-cultured with DC that expressed GFP-tagged $pMCC_{88-103}$-MHC II for life cell imaging.

3.7 Survival and proliferation assay

CFSE-labeled T cells were co-cultured with DC in collagen (5:1 ratio) for 0 to 4 days and harvested by collagenase digestion (200 U/ml, 30 min; collagenase IIV; Sigma). For some experiments, DC-conditioned supernatant was harvested, centrifuged, sterile-filtered, and used for T cell cultures. Cells were additionally stained with KJ1.26-Alexa Fluor647, washed, resuspended in PBS (450 µl) supplemented with counting beads (50 µl; Caltag), and counted by flow cytometry (FACS Canto, Becton Dickinson). Absolute T cell counts/sample were calculated as [counted number of T cells obtained from the gated $KJ1.26^+CFSE^+$ population

including cell conjugates] × [counting beads/sample]/[counted number of counting beads]. The mitotic rate in T cells was assessed from CFSE dilution monitored by flow cytometry.

3.8 Immunofluorescence, image processing, and subcellular-resolved densitometry

Co-cultures of CTx b-labeled or -unlabeled T cells immigrated into DC-containing 3D collagen lattices were fixed, washed three times, permeabilized (0.1 % Triton-x-100, 5 min), and stained with primary (18h, 4°C) and secondary antibody (2h, 4°C). Filamentous actin (F-actin) was stained with Phalloidin-Alexa Fluor 488 (2h, 4°C). 3D image stacks of T cell / DC conjugates were acquired by confocal microscopy at 0.5 µm step intervals and intensity values below saturation.

To exclude fixation artifacts potentially causing toxic cell shrinking and/or rounding the fixation quality was monitored by videomicroscopy, confirming immediate T cell arrest and preservation of T cell morphology during fixation and thereafter (Video 1). To quantify receptor location from 3D T cell-DC conjugates with amoeboid T cell morphology, the signal intensity along the interaction plane of polarized T cell/DC conjugates was measured from non-processed maximum-intensity projections encompassing the central length axis of the contact plane (1-2 µm in depth).

To capture the front-rear asymmetry of migrating T cells, T cells with polarized morphology defined by the uropod rich in CTx b and an F-actin peak in a single leading edge which formed a fully aligned contact to the DC body were analyzed. Exclusion criteria were round or multipolar (i.e. multiple leading edges) T cell morphology; multifocal contacts with DC

body or dendrites or contact discontinuities; additional contact with directly adjacent further T cells; and saturated fluorescence intensities.

Fluorescence intensities were obtained in front-rear direction i) for the T cell membrane engaged and ii) for the non-engaged membrane using Image J. The length of both membrane compartments was normalized into 50 equally sized segments (each representing a mean length of 0.26 +/- 0.06 µm and 0.33 +/- 0.07 µm for the engaged and the non-engaged membrane, respectively) and the normalized mean fluorescence intensity was obtained for each segment (Fig. 4). The fluorescence intensity range was normalized on an image-by-image basis between the brightest pixel value (100%) and background fluorescence (0%). For subcellular-resolved statistical analysis, three zones of the contact area were defined, based on cell morphology: segments 1 to 6 (front, representing the leading edge), 7 to 30 (mid-zone, representing the cell-body), and 31 to 50 (rear, representing the uropod). Statistical analysis was performed using the Mann Whittney U test for pooled data from at least three independent experiments representing 11 to 34 individual T cell/DC conjugates. For display, selected images were additionally post-processed (contrast, brightness, gamma correction) using Photoshop CS1 (Adobe).

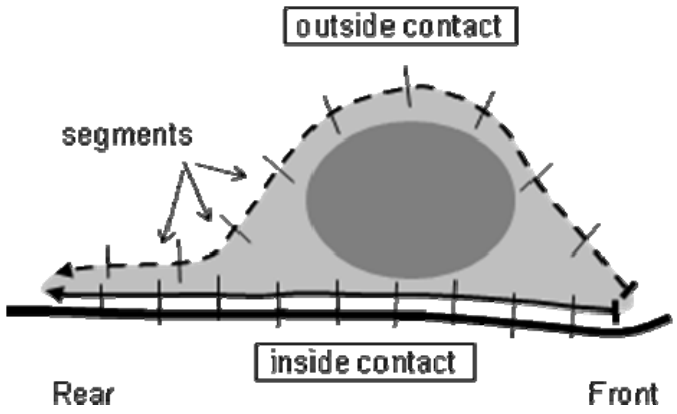

Figure 4: Normalization of T cell membranes inside and outside the contact plane. Legend and figure adapted from Storim et al., 2010.

4 Results

4.1 Establishment of an "*in vivo*-like" in vitro model for T cell/DC contacts

Conventional *in vitro* liquid culture models of T cell/APC interaction lack a pro-migratory environment and therefore impede a realistic analysis of contact dynamics. Additionally, cell migration is dispensable as cells mainly establish contacts by passive aggregation. On the other hand, the complex *in vivo* situation in lymph nodes prevents the sub-cellular resolution of T cell/DC contacts.

Using a collagen matrix model to mimic tissue-like conditions for T cell/DC interactions offers several advantages: First, a low-density 3D fibrillar collagen lattice is a pro-migratory environment for T cells and DC (Friedl and Brocker, 2004) and therefore facilitates the analysis of the impact of migration on T cell signaling under homeostatic and activating conditions. Second, the imaging properties of low-density collagen allow high resolution (i. e. sub-cellular resolution) imaging of T cell/DC contacts. And finally, passive aggregation of T cells and DC is prevented by seeding DC into the collagen matrix and placing T cells onto the surface of the collagen scaffold, thus creating initial separation of both cells which is subsequently resolved by active migration of either cell type towards each other (Fig. 5).

Despite the pro-migratory properties of fibrillar collagen, naïve T cells largely failed to spontaneously migrate into the collagen (Fig. 5A, upper row). Unexpectedly, not even the addition of the chemokines CXCL12 and/or CCL19 improved naïve T cell migration significantly (Fig. 5A, lower row). Therefore, naïve T cells could not be analyzed in this assay for technical reasons.

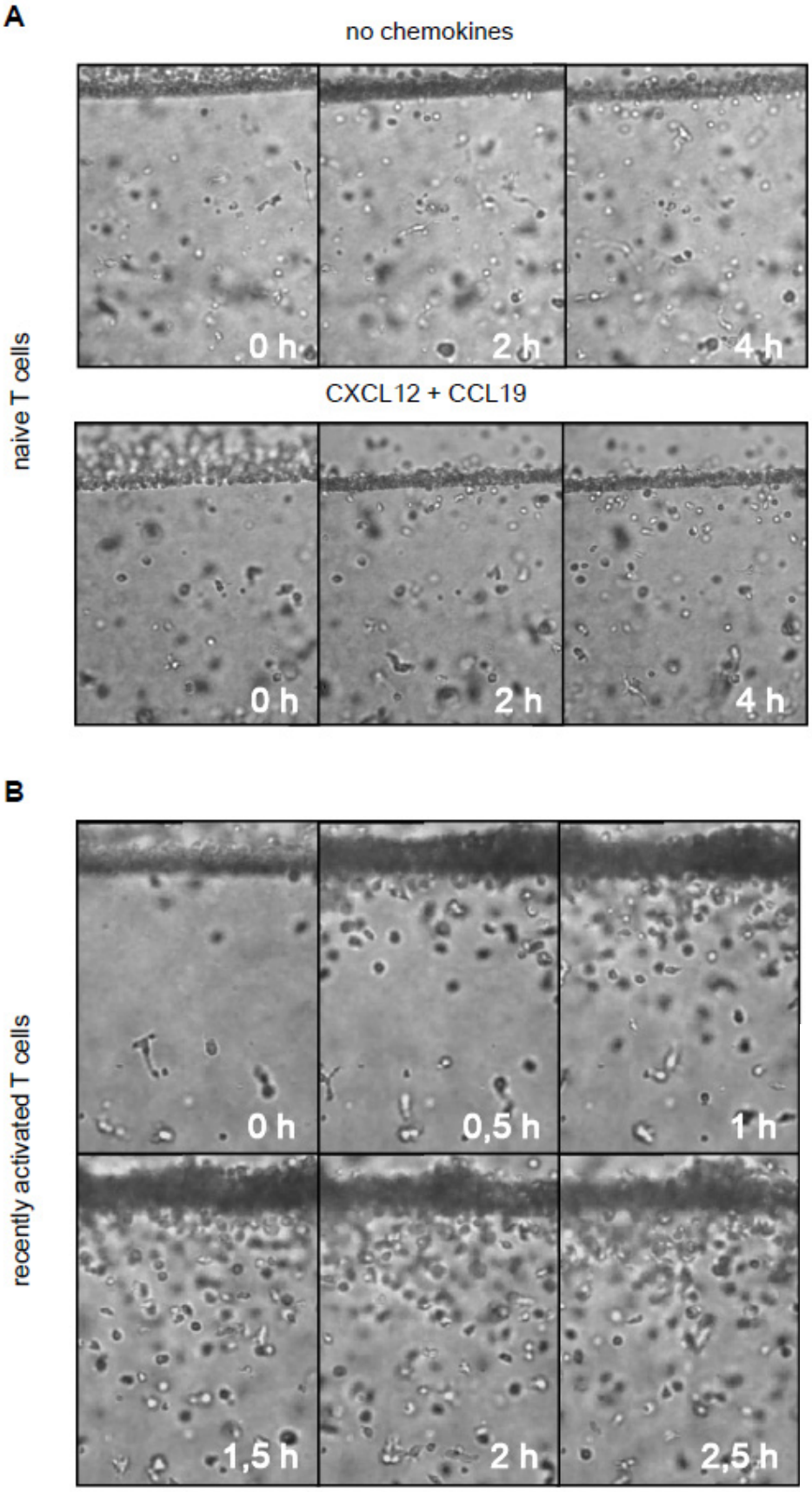

Figure 5: Immigration of DO11.10 CD4$^+$ T cells into collagen lattices containing Balb/c BMDC. (A) Spontaneous (upper row) and chemokine induced (lower row) migration of naïve DO11.10 T cells. (B) Spontaneous migration of recently activated DO11.10 T cells, compare Video 2. Legend and figure reproduced from Storim et al., 2010.

However, antigen-specific expansion of DO11.10 T cells 9 days prior to the invasion assay resulted in non-dividing T cells that displayed spontaneous migration activity, infiltrating the collagen lattices at high numbers and contacting DC (Fig. 5B, Video 2). Therefore, in the following experiments recently activated T cells were further analyzed.

4.2 Homeostatic contacts

4.2.1 Homeostatic interactions between T cells and DC in 3D collagen lattices are dynamic and short-lived

For high-resolution analysis of antigen-independent, homeostatic interactions between T cells and DC confocal life imaging was used. After infiltrating the collagen lattice, recently activated T cells migrated at high speed (approximately 10 μm/min; Fig. 6C) and frequently contacted DC. The majority of these contacts did not lead to a migratory arrest of the T cell and therefore differed from activating T cell/DC contacts that lead to temporary or long-lasting adhesion and immobilization of the T cell on the DC surface (Dustin et al., 1997). T cells rather continued to move across the DC surface and detached after a few minutes while maintaining their migration velocity at 10 μm/min (Fig. 6, Video 3).

Despite their short-lived nature and continued T cell migration, these contacts influenced T cell functions. First, T cells contacting DC while migrating survived significantly longer than T cells moving through DC-free collagen lattices (Fig. 7A and B). Second, migratory T cell/DC contacts supported slow proliferation in a small subset of T cells (Fig. 7A). This slow mitotic activity was dependent on the presence of DC as T cells failed to divide when cultured alone (Fig. 7A), which precludes background proliferation activity and confirms stringent, antigen-independent baseline conditions (see materials and methods). Conversely,

DC loaded with pOVA$_{323-339}$ induced a high rate of cell divisions within the entire T cell pool with up to 6 mitotic rounds within the 4-day observation period (Fig 7A), confirming efficient T cell stimulation under antigen-specific conditions.

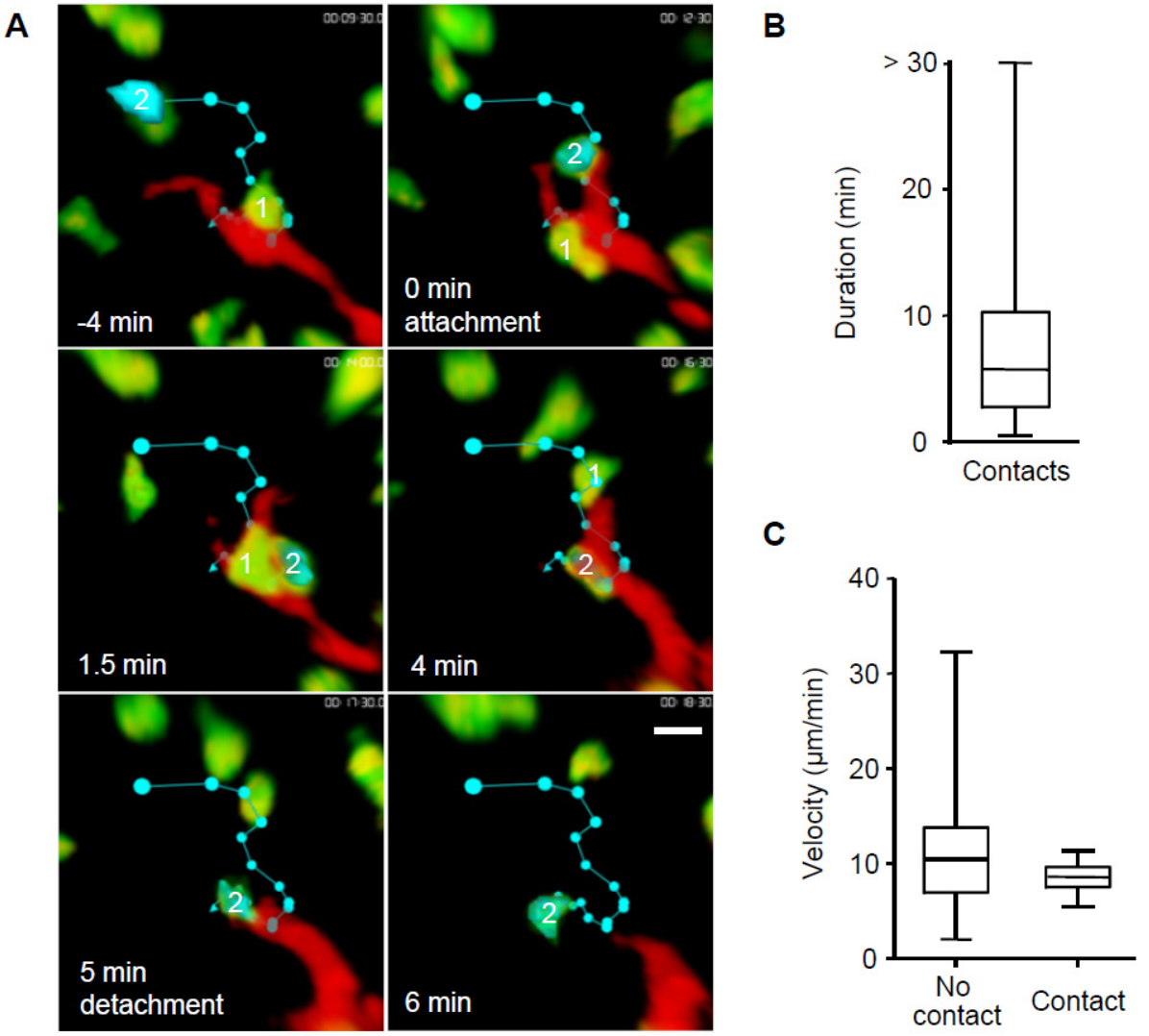

Figure 6: Dynamic homeostatic interactions in 3D collagen. (A) Amoeboid migration of CFSE labeled T cells (green) before, during and after interaction with CMTMR-labeled DC (red). Time-resolved reconstruction of confocal z-stacks illustrating two migratory contacts with one example track (cyan, cell 2; compare Video 3). (B) Contact duration of T cell-DC interactions (24 cells). (C) Velocity of T cell migration on the DC surface (14 cells) compared to contact-free migration through collagen (429 cells). Box and whiskers show median, 25-75% and total range. Bar, 5 µm. Legend and figure adapted from Storim et al., 2010.

Prolonged survival together with slow proliferation resulted in stable total T cell counts for homeostatic conditions while T cell numbers decreased to 20% and exponentially increased in the absence of DC and the presence of $pOVA_{323-339}$, respectively (Fig. 7B). Thus, completely migratory contacts between $CD4^+$ T cells and DC in the absence of cognate antigen in 3D collagen lattices support signaling leading to prolonged survival and low-level proliferation. Therefore, the 3D collagen model of T cell/DC interactions recapitulates the characteristics of homeostatic contact kinetics and outcome *in vivo* (Miller et al., 2004a; Seddon et al., 2003; Surh and Sprent, 2005).

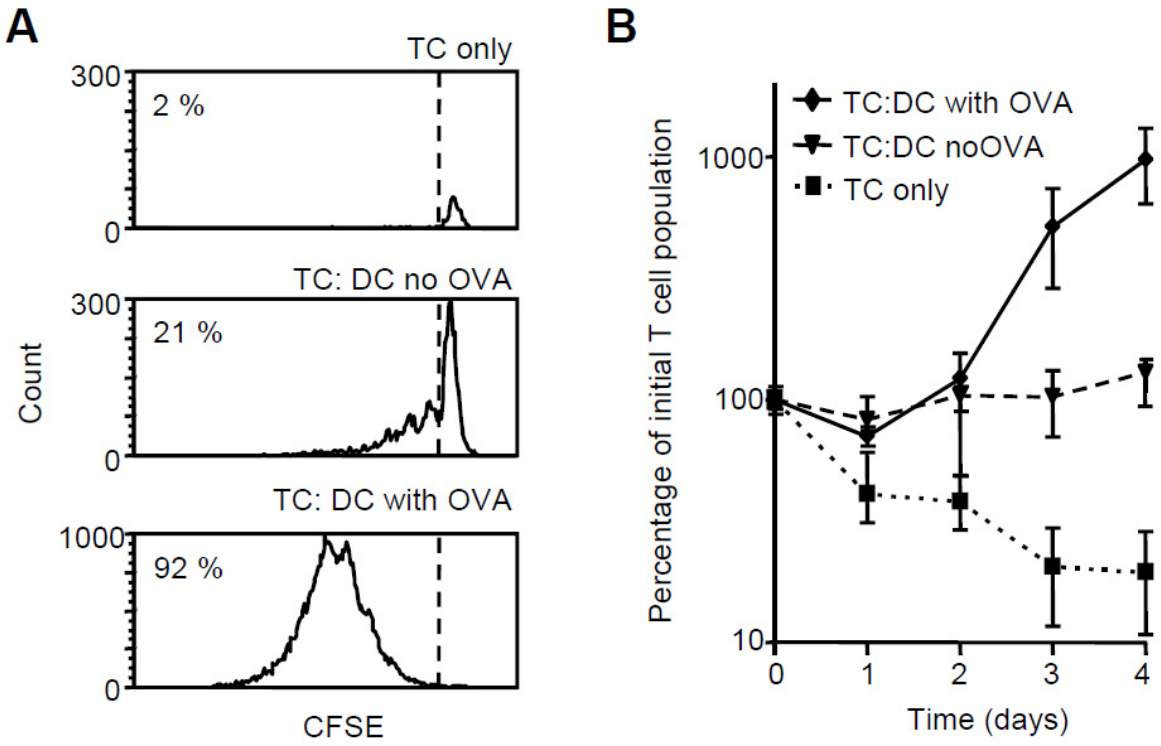

Figure 7: Homeostatic interactions in 3 D collagen support survival and low-level proliferation. (A) T cell proliferation and survival measured as CFSE-dilution after 4 days of culture. Numbers indicate the percentage of the initial T cell population that divided at least once. (B) Development of the T cell population in the presence or absence of DC after 4 days of culture. Absolute T cell numbers were obtained by quantitative flow cytometry, normalized to the initial T cell count and displayed as the means ± standard deviation (n=3). Legend and figure adapted from Storim et al., 2010.

4.2.2 The b subunit of cholera toxin labels the uropod of migrating T cells

For migration, T cells polarize into three distinct zones (del Pozo et al., 1997; Friedl and Weigelin, 2008):

- In the dynamic leading edge F-actin polymerization drives T cell polarization, the protrusion of lammelipods that probe the encountered substrate, and migration.
- A central region comprises the cell body and nucleus.
- The posterior uropod contains most of the internal membranous compartments of the cell including ER and golgi apparatus. Additionally, it is the location of T cell-substrate adhesion, receptor endocytosis, and myosin-II mediated rear-end retraction. Besides β2-integrins, CD43 and CD44 are typical uropod marker molecules.

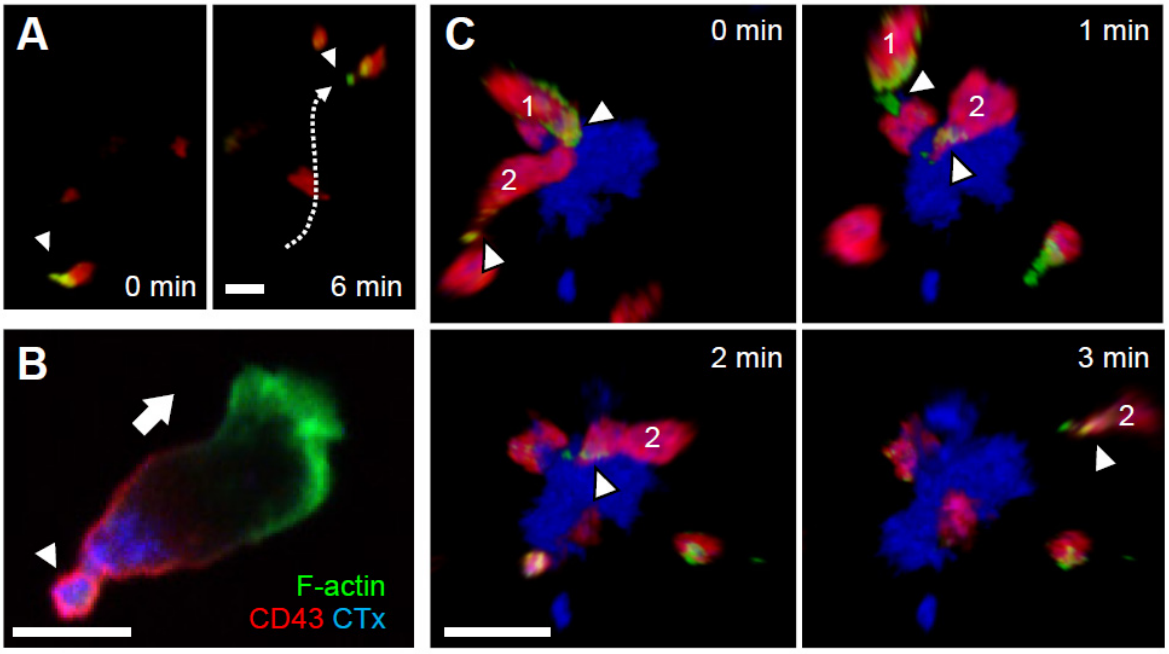

Figure 8: CTx b accumulates in the uropod of moving T cells. (A) Dynamic reconstruction of confocal z-stacks of migrating T cells labeled with CFSE (red) and Alexa Fluor 647 labeled CTx b (green). One representative cell path is indicated (compare Video 4). (B) Central section of representative T cell in migrating state pre-labeled with CTx b (blue) prior to and CD43 (Cy3, red) and F-actin (green) after fixation. Arrow, direction of migration. (C) Localization of CTx b (green) in the uropod of live T cells (CFSE, red) during migration across CMTMR labeled DC (blue) in the absence of $pOVA_{323-339}$. One detaching T cell (cell 1) and one complete interaction cycle (cell 2) are shown (compare Video 5). Bar, 5 µm. Legend and figure adapted from Storim et al., 2010.

The b subunit of cholera toxin (Ctx b) mediates binding to detergent-resistant membrane domains (Gomez-Mouton et al., 2001), leading to internalization of the toxin and accumulation in the ER and golgi apparatus (Chinnapen et al., 2007). As expected, CTx b was located in the uropod of DO11.10 T cells as soon as they polarized and started to migrate (Fig. 8A, Video 4). Additionally, a distinctive CTx b-positive uropod was maintained during migration across the DC (Fig. 8C, Video 5). Finally, CTx b-labeling of T cells remained visible after fixation and did not interfere with subsequent immunofluorescence labeling (Fig. 8B). Therefore, fluorescently labeled CTx b was used to mark the uropod of $CD4^+$ T cells.

4.2.3 Simultaneous amoeboid T cell migration and DC-induced polarization in the absence of cognate antigen

One aim of this work was the establishment of an analytical tool that allowed the comparison of the sub-cellular distribution of an array of molecules in T cells migrating on a DC surface in a 3D context. Thus, acquired data needed to be normalized for shape and signal intensity, because migrating T cells engaging with DC were morphologically diverse (e. g. they differed in length and shape while aligning to the DC), and the detected fluorescence signal intensities differed significantly (e. g. due to the distance between the fluorescent dye within the collagen and the cover slip as well as cell-to-cell expression variability of marker molecules). The T cell membrane engaging the DC in the central length axis of the contact plane ("inside contact") and the opposing non-engaged membrane ("outside contact") were divided into 50 equally sized segments and the mean fluorescence intensity for each segment was normalized (Fig. 4; see materials and methods for a detailed description). Only polarized T cells with a

morphologically clear leading edge and a CTx b positive uropod that completely engaged (i.e. longitudinally aligned to) one DC were analyzed.

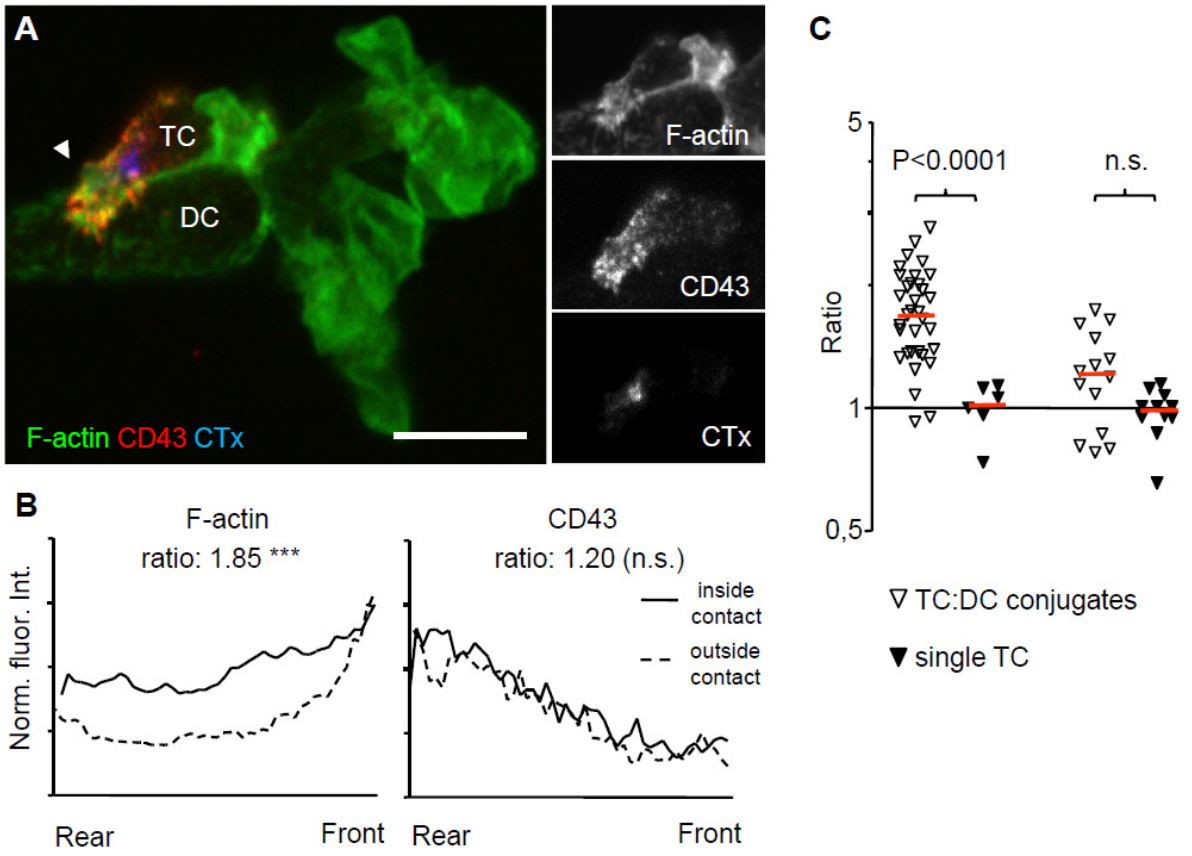

Figure 9: Front-rear asymmetry and contact-dependent redistribution of F-actin and CD43 during homeostatic interactions. (A) Three-color maximum projection of a fixed T cell / DC pair after staining for F-actin (Phalloidin-Alexa Fluor 488, green) and CD43 (Cy3, red). As reference for the rear, T cells were labeled with CTx b prior to fixation (Alexa Fluor 647, blue). Bar, 5 µm. (B) Normalized fluorescence intensities from central maximum projections of unprocessed images along the T cell membrane engaged with the DC (solid line, "inside contact") and the opposing, non-engaged membrane (dashed line; "outside contact"). Data show the median intensities from 34 (F-actin) and 14 cells (CD43). (C) Contact-dependent redistribution of F-actin and CD43, measured as median fluorescence ratio [inside contact: outside contact] of T cell/DC conjugates, compared with the ratio of both sides of contact-free T cells migrating in collagen. Significance was determined by the unpaired Mann-Whitney U test (***, $p < 0.0001$; n. s., not significant). White arrowheads in (C) and (D) indicate the rear of the T cell. Legend and figure adapted from Storim et al., 2010.

As indicated by the maintained amoeboid cell shape, contact to a DC surface did not influence the front-rear asymmetry of a migrating T cell. While F-actin clearly peaked within the T cell leading edge, CD43 was mainly located within the uropod (Fig. 9A, B; compare Fig. 8B).

However, in contrast to the symmetric F-actin distribution to both sides of a freely migrating T cell within the collagen lattice (Fig. 9C), contact with DC induced F-actin accumulation in the T cell/DC contact plane (Fig. 9 A, B).

Since most of the F-actin was CD3-colocalized, the migrating T cell rather polarized toward the DC than *vice versa* (Fig. 10), indicating a simultaneous longitudinal ("amoeboid") and DC-induced polarization of the T cell in orthogonal directions. In contrast to the F-actin distribution, contact-induced polarization did not alter the distribution of CD43 as it was neither accumulated in nor excluded from the contact plane (Fig. 9 A, B). Thus, migrating T cells polarize their actin cytoskeleton toward DC during homeostatic contacts while they maintain their default amoeboid front-rear asymmetry.

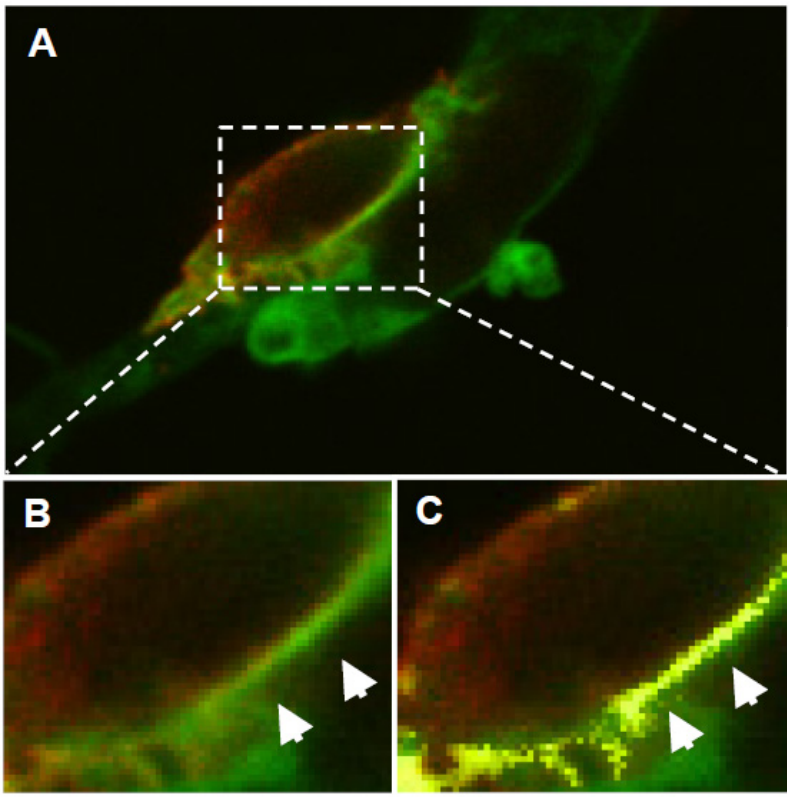

Figure 10: T cells redistribute F-actin to the contact plane. (A) CD3 and F-actin co-localize on the T cell side of the contact plane. T cell/DC co-cultures were fixed and stained with Phalloidin (green) and anti-CD3 (red). Yellow color indicates co-localization (B: higher magnification). (C) Areas with co-localized F-actin and CD3 are highlighted by false-color (intense yellow). Bar, 5 µm. Legend and figure reproduced from Storim et al., 2010.

Distribution of LFA-1, CD3 and phosphotyrosine in homeostatic contacts

DC-induced re-orientation of the actin cytoskeleton is a fast process and may be accomapnied by the redistribution of cell surface receptors in order to trancduce homeostatic signaling. As in activating interactions, candidate transmembrane proteins are the T cell receptor itself and LFA-1. Indeed, LFA-1 strongly accumulated in the homeostatic contact plane, most pronounced in the mid-zone of the contact (Fig. 11A).

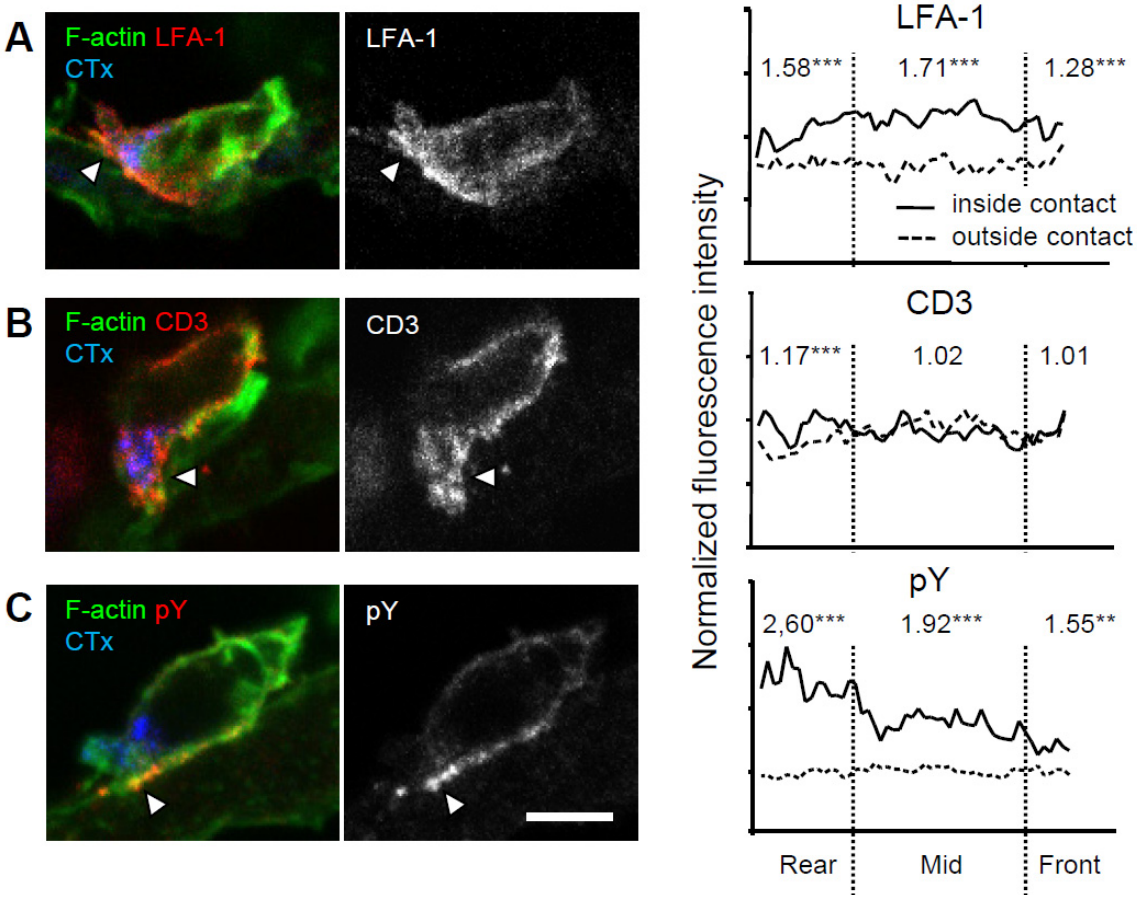

Figure 11: Distribution of LFA-1, CD3 and pY in fully developed, polarized T cell-DC contacts. CTx b-labeled (blue) T cells co-cultured with DC were fixed after collagen immigration and stained with mAbs against LFA-1 (I21/7), CD3 (500A2), or pY (4G10) (all red) and phalloidin-Alexa Fluor 488 (green), whereby phalloidin served as marker for the cell front and CTx b for the rear. Line graphs show normalized fluorescence intensities in longitudinal orientation for 20 (LFA-1), 29 (CD3) and 26 (pY) randomly selected cells. Sub-cellular-resolved enrichment of signal intensities inside versus outside the contact were averaged for the T cell front, mid-zone, and the rear (numbers) and statistically analyzed (unpaired Mann-Whitney U test; **, $p < 0.001$; ***, $p < 0.0001$). White arrowheads indicate the uropod. Bar, 5 µm. Legend and figure reproduced from Storim et al., 2010.

However, unlike CD43 or F-actin, LFA-1 did not form a longitudinal gradient within the contact plane. Cell-by-cell analysis rather suggested that LFA-1 distribution was variable during different contact phases: LFA-1 clusters were detectable in the leading edge directly after contact acquisition and even before the T cell fully aligned to the DC (Fig. 12A) while the LFA-1 signal peaked at the opposite uropod during detachment (Fig. 12C). Additionally, LFA-1 clustered at variable sites between leading edge and uropod within fully developed homeostatic contacts, further supporting the concept of a dynamic and variable LFA-1 redistribution (Fig. 12B). However, while peak levels of LFA-1 accumulation were variable, the mid-zone consistently showed LFA-1 enrichment.

Although it is established that the TCR is required for homeostatic signaling (Surh and Sprent, 2005), no accumulation of TCR within the homeostatic contact plane was detected, as shown by the distribution of CD3, a transmembrane molecule and integral part of the TCR complex: CD3 was evenly distributed within and outside the contact plane and lacked clustering except for a small but statistically significant peak in the uropod (Fig. 11B).

Next, the extent and location of signal transduction within the homeostatic contact plane was addressed. To this aim, the phosphorylation of tyrosine residues (pY) during migratory homeostatic contacts were analyzed as these phosphorylation events appear very early in antigen-specific and homeostatic signaling (Feuillet et al., 2005; Meraner et al., 2007; Smith-Garvin et al., 2009). Despite maintained motility and the lack of detectable TCR accumulation, a longitudinal gradient of tyrosine phosphorylation events with increasing pY-levels from leading edge to uropod was visualized (Fig. 11C).

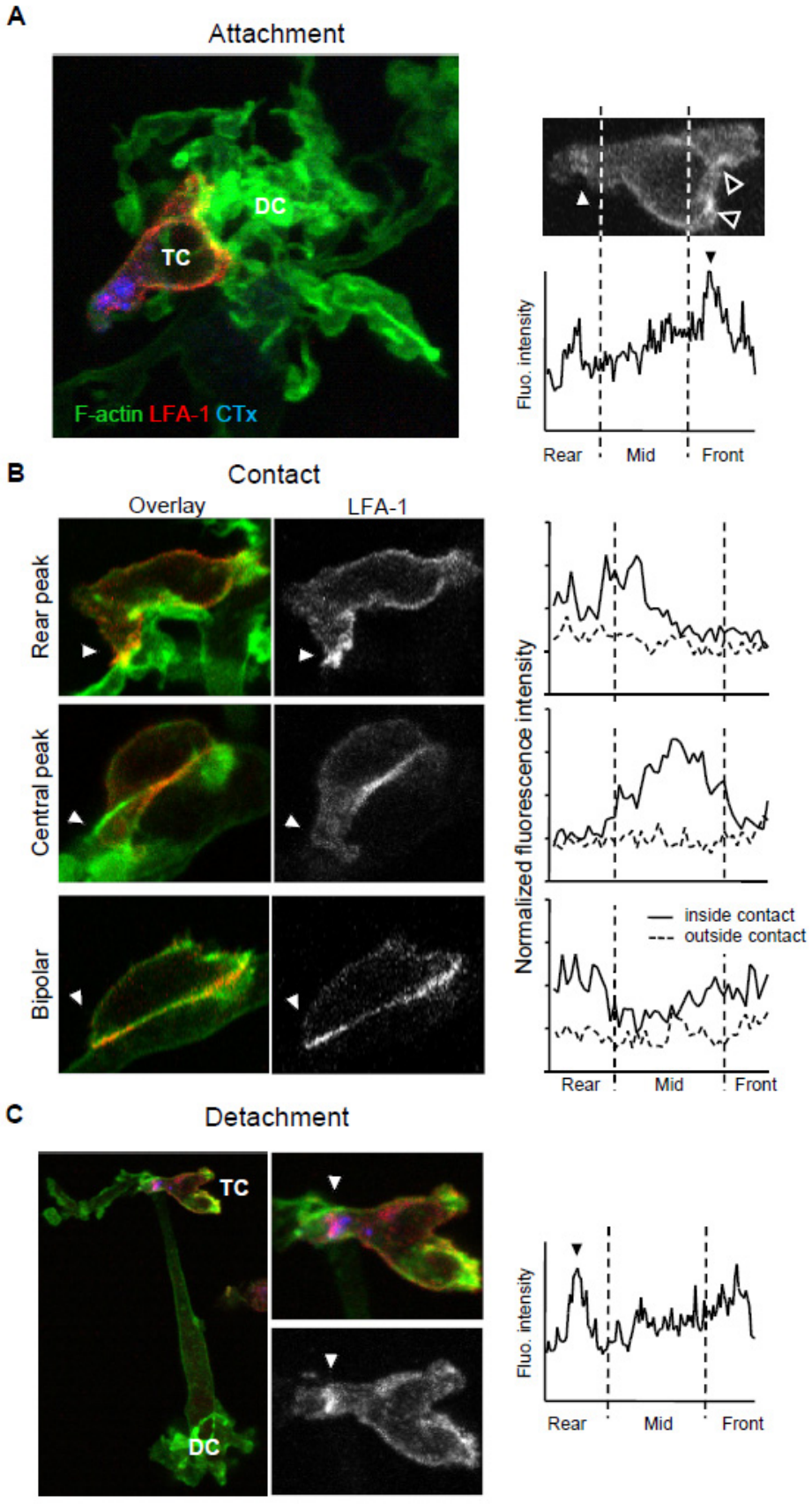

Figure 12: LFA-1 redistribution during different contact phases. T cell/DC cocultures in collagen lattices were fixed, stained with anti-LFA-1 mAb I21/7 (red) and Phalloidin (green), and cell-cell contact stages were classified using T cell and DC topographies. Images show maximum projection of adjacent slices covering the central contact region (2 µm in depth). (A) Contact acquisition, characterized by the leading edge bound to the DC and the posterior CTx b-positive uropod (blue) at the opposite cell pole. Peak intensity of LFA-1 staining (black arrowheads) at the leading edge engaged with the DC but not in lateral and posterior regions. (B) Established, elongated contact plane including leading edge and uropod. Of 20 cells analyzed LFA-1 distribution was classified as either central (6 cells), rear (7 cells), or bipolar (5 cells,), whereas two T cells lacked LFA-1 enrichment. (C) LFA-1 peak in the uropod (identified by CTx b, blue) during sub-total T cell detachment from the DC. Bar, 5 µm. Legend and figure reproduced from Storim et al., 2010.

Thus, the homeostatic contact plane is a dynamic, short-lived and asymmetric signaling platform characterized by the strong and fast redistribution of LFA-1 that enables pY signaling along a longitudinal gradient peaking in the uropod.

4.2.4 Signaling zones in dynamic homeostatic contacts

The detection of tyrosine phosphorylation allows the quantification of gross signal transduction through virtually every known signaling pathway, including TCR-dependent and –independent signals, which obviously results in a rather unspecific read-out. Pilot experiments aiming to visualize phosphorylated ZAP-70/LAT in order to detect TCR-dependent tyrosine phosphorylations did not yield specific label and thus were not further pursued (data not shown). To discriminate TCR-dependent and –independent tyrosine phosphorylation along the homeostatic T cell/DC interaction plane, MHC class II-deficient ($MHCII^{-/-}$) DC were used which provide similar levels of CD11c and CD86 but lack the capacity of TCR triggering (Fig. 13, Grusby et al., 1991).

Similar to wild-type DC, $MHCII^{-/-}$ DC supported a strong pY-peak in the uropod (Fig. 14). However, interference with TCR-signaling nearly abrogated signaling in the mid-zone (Fig. 14), suggesting a special role of this region for the TCR contribution to homeostatic signaling.

Interestingly, pY-signals and CD3 co-localized within the mid-zone but not the uropod in single sections of some analyzed T cell/DC couples (Fig. 15), which further supported the importance of the mid-zone for TCR-signaling.

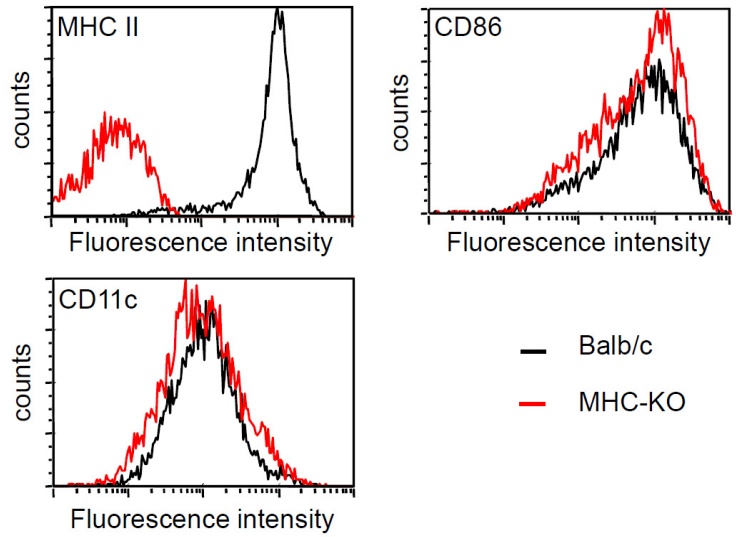

Figure 13: Phenotype of wild-type Balb/c and MHCII$^{-/-}$ DC. At day 8 of culture including a maturation step for 24 h with 1 µg/ml LPS DC were stained with anti-MHC class II, anti-CD11c and anti-CD86 mAbs and analyzed by flow cytometry. Legend and figure adapted from Storim et al., 2010.

Despite the stark influence on the signaling pattern in homeostatic contacts, the presence or absence of MHC class II molecules did not alter the principle polarization of the T cell toward the DC: both F-actin and LFA-1 accumulated in the contact plane of MHC$^{-/-}$ DC (Fig. 16).

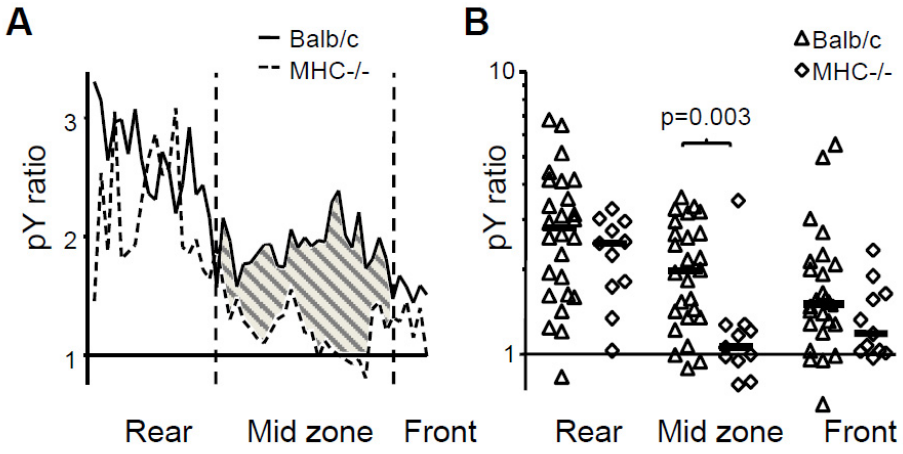

Figure 14: TCR-dependent and -independent pY signals in migratory contacts. Gradients (A) and subcellular resolved population statistics (B) of pY signal enrichment in the contact plane of DO11.10 T cells engaged with wild-type or MHCII$^{-/-}$ DC. (A) Median fluorescence ratios [inside contact : outside contact] for 11 (MHC$^{-/-}$) and 26 (Balb/c) interactions. Dashed area indicates the amplitude of TCR-dependent pY signaling. (B) Scatter plot of pY-ratios in the cell front, mid-zone and rear for individual contacts (unpaired Mann-Whitney U test). Legend and figure adapted from Storim et al., 2010.

However, MHC$^{-/-}$ DC failed to induce the minor CD3 accumulation in the uropod (Fig. 16). Thus, T cells migrating on a DC surface develop a contact-dependent asymmetric signaling platform that facilitates TCR-dependent and -independent signaling in distinct signaling zones.

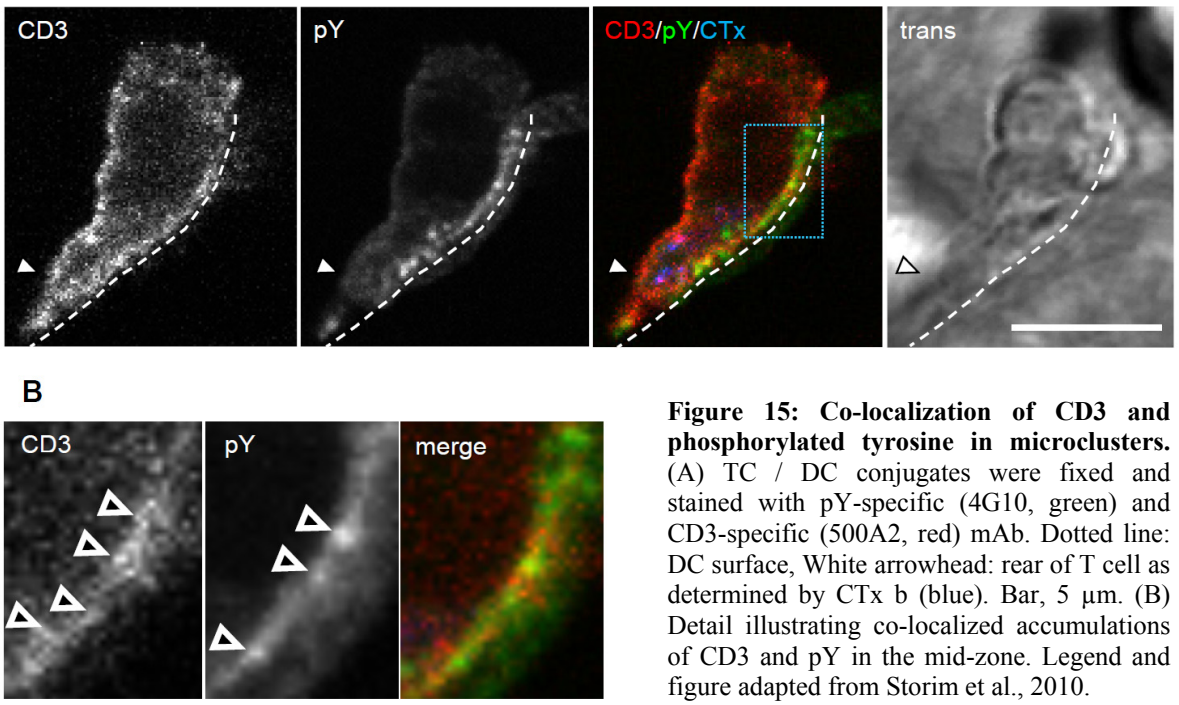

Figure 15: Co-localization of CD3 and phosphorylated tyrosine in microclusters. (A) TC / DC conjugates were fixed and stained with pY-specific (4G10, green) and CD3-specific (500A2, red) mAb. Dotted line: DC surface, White arrowhead: rear of T cell as determined by CTx b (blue). Bar, 5 µm. (B) Detail illustrating co-localized accumulations of CD3 and pY in the mid-zone. Legend and figure adapted from Storim et al., 2010.

To analyze the role of TCR-dependent and –independent signaling in specialized zones of the homeostatic contact plane, the influence of i) TCR-signaling, ii) LFA-1 signaling and iii) DC-derived soluble factors on homeostatic proliferation and survival was addressed. While survival of non-dividing T cells was supported by MHCII$^{-/-}$ DC, these interactions failed to induce homeostatic T cell proliferation (Fig. 17A).

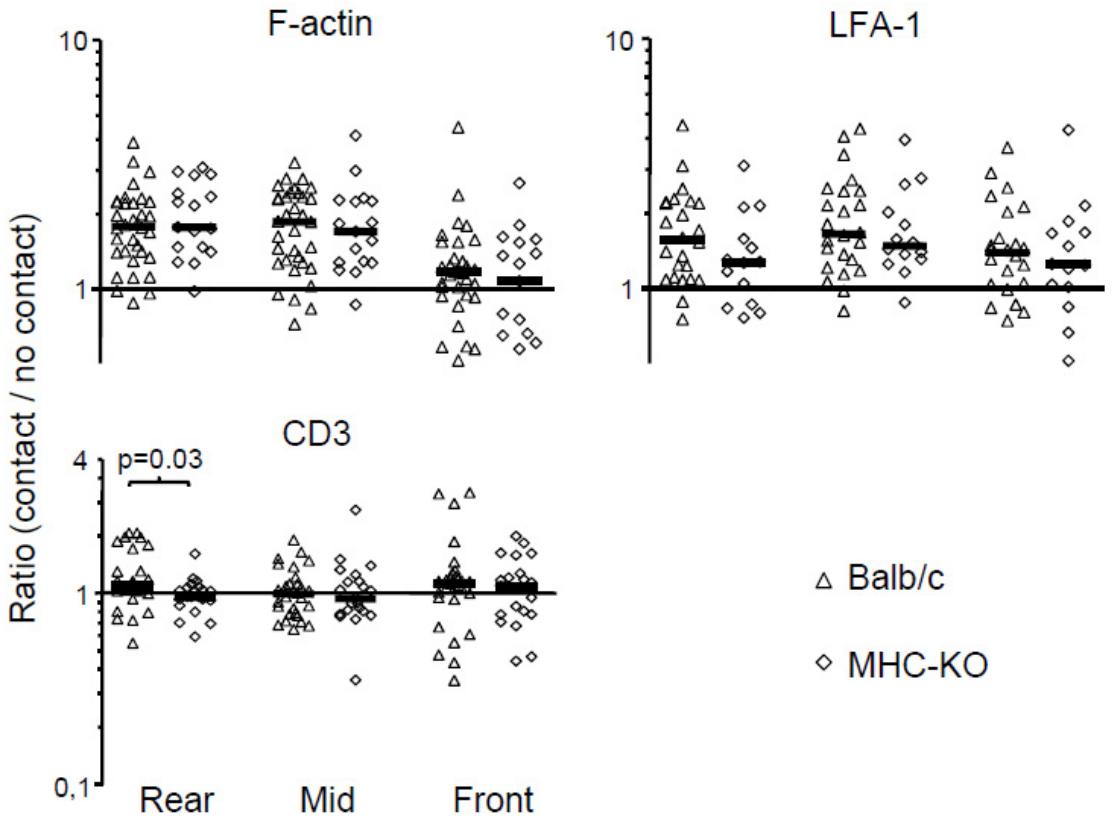

Figure 16: Redistribution of CD3 but not of LFA-1 and F-actin is dependent on TCR signaling. PFA-fixed conjugates of DO11.10 T cells and Balb/c or MHC$^{-/-}$ DC were stained and analyzed as in Fig. 11. Ratiometric analysis of single cells for front, mid-zone and rear of the contact membrane. Bars indicate median. Unpaired Mann-Whitney U test. F-actin: Balb/c, 34 cells; MHC$^{-/-}$, 17 cells. CD3: Balb/c, 29 cells; MHC$^{-/-}$, 21 cells. LFA-1: Balb/c 24, cells; MHC$^{-/-}$, 14 cells. Legend and figure adapted from Storim et al., 2010.

Contact with wild-type DC in the presence of LFA-1 function blocking antibody M17/4 had similar effects (Fig. 17A). Consequently, interference with TCR- or LFA-1 signaling resulted in a decay of viable T cells after 4 days of co-culture (Fig. 17B). Interference with LFA-1 in T cells contacting MHC$^{-/-}$ DC did, however, not lead to additional effects (Fig 17A, B).

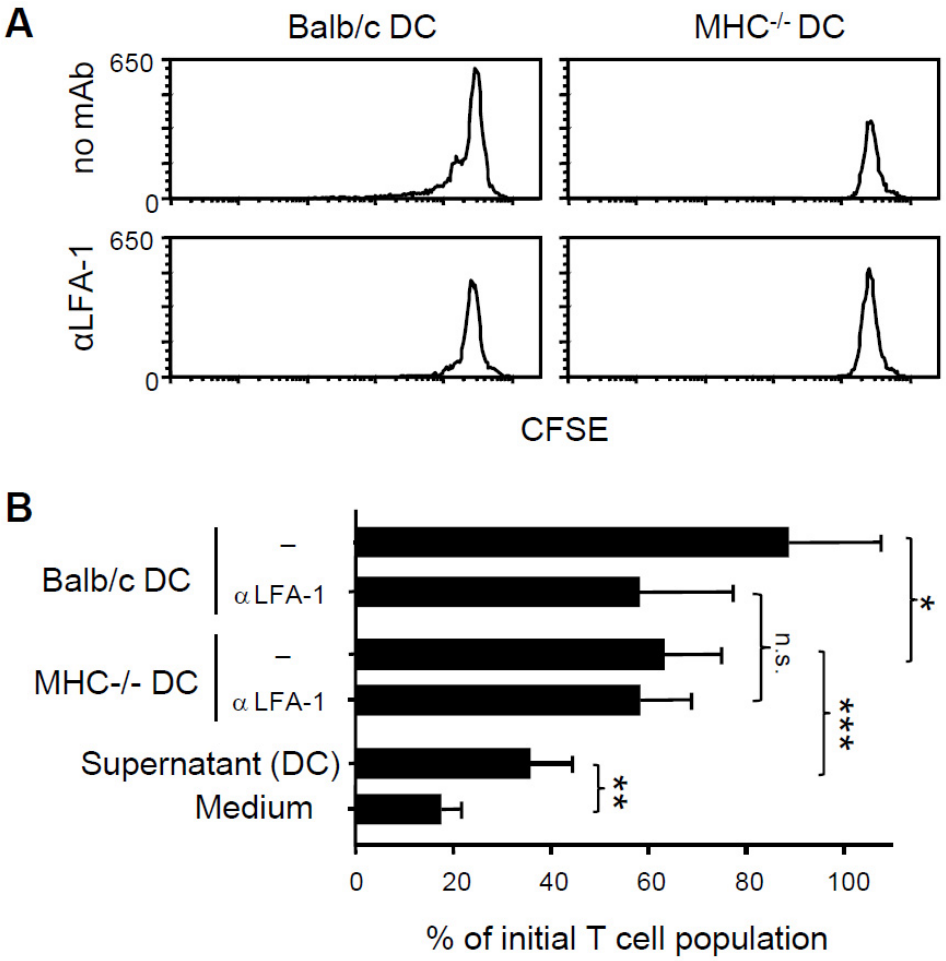

Figure 17: Mechanisms of homeostatic T cell proliferation and survival. DO11.10 T cells after 4 days of co-culture with MHCII$^{-/-}$ or wild-type DC in the presence or absence of function-blocking anti-LFA-1 mAb M17/4 compared with T cells cultured in the absence of DC with or without DC-conditioned supernatant. (A) CFSE profiles of gated transgenic TCR-positive cells stained by mAb KJ1.26. Graphs are representative for 3 independent experiments. (B) Change of T cell counts after 4 days of culture relative to day 0. Absolute numbers were obtained for gated KJ1.26-positive cells using counting beads as internal reference. Data show the means and SD for 3 independent experiments. *, $p = 0.02$; **, $p < 0.01$; ***, $p < 0.0001$. Legend and figure adapted from Storim et al., 2010.

In order to verify the contribution of physical T cell/DC engagement to homeostatic T cell survival, T cells were cultured in DC-conditioned media (harboring DC-derived soluble factors) but in the absence of DC, which resulted in increased survival compared to

unconditioned medium (Fig. 17B). However, the presence of DC in the collagen matrix (with or without intact TCR- and/or LFA-1 signaling) led to a significant increase of T cell survival compared with DC-free conditions (Fig. 17B). In conclusion, low affinity TCR-signaling and/or engagement of LFA-1 in the mid-zone of dynamic homeostatic contacts are sufficient to trigger homeostatic T cell proliferation, while other contact-dependent mechanisms and DC-derived soluble factors together support T cell survival.

4.3 Antigen specific contacts

In contrast to homeostatic contacts, the dynamics of TCR-specific, activating interactions between APC and T cells are more heterogeneous in duration, kinetics and composition (Fig. 18; Friedl and Storim, 2004). *In vivo*, both short-lived and long-lasting interactions co-exist, dependent on the phase of activation, the strength of the antigenic peptide, and the type of APC (Azar et al., 2010; Henrickson et al., 2008; Mempel et al., 2006; Miller et al., 2004b). *In vitro* both, “classical” concentric immunological synapses and multifocal contact structures support T cell activation (Friedl et al., 2005). However, how molecular contact structure and dynamics impact the resulting T cell activation strength and ensuing effector function remains elusive. Collagen matrices were reported to support predominantly short-lived T cell/APC contacts leading to full T cell activation (Gunzer et al., 2000; Gunzer et al., 2004). However, here an unselected T cell population that was not sorted for migration activity was analyzed. To exclude non-migrating T cells that potentially may undergo passive aggregation with DC, the 3D collagen invasion model was used to monitor the dynamics of antigen-specific interactions between T cells and DC under pro-migratory conditions.

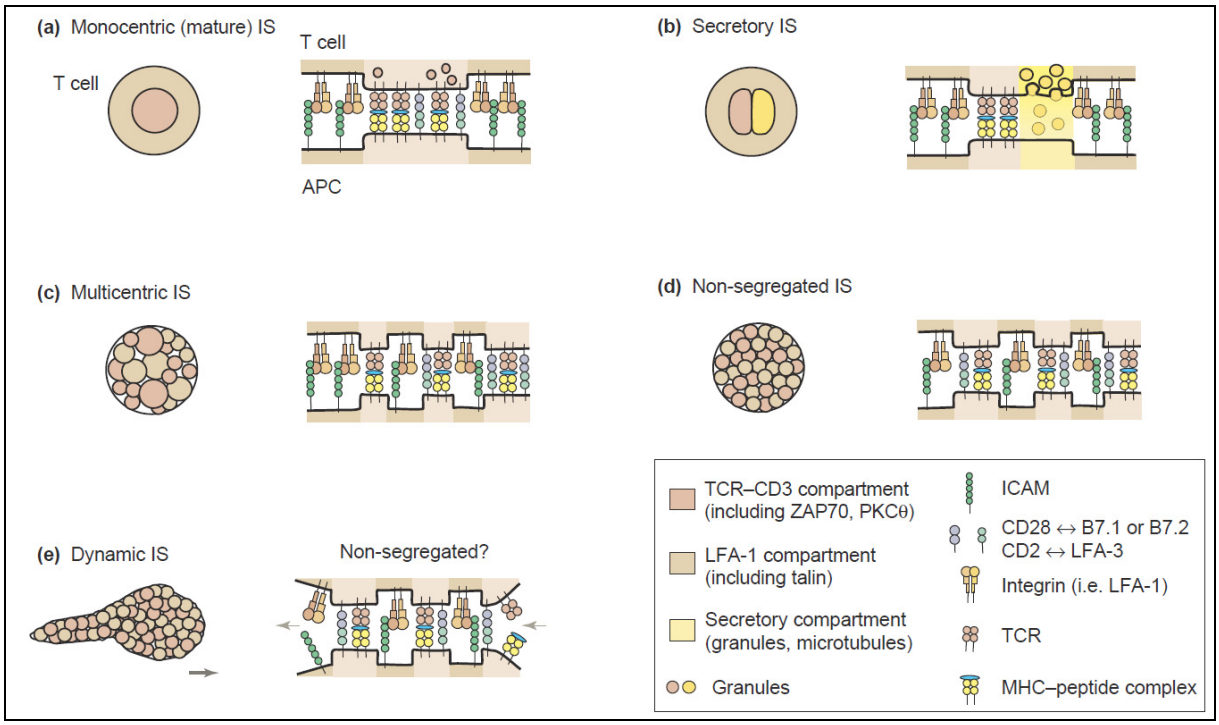

Figure 18: Diversity of morphology and molecular organization of the immunological synapse. (a) Monocentric mature IS; (b) secretory IS; (c) multicentric IS; (d) non-segregated IS; and (e) dynamic IS. Transition forms probably exist for all of these states. In (a)–(e), the left-hand image shows the view from above, whereas the right-hand image shows the view from the side. Legend and figure reproduced from Friedl and Storim, 2004.

4.3.1 Contact dynamics and MHC II redistribution

As for homeostatic contacts, the dynamics of antigen-specific T cell/DC interactions were analyzed in high resolution using confocal life imaging. To monitor T cell dynamics relative to antigen-specific MCH II engagement, recently activated 5C.C7 T cells recognizing $pMCC_{88\text{-}103}$ (Seder et al., 1992) were confronted with mature DC from B10.A mice infected with a Moloney Murine Leukemia Virus encoding for an EGFP-tagged MHC II molecule that was covalently linked to their cognate antigen (pMCC-MHC-GFP). Antigen-independent, homeostatic contacts with DC expressing an MHC class II complex linked to a non-activating $pMCC_{88\text{-}103}$ variant ($MCC^{D93E,K99T,T102A}$; null-MHC-GFP) served as control.

Similar to the DO11.10 model (compare section 4.2), the majority of homeostatic contacts were dynamic and MHC II accumulation in the contact plane was not detectable (data not shown). Conversely, recognition of pMCC-MHC-GFP by 5C.C7 T cells led to MHC II cluster formation in 73% of the contacts (Fig. 19 A). MHC II clusters were detectable only 2 min after contact acquisition (Fig. 19 B, Video 6) and persisted throughout the observed time span along the interphase between T cell and DC, but not in DC regions outside the interaction plane.

Contact dynamics were classified as i) “stable” when T cell movement relative to the DC was low to undetectable; as ii) “dynamic” when the T cell migrated across the DC surface, similar to homeostatic interactions; and as iii) “not classified” when vigorous DC movement prevented the classification of T cell dynamics. Unexpectedly, the motility of the majority of 5C.C7 T cells within antigen specific contacts was classified as stable while only a minority of the T cells was clearly moving on the DC surface (Fig. 19 C). In line with low contact dynamics, contact duration was considerably longer than reported for the collagen matrix model (Gunzer et al., 2000; Gunzer et al., 2004; Rothoeft et al., 2006) and no contact termination was observed in any imaging session (duration range 10 to 30 min). Thus, for recently activated 5C.C7 T cells interacting with DC in 3D collagen the recognition of cognate pMCC antigen predominantly leads to long lasting and stable interactions that support the accumulation and focalization of peptide-MHC II complexes along the junction.

The TCR / peptide-MHC affinity of the 5C.C7 model is low compared to the DO11.10 model (Purtic et al., 2005) and the antigenic potency of peptide-MHC complexes is positively correlated with the deceleration of T cells *in vivo* (Skokos et al., 2007). Therefore, binding kinetics and contact structure might also differ between T cell activation models.

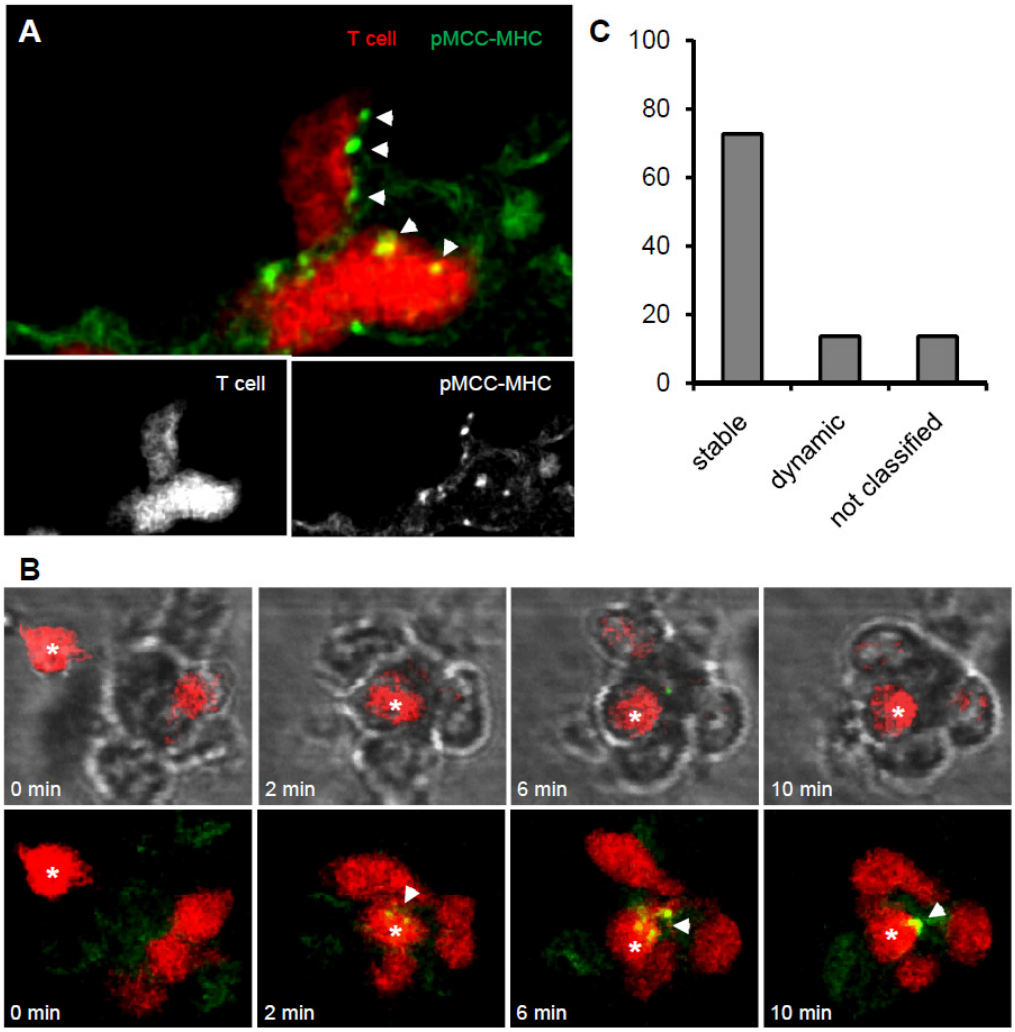

Figure 19: Contact dynamics and MHC class II accumulation during antigen specific contacts. 5C.C7 T cells were stained with SNRAF (red) and co-cultured with mature B10A DC expressing pMCC-MHC-GFP (green). (A) Z-reconstruction from a confocal time lapse series. Arrowheads indicate pMCC-MHC-GFP clusters in the contact plane. Bar, 5 µm. (B) Time-resolved reconstruction of confocal z-stacks illustrating the contact acquisition of a T cell (*) to a small T cell / DC cluster and the accumulation of pMCC-MHC-GFP in the contact plane (arrowheads; compare Video 6). Bar, 5 µm. (C) Classification of the interaction dynamics of 22 T cells from 3 independent experiments.

In order to further characterize contact characteristics during activating T cell/DC interactions, the high-affinity DO11.10 model and the quantitative analysis tools used to analyze homeostatic contacts were adapted in a series of preliminary experiments.

4.3.2 T cells polarize towards the DC and form a symmetrical contact plane

CTx b was used to stain ER/golgi in antigen-specific contacts. In line with the fast occurrence of MHC II clusters, CTx b relocated from the uropod of DO11.10 CD4+ cells towards the center of the interaction plane within a few minutes after contact acquisition with Balb/c DC pulsed with $pOVA_{323-393}$ (Fig. 20A, Video 7). Concomitantly, the uropod of the T cell disappeared followed by transition towards a round, non-migratory phenotype (Fig. 20A, Video 7). Consequently, in fixed samples, rounded T cells were polarized towards the pOVA-loaded DC, formed a flat contact plane rich in F-actin and pY, and lacked a distinct uropod (Fig. 20B). The distribution of tyrosine phosphorylation revealed a strong signal along the contact plane peaking in the centre without obvious signs of a front-rear asymmetry (Fig. 20C, D). Thus, CTx b staining and ratiometric analysis allowed the characterization of symmetric, activating interactions. Contact dynamics in the pOVA model were as low as in the pMCC model. The stable contact plane between T cells and DC in 3D collagen is strongly reminiscent of contact structures known from liquid culture models (Brossard et al., 2005; Fisher et al., 2008; Tseng et al., 2008).

4.3.3 T cells accumulate at the uropod of dendritic cells during specific interactions

When co-cultured for 3 hours, stable contacts of DO11.10 T cells to pOVA-pulsed DC formed and underwent secondary relocation. After contact initiation at the DC leading edge, bound T cells slowly changed position on the DC surface and finally accumulated in a microcluster at the DC's trailing edge while the anterior portion of the DC was free of T cells (Fig. 21A; Video 8).

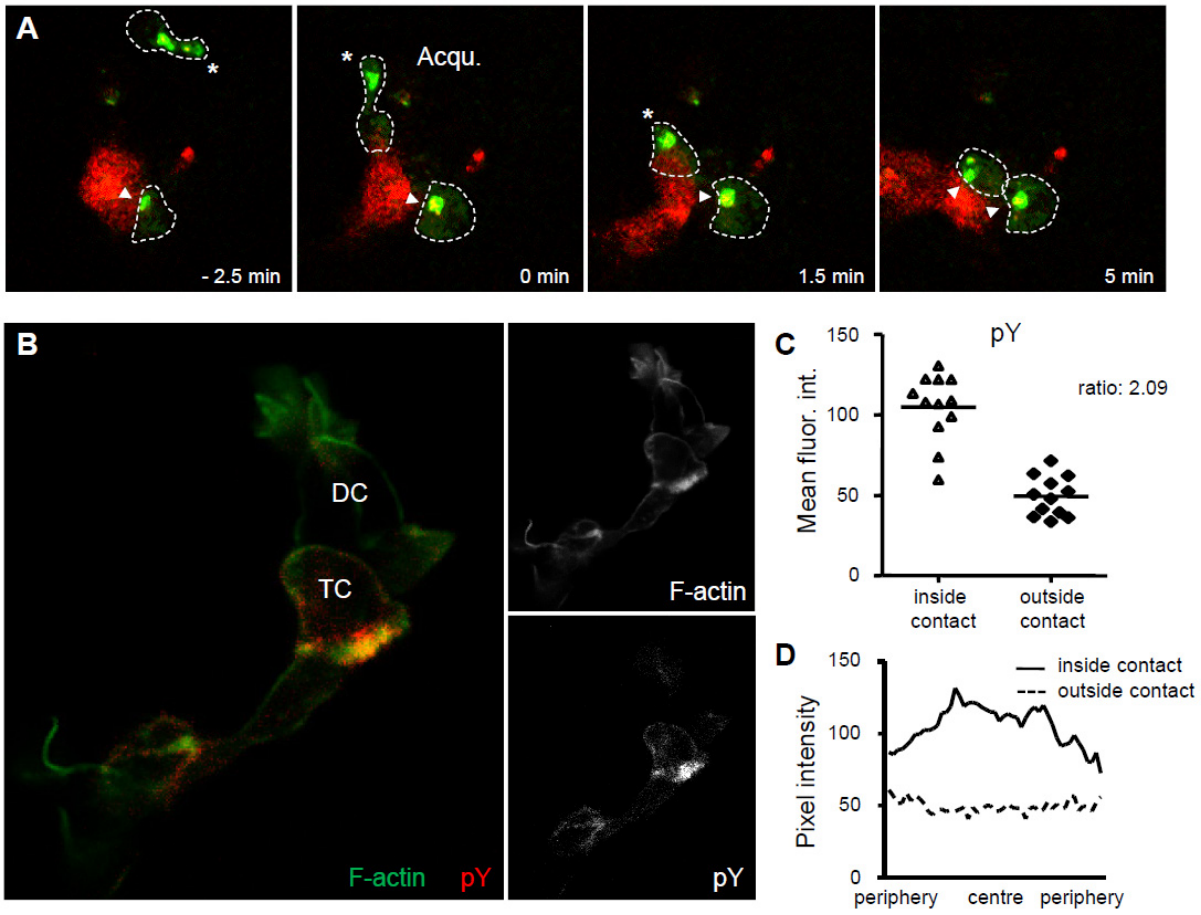

Figure 20: T cell polarity and contact plane assembly during antigen specific T cell / DC contacts in 3D collagen. (A) DO11.10 T cells were stained with CTx b (green) and co-cultured with pOVA pulsed Balb/c DC (CMTMR, red). Z-reconstructions from a confocal time-lapse series (compare Video 7) illustrate contact acquisition, disassembly of the uropod (*) and redistribution of ER/golgi to the contact plane (arrowhead). Additionally, another T cell bound to the DC is depicted with ER/golgi constantly in the center of the contact plane (arrowhead). (B) A T cell in contact with a pOVA pulsed DC was fixed and stained for pY (Cy3, red) and F-actin (Phalloidin-Alexa 488, green). (C, D) Analysis of pY accumulation in the contact plane (12 T cells, one experiment). Bar, 5 µm.

These binding kinetics suggested that the DC provide two compartments with distinct binding properties: an anterior compartment, driving locomotion and initiating contact with T cells, and a posterior compartment (i.e. the DC uropod), sustaining antigen dependent contacts.

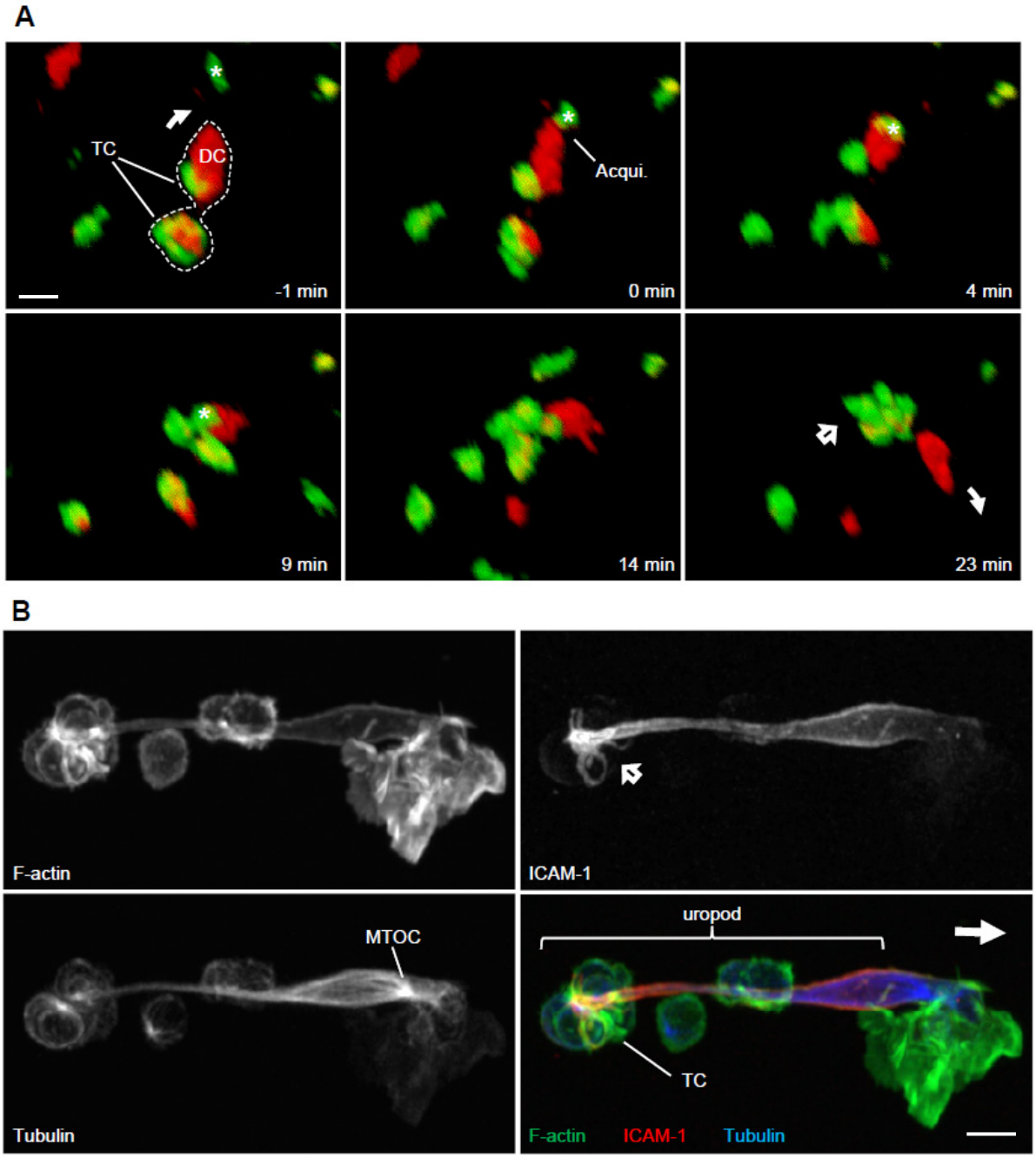

Figure 21: T cells form microclusters at the uropod of antigen-pulsed DC. (A) Z-reconstruction of a confocal time-lapse series of T cells (CFSE, green) co-cultured with pOVA pulsed DC (CMTMR, red). (*) T cell that contacts the DC at the DC leading edge and then slowly proceeds to the DC uropod to join a microcluster of already bound T cells (open arrow). Arrow: direction of DC migration. Bar, 10 µm. Compare Video 8. (B) T cells in contact with pOVA-pulsed DC were fixed and stained for F-actin (Phalloidin-Alexa488, green), ICAM-1 (Cy3, red) and microtubules (Alexa 647, blue). Bar, 5 µm.

In fixed T cell/DC conjugates the leading edge of the DC consisted of several veils and dendrites rich in F-actin but free of T cells, whereas the DC uropod was rich in ICAM-1 and bound several round, non-migratory T cells forming a small cluster (Fig. 21B). Tubulin filaments orienting from the MTOC in mid-cell position were predominantly oriented towards the DC uropod, near to the T cell cluster (Fig. 21B). Thus, the uropod of moving DC shows high levels of ICAM-1 and supports prolonged interactions to T cells in an antigen-dependent manner, whereas the leading edge appears prone to T cell mobility and/or drift. Whether binding to a specialized compartment of the DC is functionally relevant for T cell activation and/or effector function needs to be addressed in future studies.

5 Discussion

Using live-cell microscopy together with high-resolution 3D reconstruction of fixed T cell/DC conjugates in 3D collagen lattices, we here show how T cells interact with DC in both homeostatic and activating conditions. While continuously migrating T cells integrate proliferation and survival signals during homeostatic cell-cell contacts, T cells accumulate at a distinct, newly described zone at the DC uropod to receive sustained TCR signaling during T cell activation. Thus, the 3D collagen lattice model reveals aspects of T cell/DC immunology that are masked in conventional 2D liquid culture models due to the lack of pro-migratory stimuli and a matrix that supports the physiological spreading of DC. Additionally, the superior imaging characteristics of low density 3D collagen compared with *in vivo* imaging allows immunofluorescence studies on a sub-cellular level. Therefore, the 3D collagen matrix model complements *in vitro* and *in vivo* studies.

5.1 Homeostatic contacts

5.1.1 Homeostatic interactions: a model for a dynamic immunological synapse

Under homeostatic conditions, contacts with DC presenting low-affinity, self-peptide MHC complexes on their surfaces do not lead to a “stop signal” but to continued T cell migration on the DC surface. The T cell aligns side-to-side with the DC and maintains its polarized amoeboid morphology, cytoskeletal organization and surface receptor topography (Fig. 22A, B). Simultaneously, the T cell polarizes towards the DC resulting in redistribution of the actin cytoskeleton and adhesion receptors (Fig. 22C). The concomitance of migratory and DC-induced polarization in orthogonal direction results in the generation of an asymmetric contact

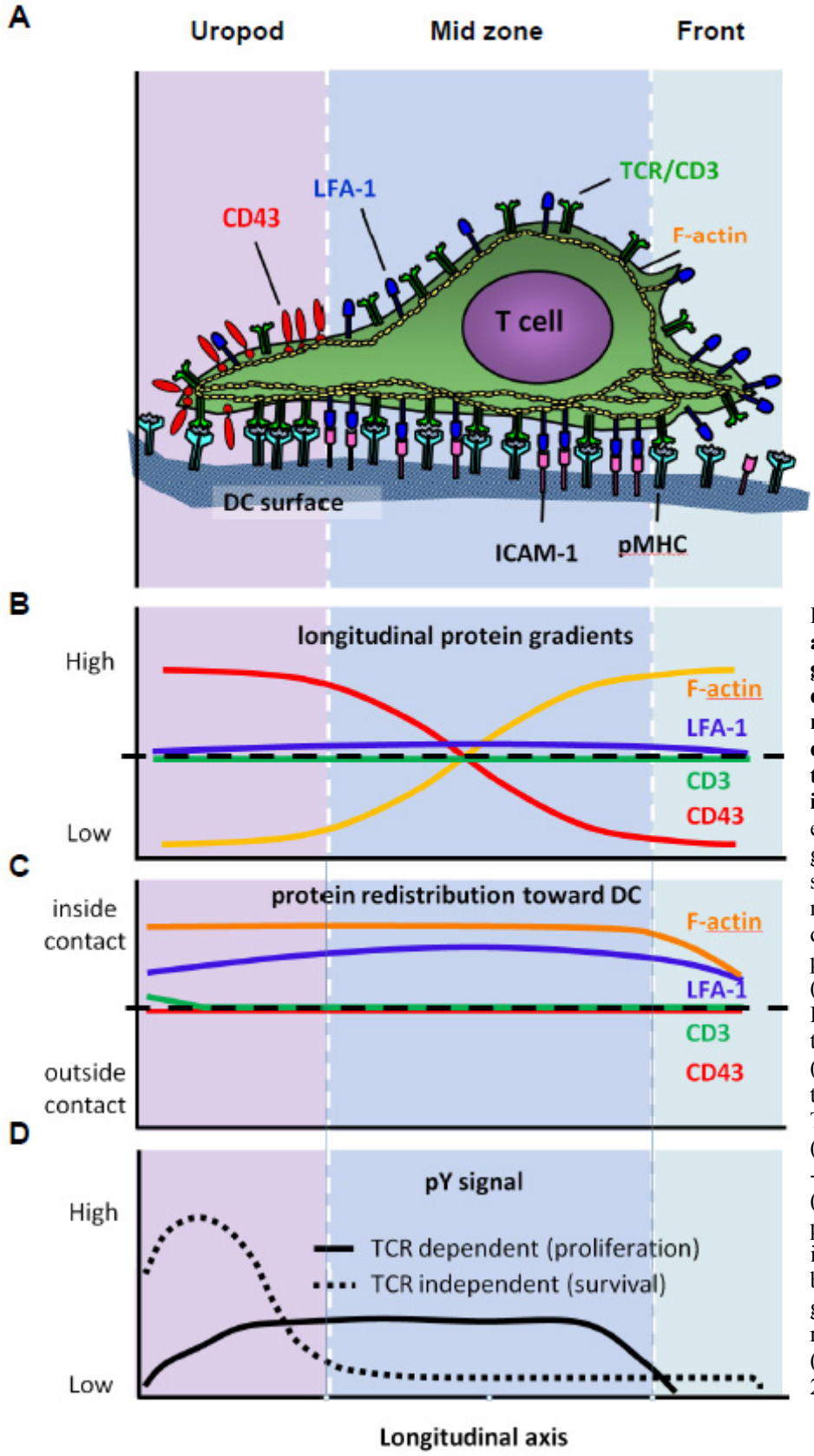

Figure 22: Zones and molecular gradients in the dynamic immunological synapse during homeostatic T cell / DC interactions. Amoeboid T cell migrating across a DC surface (A) with maintained longitudinal ("amoeboid") protein gradients (B) and LFA-1 and F-actin redistribution toward the DC (C) within the contact plane. (D) TCR-dependent (straight line) and -independent (dashed line) phosphotyrosine signaling along the mobile junction. Legend and figure reproduced from (Storim et al., 2010).

plane which promotes TCR/MHC class II-dependent and –independent signaling (Fig. 22B, C). As TCR-dependent proliferation is associated with signaling in the mid-zone and contact-dependent but TCR-independent survival might be mediated within the T cell uropod, distinct signaling zones can be distinguished (Fig. 22D). This migratory contact plane that mediates cell-to-cell signal transduction and homeostatic T cell functions thus fulfills the criteria of a dynamic immunological synapse (Friedl and Brocker, 2002; Friedl and Storim, 2004), also named “kinapse” (Dustin, 2008).

5.1.2 DC-induced T cell polarization

Homeostatic contacts prompt a strong, TCR-signaling-independent polarization of the T cell towards the contact plane. For the duration of the interaction, the DC surface becomes the leading guidance structure for the migrating T cell turning a fiber-guided migration in 3D collagen (Wolf et al., 2003) into a 2D-like migration along a cell-surface with a 3D component as the extracellular matrix (ECM) is still in contact with most parts of the T cell. In contrast to amoeboid migration in a 3D environment (Friedl et al., 1998; Lämmermann et al., 2008) and in line with accumulation of LFA-1 within in the contact plane, leukocyte migration on a 2D surface is adhesion-receptor dependent (Lämmermann and Sixt, 2009). Indeed, LFA-1 function was shown to be mandatory for T cell migration on endothelial cells in the lumen of blood vessels under shear stress (Ley et al., 2007; Shulman et al., 2009). However, in the homeostatic T cell/DC interaction model antibody-mediated blockade of LFA-1/ICAM-1 binding did not affect contact-dependent T cell survival (Fig. 17B) and $ICAM^{-/-}$ DC support short and dynamic activating interactions to $CD8^{+}$ T cells *in vivo* (Scholer et al., 2008). Thus, LFA-1 function is dispensable for the establishment of short, migratory T cell/DC contacts, possibly because the lack of LFA-1 is compensated by other

adhesion receptors like α_4 integrins that also might mediate DC-induced polarization (Kinashi, 2005). Alternatively, ligation of the DC and/or T cell gylcocalyx by lectin-type receptors might be sufficient to induce T cell polarization and migration on the DC surface in the absence of shear forces (Erbacher et al., 2009). Or the concomitant availability of a 3D collagen network provides the environmental 3D conditions for adhesion receptor independent migration on the DC surface (Lämmermann and Sixt, 2009) and DC-induced polarization is an independent event with no major influence on T cell migration. Future experiments that address the minimum requirements for DC-induced T cell polarization will need to clarify these open questions.

5.1.3 The dual role of the actin cytoskeleton

DC-induced T cell polarization during dynamic homeostatic interactions leads to strong accumulation of F-actin in the contact plane, similar to non-cognate contacts in liquid culture (Revy et al., 2001) and activating, high-affinity T cell/APC contacts (Valitutti et al., 1995). The dependence of homeostatic signaling on actin function has not formally been demonstrated. However, abolishment of high-affinity TCR signaling upon F-actin disruption (Campi et al., 2005; Valitutti et al., 1995; Varma et al., 2006) and the usage of a similar signal transduction machinery in activating and homeostatic signaling (Sprent and Surh, 2011) suggest a role for F-actin in homeostatic signaling. Moreover, sustained T cells migration across the DC surface, implies a dual role of the actin cytoskeleton and a unique molecular architecture of the contact plane compared to symmetrical, stable contact forms:

- F-actin not only promotes signal transduction but also drives migration.
- Therefore receptor traffic, most likely from the front to the back of the contact plane, is driven by the actin cytoskeleton.

- In contrast to the diffusely patched concentric and symmetrical “pre-synapse” seen in liquid cultures (Revy et al., 2001), leading edge, cell body and uropod together form an asymmetrical contact structure.
- Thus, actin dynamics drive receptor transitions through different cellular compartments that most likely offer distinct preconditions for signaling (Friedl and Weigelin, 2008).

Thus, a unique actin-dependent molecular architecture of the contact plane forms, which is morphologically and functionally distinct from the symmetrical, stable contact types.

5.1.4 The leading edge

The actin-rich leading edge with its protruding lamellipods represent the T cell’s sensor for its environment (Negulescu et al., 1996) and therefore is the default location for initial receptor-ligand engagement during migratory T cell/DC contacts (Friedl and Brocker, 2002). Signaling in the front part of the contact plane is detectable by a moderately strong phosphotyrosine signal. However, despite its particular sensitivity for TCR triggering in a 2D model (Negulescu et al., 1996), TCR signaling does not statistically significantly contribute to tyrosine phosphorylation in the leading edge. This may be due to masking of low-affinity TCR-signaling through TCR-independent events, e.g. the regulation of actin polymerization (Insall and Machesky, 2009). In particular, WASP-family proteins and HS-1 (hematopoietic lineage cell-specific protein 1), an actin stabilizing adaptor which is found in the leading edge of leukocytes, need to become tyrosine-phosphorylated to become fully active (Caron, 2003; Dehring et al., 2011; Huang et al., 2008). Alternatively, the lack of TCR-dependent tyrosine

phosphorylation may result from rapid retrograde exit of newly formed TCR/self-MHC class II-pairs during migratory interactions.

5.1.5 The mid-zone

In the mid-zone of moving leukocytes RhoA counteracts highly dynamic membrane protrusions and facilitates the formation of parallel F-actin-myosin fibers (Li et al., 2005; Xu et al., 2003) resulting in a less dynamic signaling region. TCR/MHC class II pairs entering this region from the leading edge are productively signaling as suggested by high levels of TCR-dependent tyrosine phosphorylation and its association with homeostatic proliferation. TCR signaling is not accompanied by large-scale TCR accumulation in any zone of the dynamic homeostatic contact (as demonstrated by CD3 and pY co-staining) consistent with high receptor dynamics (Lee et al., 2002) which are most likely due to fast retrograde transport of signaling TCR/MHC class II pairs through the mid-zone. This transport may be achieved via TCR binding to the DC surface, cross-talk with LFA-1 function and/or actin-myosin contraction:

- Stabilized by LFA-1 (which binds to ICAM-1 and is enriched in the mid zone of dynamic contacts, Fig. 11A and 12), the TCR is “fixed” to (self-)peptide-MHC complexes on the DC surface.

- Together with LFA-1, which is linked to F-actin, the TCR moves backwards upon contraction of actin-myosin fibers while the cell pushes forward (Jacobelli et al., 2004; Kinashi, 2005).

- This would imply, that the TCR/CD3 complex and LFA-1 form small functional units (or “microclusters”) as reported for activating T cell/APC contacts (Varma et al., 2006).

In line with the formation of microclusters and the requirement of LFA-1 for cognate TCR signaling under conditions of limited antigen affinity or availability (Bachmann et al., 1997; Suzuki et al., 2007; Wulfing et al., 1998), productive TCR signaling in the mid-zone is connected to LFA-1 function as homeostatic proliferation is abrogated by a function-blocking anti-LFA-1 antibody.

The affinity of LFA-1 for ICAM-1 ligation in homeostatic contacts is not known. Recognition of cognate antigen but not of low-affinity self-peptides leads to high-affinity ICAM-1 ligation (Dustin et al., 1997; Kinashi, 2005), and lymphopenia induced proliferation appears to be independent of LFA-1 function (Surh and Sprent, 2008). However, independent of TCR signaling, chemokines like CCL21 - which is bound to the surface of DC - are also able to induce the high-affinity conformation of LFA-1 (Feigelson et al., 2011; Friedman et al., 2006). In another model of TCR-independent LFA-1 engagement, migration on an ICAM-coated surface promotes formation of an area with high-affinity LFA-1, the so called focal zone, which forms without terminating T cell migration (Smith et al., 2005). Interestingly, the focal zone is a polar adhesion and signaling zone located in the middle of a moving T cell and therefore correlates to the mid-zone of dynamic homeostatic contacts (Smith et al., 2005). The mid-zone may thus represent a platform where subsets of high affinity LFA-1 molecules stabilize microclusters of low-affinity TCR/MHC complexes and therefore promote TCR-dependent homeostatic proliferation.

5.1.6 The uropod

While the posterior uropod of freely-moving T cells is not known to be critical for cell signaling, the posterior region of the dynamic homeostatic synapse has at least two functions. First, the contribution of TCR/MHC to tyrosine phosphorylation in the uropod is statistically not significant, consistent with a role of the uropod in blunting the TCR signal. Like receptor entry into the leading edge, signal termination in the uropod is suggested by the architecture of the dynamic contact plane and may result from a variety of mechanisms that might synergize:

- As in the center of activating T cell/APC contacts (Varma et al., 2006), surface receptors may be removed from the plasma membrane of the uropod via endocytosis (Samaniego et al., 2007).
- CD43, an established negative regulator of TCR signaling, is strongly accumulated in the uropod and might abrogate TCR signaling (Tong et al., 2004).
- As in T cells migrating on ICAM-1 (Smith et al., 2005), LFA-1 located in the uropod of the dynamic contact may be in low-affinity conformation and therefore destabilize TCR/MHC interaction.
- When ligand binding is weak, receptors may just exit to non-engaged parts of the T cell membrane.

Second, besides terminating TCR signaling, the uropod of the dynamic homeostatic synapse actively participates in T cell signaling as the phosphotyrosine signal peaks in the rear part of the contact plane (Fig. 14). However, signal transduction pathways and functional outcomes connected to this massive tyrosine phosphorylation are unknown. First, the regulation of cell adhesion and actin-myosin contraction may account for a part of the uropod-localized pY. In

line with this hypothesis, β_1 integrins and the cytoskeletal linkers ezrin/radixin/moesin (ERM proteins), show peak location in the uropod of T cells migrating across surfaces or within 3D environments (del Pozo et al., 1997; Friedl et al., 1998). Then, similar to T cell activation (Burack et al., 2002; Tomassian et al., 2011; Viola et al., 1999) signaling within cholesterol rich membrane domains ("lipid rafts") may contribute to tyrosine phosphorylation within the uropod (Gomez-Mouton et al., 2001). And finally, the contact dependence of T cell survival seen in our system and liquid culture models (Feuillet et al., 2005) might be associated with signaling events within the uropod. Cytokines and/or chemokines presented on the DC surface might trigger signaling in the T cell uropod involved in T cell survival (Guimond et al., 2009; Kaiser et al., 2005). The rear zone of the homeostatic synapse which is formed by the T cell uropod is thus a signaling zone that is involved in TCR signal termination and may contribute to diverse T cell functions including adhesion, migration and survival.

5.1.7 Comparison of the dynamic homeostatic synapse with the activating immunological synapse

The trafficking of TCR/MHC class II pairs from the T cell front to the rear and their preferential signaling in the mid-zone are reminiscent of cognate TCR/MHC dynamics and signaling in the mature IS. Here TCR/MHC pairs form in the periphery, move inward (while generating pY signaling), and enter the IS center where TCR signaling is terminated (Campi et al., 2005; Varma et al., 2006; Yokosuka et al., 2005). Moreover, in a lipid bilayer model, short-lived conversions of the IS periphery and center into a polar leading lamella and a posterior region, respectively, where termed "kinapse" and recapitulate the longitudinal segregation of the dynamic homeostatic synapse to a certain extent (Sims et al., 2007) (Dustin, 2008). However, the amoeboid phenotype of this kinapse is incomplete, i.e., it lacks a

bona fide uropod. Therefore, neither the signal termination mechanisms discussed above nor a signaling zone for TCR-independent events are described by this model. Thus, the dynamic homeostatic synapse is the most comprehensive model to explain simultaneous migration and cell-to-cell communication.

5.1.8 The role of the dynamic homeostatic synapse in T cell immunology and other types of cell-cell communication

In secondary lymphoid tissues, migrating T cells are in continuous contact with dendritic cells and fibroblastic reticular cells (Bajenoff et al., 2006; Lindquist et al., 2004). Under homeostatic conditions, these cells deliver self-peptide-MHC complexes, survival-mediating surface receptors and surface-bound cytokines (Friedman et al., 2006; Guimond et al., 2009; Link et al., 2007). The here described dynamic signaling platform of recently activated $CD4^+$ T cells is suited to integrate all these signals and therefore mediate T cell homeostasis. Due to technical limitations of the 3D collagen model, in particular the poor spontaneous or chemokine-induced migration of naïve $CD4^+$ T cells under non-stimulating conditions, this work could not include the analysis of naïve T cells. However, *in vivo* imaging setups suggest that naïve T cells form similar dynamic contacts while moving across and sampling DC in lymph nodes (Miller et al., 2004a).

Furthermore, a dynamic signaling platform, like the dynamic homeostatic synapse, may also contribute to signaling mechanisms during T cell interaction with stronger, cognate antigen. In fact, migratory interactions during antigen-specific T cell interactions with APC and target cells were shown in diverse experimental setups: the serial sampling of DC during early and late phases of T cell activation (Azar et al., 2010; Henrickson et al., 2008; Mempel et al.,

2004; Miller et al., 2004b) as well as during anergy induction (Hugues et al., 2004; Skokos et al., 2007); the dynamics of thymocyte/stromal cell interactions during T cell development (Bousso et al., 2002), Fas/FasL-dependent-killing of target cells by cytotoxic T cells (O'Keefe and Gajewski, 2005); and T cell activation on lipid bilayers (Sims et al., 2007). Ultimately, this dynamic signaling platform is capable of integrating a diverse array of signals in one contact plane consisting of distinct contact zones during amoeboid T cell scanning. It might therefore represent a universal starting point for all types of migratory and adhesive T cell contacts during trafficking, activation and effector function.

5.2 Antigen specific contacts

Compared with homeostatic contacts, the kinetics of activating, antigen-dependent contacts between T cells and DC are more heterogeneous, ranging from dynamic to fully adhesive, whereby the contribution of dynamic phases to T cell activation remains largely elusive. Using high-resolution confocal imaging in a pro-migratory environment, interaction dynamics between recently activated T cells and antigen-laden DC were studied in a 3D collagen invasion model. In contrast to the largely dynamic interaction kinetics of naïve T cells (Gunzer et al., 2000; Gunzer et al., 2004), the contacts were mainly long-lasting and stable, leading to focalized MHC class II enrichment in the contact plane. Moreover, T cells accumulated in a distinctive region of the DC, the adhesive DC uropod, which is rich in ICAM-1. Thus, for recently activated T cells DC provide a “sticky” uropod enabling sustained T cell binding and TCR triggering, promoting improved re-stimulation, differentiation and effector function.

5.2.1 Contact kinetics and IS organization between recently activated T cells and DC

Despite its pro-migratory properties enabling T cell transition from one DC to another, the 3D collagen invasion model together with recently activated T cells and antigen-laden DC favored “stable” and mono-cellular rather than “dynamic” and serial activating contacts between T cells and DC. Although T cells clearly change positions on the DC surface and produce occasional lamellipodial protrusions (Fig. 18A), this T cell movement is slow compared to T cells migrating across DC during homeostatic interactions, and it lacks the hallmarks of amoeboid movement, including a leading lamellipod and a posterior uropod. Thus, passive T cell transport via DC associated mechanisms involving the DC cytoskeleton rather than active T cell migration is likely to lead to T cell accumulation at the DC uropod. These transport mechanisms might contribute to T cell activation as interference with the DC cytoskeleton leads to hampered T cell activation (Al-Alwan et al., 2003) (Kobayashi et al., 2001).

Due to technical limitations in this study which focused on short-term confocal imaging, complete contact duration from contact acquisition until detachment could not be addressed directly. A typical imaging session covered up to 30 min, and no contact termination was observed in any session, suggesting that contact duration largely exceeded the time span reported for naïve T cells with a median in the 10 to 20 min range (Gunzer et al., 2000; Gunzer et al., 2004). This difference may be partly explained by the activation state of the T cells. In contrast to naïve T cells, pre-activated T cells express higher amounts of adhesion-receptors and/or pre-clustered integrins on the cell surface which may lead to increased avidity and in turn prolonged interactions with DC (Friedl and Gunzer, 2001; Springer et al., 1987). In line with receptor avidity regulation, the interaction time between T cells and DC in

3D collagen lattices increases, when T cells were previously activated (Rothoeft et al., 2006). In accordance with increased contact stability in the 3D collagen model, activated T cells engaged in different models of antigen presentation consistently display contact durations exceeding 30 min at high stability (Freiberg et al., 2002; Monks et al., 1998).

Another reason for the discrepancy between contact duration and dynamics reported here compared to earlier studies may result from differing imaging techniques. Earlier studies used bright-field time-lapse microscopy to asses T cell/DC interaction kinetics lacking z-resolution, whereas the here-used time-lapse confocal microscopy allows exact denomination of cellular interactions and contact planes. Thus, using low-resolution bright-field imaging, T cells migrating above or below DC might be misinterpreted as T cells contacting DC and thereby impose a bias towards shorter contact duration and more vigorous contact dynamics during visual analysis.

Using paraformaldehyde fixation together with the collagen invasion model allows end-point analyses of protein localization in moving cells but precludes the analysis of receptor or signaling dynamics within T cell/DC interactions. Therefore, the time resolved analysis of receptor redistribution during cell-cell contacts like in more artificial liquid culture models (Freiberg et al., 2002; Grakoui et al., 1999; Monks et al., 1998) was impossible using primary T cells and DC that did not express fluorescent receptor proteins. Although preliminary, our results, however, are in line with an IS between T cells and DC that is stable over minutes and possibly hours but lacks large-scale segregation as reported before (Brossard et al., 2005; Tseng et al., 2008).

In conclusion, future studies on interaction dynamics, contact duration and IS organization should be addressed with techniques that allow both, high (x, y and z) resolution for sufficient cell/receptor tracking and prolonged live-cell imaging.

5.2.2 The DC uropod predisposes for T cell clustering

This study suggests the existence of two functionally distinct compartments in migrating DC, an anterior more dynamic region that preferentially initiates contacts to T cells and a posterior zone with increased adhesiveness towards T cells for sustained cell-cell contacts. Contact initiation at the DC leading edge is consistent with the known preference of DC veils and dendrites to engage with T cells (Benvenuti et al., 2004; Fisher et al., 2008), and dendrite formation is pronounced in the DC leading edge (Lämmermann et al., 2009). Furthermore, T cell binding preferentially occurs in membrane compartments on the DC surface that lack veils but consist of clustered microvilli (Fisher et al., 2008). However, the DC uropod so far has not been linked to T cell binding and/or T cell activation.

Two previously published observations suggest that the DC uropod might be the region for sustained T cell binding and effective T cell activation. First, uropod formation is associated with DC maturation (Mattioli et al., 2008; Mattioli et al., 2005; Quaranta et al., 2003) as DC convert from a sessile into a migratory phenotype (Alvarez et al., 2008). Second, the uropod is an adhesive structure rich in ICAM-1 (Fig. 18B) and integrins (Madruga et al., 1999). It is thus likely that the accumulation of T cells at the DC uropod is dependent on these or similar adhesion receptors.

Besides providing locally accumulated adhesion receptors, the function of the DC uropod in T cell activation remains unknown. Region-confined T cell binding to and receptor

engagement within the DC uropod might facilitate the delivery of new peptide-MHC complexes and adhesion molecules to multiple bound T cells from intracellular stocks (Boes et al., 2002; Jo et al., 2010). Consistent with a secretory uropod function, the DC microtubules are oriented towards and extent into the uropod and might provide a scaffold for vesicle trafficking (Fig. 19B).

The biological function and relevance of local T cell adhesion to DC may include activating/modulating cross-talk between T cell subsets. During a pathogen-specific immune response, a microcluster of T cells at the DC uropod might not only consist of $CD4^+$ helper T cells but also comprise $CD8^+$ cytotoxic T cells and $CD4^+CD25^+$ regulatory T cells, sharing specificity for a particular pathogen. Thereby, in one DC uropod-localized microcluster, regulatory T cells could limit the activation of neighboring $CD4^+$ and/or $CD8^+$ cells via paracrine secretion of cytokines, e. g. IL-10 and TGF-β, and the lysis of T cells in an antigen-dependent manner (Vignali et al., 2008). In line with this hypothesis, it was shown, that regulatory T cell function requires direct cell-cell interaction or at least the immediate vicinity of the target T cell (Takahashi et al., 1998; Thornton and Shevach, 1998). Likewise, a direct cell-cell interaction within this microcluster might enable or enhance $CD4^+$ T cell help for the development of a cytotoxic T cell response (Bourgeois et al., 2002). To summarize, the DC uropod is an interesting cell compartment that is characterized by a distinctive composition of surface receptors along with the facility to secrete T cell-activating molecules (e.g. peptide-MHC complexes and cytokines). These properties enable the DC uropod not only to coordinate the activation of bound T cells but also to orchestrate an entire antigen-specific immune response.

5.3 Outlook

The 3D collagen matrix model enabled new insights into the kinetics and biology of T cell homeostasis and activation. A key disadvantage of *ex vivo* models, the poor spontaneous or chemokine-induced migration of naïve $CD4^+$ T cells, hitherto limited these observations to pre-activated T cells. Therefore, future work will need to optimize the experimental setup to enhance migration of naïve T cells without cross-talk to antigen-specific activation, e.g. by directly coupling chemokines to collagen fibers in order to enhance their bioactivity (Stachowiak and Irvine, 2008; Woolf et al., 2007) or pre-treating naïve T cells with adhesion receptor-triggering multimeric ligands. To further confirm the "tunability" of antigen recognition dynamics, sets of antigenic peptides with defined immunogenicity ranging from "homeostatic" (i.e. self-antigens) to strong affinity will show thresholds for dynamic and stable phases of antigen-recognition and resulting effector cell fate (Henrickson et al., 2008; Rothoeft et al., 2006; Skokos et al., 2007). Extending the initial findings on DC uropod function, it will be interesting to test which mechanisms regulate local T cell accumulation and how sustained engagement in this specialized region orchestrates distinct effector outcome, including anergy induction and/or helper/effector fate. In summary, due to its superior imaging resolution and experimental control conditions, monitoring immune cell interactions and activation in 3D extracellular scaffolds will be a valuable tool for studying the role of the dynamics and polarity during immune cell interactions.

6 Summary

Polarity and migration are essential for T cell activation, homeostasis, recirculation and effector function. To address how T cells coordinate polarization and migration when interacting with dendritic cells (DC) during homeostatic and activating conditions, a low density collagen model was used for confocal live-cell imaging and high-resolution 3D reconstruction of fixed samples. During short-lived (5 to 15 min) and migratory homeostatic interactions, recently activated T cells simultaneously maintained their amoeboid polarization and polarized towards the DC. The resulting fully dynamic and asymmetrical interaction plane comprised all compartments of the migrating T cell: the actin-rich leading edge drove migration but displayed only moderate signaling activity; the mid-zone mediated TCR/MHC induced signals associated with homeostatic proliferation; and the rear uropod mediated predominantly MHC independent signals possibly connected to contact-dependent T cell survival. This “dynamic immunological synapse” with distinct signaling sectors enables moving T cells to serially sample antigen-presenting cells and resident tissue cells and thus to collect information along the way. In contrast to homeostatic contacts, recognition of the cognate antigen led to long-lasting T cell/DC interaction with T cell rounding, disintegration of the uropod, T cell polarization towards the DC, and the formation of a symmetrical contact plane. However, the polarity of the continuously migrating DC remained intact and T cells aggregated within the DC uropod, an interesting cellular compartment potentially involved in T cell activation and regulation of the immune response. Taken together, 3D collagen facilitates high resolution morphological studies of T cell function under realistic, *in vivo*-like conditions.

7 Zusammenfassung

Zellpolarität und Migration sind essentielle Voraussetzungen für T-Zellaktivierung und -homöostase sowie für Rezirkulation, und Effektorfunktionen. Um unter homöostatischen bzw. aktivierenden Bedingungen die Koordination von Polarisation und Migration von T-Lymphozyten, die mit dendritischen Zellen (DC) interagieren, zu untersuchen, wurde ein Kollagenmatrix-Model mit niedriger Kollagendichte für konfokale Zeitraffermikroskopie und die hochaufgelöste Rekonstruktion fixierter Proben genutzt. Bei kurzen (5-15 min), migratorischen homöostatischen Kontakten behielten voraktivierte T-Zellen ihr amöboide Polarisation bei, während sie sich gleichzeitig Richtung DC polarisierten. Die hieraus resultierende, dynamische und asymmetrische Kontaktfläche bestand aus allen Kompartimenten der migrierenden T-Zelle: Der F-Aktin-reiche vordere Zellpol („leading edge“) sorgte für Vorschub, hatte aber nur einen geringen Anteil an der Singaltransduktion; im mittleren Bereich („mid-zone“) waren MHC/TCR-abhängige Signale mit homöostatischer Proliferation assoziiert; und im als Uropod bezeichneten hintere Zellpol fanden sich vor allem MHC-unabhängige Signale, die möglicherweise im Zusammenhang mit kontaktabhängigem Überleben stehen. Diese „dynamische immunologische Synapse“ mit ihren Signaltransduktionsbereichen versetzt wandernde T-Zellen in die Lage, nacheinander Kontakt zu mehreren antigenpräsentierenden oder gewebsspezifischen Zellen aufzunehmen und so Informationen „im Vorbeigehen“ zu sammeln. Im Gegensatz zu homöostatischen Kontakten führte die Bindung des spezifischen Antigens zu langlebigen T-Zellen/DC Kontakten, die mit der Abrundung der T-Zelle und der Polarisation Richtung DC, der Auflösung ihres Uropods sowie der Ausbildung einer symmetrischen Kontaktfläche einher gingen. Die Polarität der währenddessen fortgesetzt migrierenden DC blieb dem gegenüber erhalten und T-Zellen

akkumulierten im DC-Uropod, einem interessanten Zellkompartiment, dass an T-Zell-aktivierung und der Regulation der Immunantwort beteiligt sein könnte. Zusammengefasst ermöglicht das 3D Kollagenmatrix-Modell die hoch aufgelöste morphologische Untersuchung von T-Zellfunktionen unter realistischen, *in vivo*-artigen Bedingungen.

8 References

Affolter, M., and Weijer, C.J. (2005). Signaling to cytoskeletal dynamics during chemotaxis. Dev. Cell *9*, 19-34.

Al-Alwan, M.M., Liwski, R.S., Haeryfar, S.M., Baldridge, W.H., Hoskin, D.W., Rowden, G., and West, K.A. (2003). Cutting Edge: Dendritic Cell Actin Cytoskeletal Polarization during Immunological Synapse Formation Is Highly Antigen-Dependent. J. Immunol. *171*, 4479-4483.

Allenspach, E.J., Cullinan, P., Tong, J., Tang, Q., Tesciuba, A.G., Cannon, J.L., Takahashi, S.M., Morgan, R., Burkhardt, J.K., and Sperling, A.I. (2001). ERM-dependent movement of CD43 defines a novel protein complex distal to the immunological synapse. Immunity *15*, 739-750.

Alvarez, D., Vollmann, E.H., and von Andrian, U.H. (2008). Mechanisms and consequences of dendritic cell migration. Immunity *29*, 325-342.

Azar, G.A., Lemaitre, F., Robey, E.A., and Bousso, P. (2010). Subcellular dynamics of T cell immunological synapses and kinapses in lymph nodes. Proc. Natl. Acad. Sci. U S A *107*, 3675-3680.

Bachmann, M.F., McKall-Faienza, K., Schmits, R., Bouchard, D., Beach, J., Speiser, D.E., Mak, T.W., and Ohashi, P.S. (1997). Distinct roles for LFA-1 and CD28 during activation of naive T cells: adhesion versus costimulation. Immunity *7*, 549-557.

Bajenoff, M., Egen, J.G., Koo, L.Y., Laugier, J.P., Brau, F., Glaichenhaus, N., and Germain, R.N. (2006). Stromal cell networks regulate lymphocyte entry, migration, and territoriality in lymph nodes. Immunity *25*, 989-1001.

Banchereau, J., and Steinman, R.M. (1998). Dendritic cells and the control of immunity. Nature *392*, 245-252.

Benvenuti, F., Hugues, S., Walmsley, M., Ruf, S., Fetler, L., Popoff, M., Tybulewicz, V.L., and Amigorena, S. (2004). Requirement of Rac1 and Rac2 expression by mature dendritic cells for T cell priming. Science *305*, 1150-1153.

Boes, M., Cerny, J., Massol, R., Op den Brouw, M., Kirchhausen, T., Chen, J., and Ploegh, H.L. (2002). T-cell engagement of dendritic cells rapidly rearranges MHC class II transport. Nature *418*, 983-988.

Bompard, G., and Caron, E. (2004). Regulation of WASP/WAVE proteins: making a long story short. J. Cell Biol. *166*, 957-962.

Bourgeois, C., Rocha, B., and Tanchot, C. (2002). A role for CD40 expression on CD8+ T cells in the generation of CD8+ T cell memory. Science *297*, 2060-2063.

Bousso, P., Bhakta, N.R., Lewis, R.S., and Robey, E. (2002). Dynamics of thymocyte-stromal cell interactions visualized by two-photon microscopy. Science *296*, 1876-1880.

Brossard, C., Feuillet, V., Schmitt, A., Randriamampita, C., Romao, M., Raposo, G., and Trautmann, A. (2005). Multifocal structure of the T cell - dendritic cell synapse. Eur. J. Immunol *35*, 1741-1753.

Burack, W.R., Lee, K.H., Holdorf, A.D., Dustin, M.L., and Shaw, A.S. (2002). Cutting edge: quantitative imaging of raft accumulation in the immunological synapse. J. Immunol. *169*, 2837-2841.

Campi, G., Varma, R., and Dustin, M.L. (2005). Actin and agonist MHC-peptide complex-dependent T cell receptor microclusters as scaffolds for signaling. J. Exp. Med. *202*, 1031-1036.

Caron, E. (2003). Regulation by phosphorylation. Yet another twist in the WASP story. Dev. Cell *4*, 772-773.

Cernuda-Morollon, E., Millan, J., Shipman, M., Marelli-Berg, F.M., and Ridley, A.J. (2010). Rac activation by the T-cell receptor inhibits T cell migration. PLoS One *5*, e12393.

Charest, P.G., and Firtel, R.A. (2007). Big roles for small GTPases in the control of directed cell movement. Biochem. J. *401*, 377-390.

Chinnapen, D.J., Chinnapen, H., Saslowsky, D., and Lencer, W.I. (2007). Rafting with cholera toxin: endocytosis and trafficking from plasma membrane to ER. FEMS Microbiol. Lett. *266*, 129-137.

Davis, M.M., and Bjorkman, P.J. (1988). T-cell antigen receptor genes and T-cell recognition. Nature *334*, 395-402.

De Riva, A., Bourgeois, C., Kassiotis, G., and Stockinger, B. (2007). Noncognate interaction with MHC class II molecules is essential for maintenance of T cell metabolism to establish optimal memory CD4 T cell function. J. Immunol. *178*, 5488-5495.

Dehring, D.A., Clarke, F., Ricart, B.G., Huang, Y., Gomez, T.S., Williamson, E.K., Hammer, D.A., Billadeau, D.D., Argon, Y., and Burkhardt, J.K. (2011). Hematopoietic lineage cell-specific protein 1 functions in concert with the Wiskott-Aldrich syndrome protein to promote podosome array organization and chemotaxis in dendritic cells. J. Immunol. *186*, 4805-4818.

del Pozo, M.A., Cabanas, C., Montoya, M.C., Ager, A., Sanchez-Mateos, P., and Sanchez-Madrid, F. (1997). ICAMs redistributed by chemokines to cellular uropods as a mechanism for recruitment of T lymphocytes. J. Cell. Biol. *137*, 493-508.

Dustin, M.L. (2008). T-cell activation through immunological synapses and kinapses. Immunol. Rev. *221*, 77-89.

Dustin, M.L., Bromley, S.K., Kan, Z., Peterson, D.A., and Unanue, E.R. (1997). Antigen receptor engagement delivers a stop signal to migrating T lymphocytes. Proc. Natl. Acad. Sci. U S A *94*, 3909-3913.

Erbacher, A., Gieseke, F., Handgretinger, R., and Muller, I. (2009). Dendritic cells: functional aspects of glycosylation and lectins. Hum. Immunol. *70*, 308-312.

Ernst, B., Lee, D.S., Chang, J.M., Sprent, J., and Surh, C.D. (1999). The peptide ligands mediating positive selection in the thymus control T cell survival and homeostatic proliferation in the periphery. Immunity *11*, 173-181.

Feigelson, S.W., Grabovsky, V., Manevich-Mendelson, E., Pasvolsky, R., Shulman, Z., Shinder, V., Klein, E., Etzioni, A., Aker, M., and Alon, R. (2011). Kindlin-3 is required for the stabilization of TCR-stimulated LFA-1:ICAM-1 bonds critical for lymphocyte arrest and spreading on dendritic cells. Blood *117*, 7042-7052.

Feuillet, V., Lucas, B., Di Santo, J.P., Bismuth, G., and Trautmann, A. (2005). Multiple survival signals are delivered by dendritic cells to naive CD4+ T cells. Eur. J. Immunol. *35*, 2563-2572.

Figdor, C.G., van Kooyk, Y., and Adema, G.J. (2002). C-type lectin receptors on dendritic cells and Langerhans cells. Nat. Rev. Immunol. *2*, 77-84.

Fischer, U.B., Jacovetty, E.L., Medeiros, R.B., Goudy, B.D., Zell, T., Swanson, J.B., Lorenz, E., Shimizu, Y., Miller, M.J., Khoruts, A., and Ingulli, E. (2007). MHC class II deprivation impairs CD4 T cell motility and responsiveness to antigen-bearing dendritic cells in vivo. Proc. Natl. Acad. Sci. U S A *104*, 7181-7186.

Fisher, P.J., Bulur, P.A., Vuk-Pavlovic, S., Prendergast, F.G., and Dietz, A.B. (2008). Dendritic cell microvilli: a novel membrane structure associated with the multifocal synapse and T-cell clustering. Blood *112*, 5037-5045.

Freiberg, B.A., Kupfer, H., Maslanik, W., Delli, J., Kappler, J., Zaller, D.M., and Kupfer, A. (2002). Staging and resetting T cell activation in SMACs. Nat. Immunol. *3*, 911-917.

Fremont, D.H., Hendrickson, W.A., Marrack, P., and Kappler, J. (1996). Structures of an MHC class II molecule with covalently bound single peptides. Science *272*, 1001-1004.

Friedl, P., and Brocker, E.B. (2002). TCR triggering on the move: diversity of T-cell interactions with antigen-presenting cells. Immunol. Rev. *186*, 83-89.

Friedl, P., and Brocker, E.B. (2004). Reconstructing leukocyte migration in 3D extracellular matrix by time-lapse videomicroscopy and computer-assisted tracking. Methods Mol. Biol. *239*, 77-90.

Friedl, P., den Boer, A.T., and Gunzer, M. (2005). Tuning immune responses: diversity and adaptation of the immunological synapse. Nat. Rev. Immunol. *5*, 532-545.

Friedl, P., Entschladen, F., Conrad, C., Niggemann, B., and Zanker, K.S. (1998). CD4+ T lymphocytes migrating in three-dimensional collagen lattices lack focal adhesions and utilize beta1 integrin-independent strategies for polarization, interaction with collagen fibers and locomotion. Eur. J. Immunol. *28*, 2331-2343.

Friedl, P., and Gunzer, M. (2001). Interaction of T cells with APCs: the serial encounter model. Trends Immunol. *22*, 187-191.

Friedl, P., Noble, P.B., and Zanker, K.S. (1995). T lymphocyte locomotion in a three-dimensional collagen matrix. Expression and function of cell adhesion molecules. J. Immunol. *154*, 4973-4985.

Friedl, P., and Storim, J. (2004). Diversity in immune-cell interactions: states and functions of the immunological synapse. Trends. Cell Biol. *14*, 557-567.

Friedl, P., and Weigelin, B. (2008). Interstitial leukocyte migration and immune function. Nat. Immunol. *9*, 960-969.

Friedman, R.S., Jacobelli, J., and Krummel, M.F. (2006). Surface-bound chemokines capture and prime T cells for synapse formation. Nat. Immunol. *7*, 1101-1108.

Fujikawa, K., Miletic, A.V., Alt, F.W., Faccio, R., Brown, T., Hoog, J., Fredericks, J., Nishi, S., Mildiner, S., Moores, S.L.*, et al.* (2003). Vav1/2/3-null mice define an essential role for Vav family proteins in lymphocyte development and activation but a differential requirement in MAPK signaling in T and B cells. J. Exp. Med. *198*, 1595-1608.

Genot, E., and Cantrell, D.A. (2000). Ras regulation and function in lymphocytes. Curr. Opin. Immunol. *12*, 289-294.

Glimcher, L.H., and Murphy, K.M. (2000). Lineage commitment in the immune system: the T helper lymphocyte grows up. Gene.s Dev. *14*, 1693-1711.

Goldrath, A.W., and Bevan, M.J. (1999). Low-affinity ligands for the TCR drive proliferation of mature CD8+ T cells in lymphopenic hosts. Immunity *11*, 183-190.

Gomez-Mouton, C., Abad, J.L., Mira, E., Lacalle, R.A., Gallardo, E., Jimenez-Baranda, S., Illa, I., Bernad, A., Manes, S., and Martinez, A.C. (2001). Segregation of leading-edge and uropod components into specific lipid rafts during T cell polarization. Proc. Natl. Acad. Sci. USA *98*, 9642-9647.

Grakoui, A., Bromley, S.K., Sumen, C., Davis, M.M., Shaw, A.S., Allen, P.M., and Dustin, M.L. (1999). The Immunological Synapse: A Molecular Machine Controlling T Cell Activation. Science *285*, 221-227.

Grusby, M.J., Johnson, R.S., Papaioannou, V.E., and Glimcher, L.H. (1991). Depletion of CD4+ T cells in major histocompatibility complex class II-deficient mice. Science *253*, 1417-1420.

Guimond, M., Veenstra, R.G., Grindler, D.J., Zhang, H., Cui, Y., Murphy, R.D., Kim, S.Y., Na, R., Hennighausen, L., Kurtulus, S.*, et al.* (2009). Interleukin 7 signaling in dendritic cells regulates the homeostatic proliferation and niche size of CD4+ T cells. Nat. Immunol. *10*, 149-157.

Gunzer, M., Schafer, A., Borgmann, S., Grabbe, S., Zanker, K.S., Brocker, E.B., Kampgen, E., and Friedl, P. (2000). Antigen presentation in extracellular matrix: interactions of T cells with dendritic cells are dynamic, short lived, and sequential. Immunity *13*, 323-332.

Gunzer, M., Weishaupt, C., Hillmer, A., Basoglu, Y., Friedl, P., Dittmar, K.E., Kolanus, W., Varga, G., and Grabbe, S. (2004). A spectrum of biophysical interaction modes between T cells and different antigen-presenting cells during priming in 3-D collagen and in vivo. Blood *104*, 2801-2809.

Hawiger, D., Inaba, K., Dorsett, Y., Guo, M., Mahnke, K., Rivera, M., Ravetch, J.V., Steinman, R.M., and Nussenzweig, M.C. (2001). Dendritic cells induce peripheral T cell unresponsiveness under steady state conditions in vivo. J. Exp. Med. *194*, 769-779.

Heasman, S.J., Carlin, L.M., Cox, S., Ng, T., and Ridley, A.J. (2010). Coordinated RhoA signaling at the leading edge and uropod is required for T cell transendothelial migration. J. Cell Biol. *190*, 553-563.

Henrickson, S.E., Mempel, T.R., Mazo, I.B., Liu, B., Artyomov, M.N., Zheng, H., Peixoto, A., Flynn, M.P., Senman, B., Junt, T.*, et al.* (2008). T cell sensing of antigen dose governs interactive behavior with dendritic cells and sets a threshold for T cell activation. Nat. Immunol. *9*, 282-291.

Hochweller, K., Wabnitz, G.H., Samstag, Y., Suffner, J., Hammerling, G.J., and Garbi, N. (2010). Dendritic cells control T cell tonic signaling required for responsiveness to foreign antigen. Proc. Natl. Acad. Sci. USA *107*, 5931-5936.

Hogg, N., Laschinger, M., Giles, K., and McDowall, A. (2003). T-cell integrins: more than just sticking points. J. Cell Sci. *116*, 4695-4705.

Huang, Y., Comiskey, E.O., Dupree, R.S., Li, S., Koleske, A.J., and Burkhardt, J.K. (2008). The c-Abl tyrosine kinase regulates actin remodeling at the immune synapse. Blood *112*, 111-119.

Hugues, S., Fetler, L., Bonifaz, L., Helft, J., Amblard, F., and Amigorena, S. (2004). Distinct T cell dynamics in lymph nodes during the induction of tolerance and immunity. Nat. Immunol. *5*, 1235-1242.

Im, S.H., and Rao, A. (2004). Activation and deactivation of gene expression by Ca2+/calcineurin-NFAT-mediated signaling. Mol. Cells *18*, 1-9.

Insall, R.H., and Machesky, L.M. (2009). Actin dynamics at the leading edge: from simple machinery to complex networks. Dev. Cell *17*, 310-322.

Jacobelli, J., Chmura, S.A., Buxton, D.B., Davis, M.M., and Krummel, M.F. (2004). A single class II myosin modulates T cell motility and stopping, but not synapse formation. Nat. Immunol. *5*, 531-538.

Jo, J.H., Kwon, M.S., Choi, H.O., Oh, H.M., Kim, H.J., and Jun, C.D. (2010). Recycling and LFA-1-dependent trafficking of ICAM-1 to the immunological synapse. J. Cell Biochem. *111*, 1125-1137.

Jung, D., and Alt, F.W. (2004). Unraveling V(D)J recombination; insights into gene regulation. Cell *116*, 299-311.

Kaiser, A., Donnadieu, E., Abastado, J.P., Trautmann, A., and Nardin, A. (2005). CC chemokine ligand 19 secreted by mature dendritic cells increases naive T cell scanning behavior and their response to rare cognate antigen. J. Immunol. *175*, 2349-2356.

Kassiotis, G., Garcia, S., Simpson, E., and Stockinger, B. (2002). Impairment of immunological memory in the absence of MHC despite survival of memory T cells. Nat. Immunol. *3*, 244-250.

Khaled, A.R., and Durum, S.K. (2002). Lymphocide: cytokines and the control of lymphoid homeostasis. Nat. Rev. Immunol. *2*, 817-830.

Kinashi, T. (2005). Intracellular signalling controlling integrin activation in lymphocytes. Nat. Rev. Immunol. *5*, 546-559.

Kinsella, T.M., and Nolan, G.P. (1996). Episomal vectors rapidly and stably produce high-titer recombinant retrovirus. Hum. Gene Ther. *7*, 1405-1413.

Kobayashi, M., Azuma, E., Ido, M., Hirayama, M., Jiang, Q., Iwamoto, S., Kumamoto, T., Yamamoto, H., Sakurai, M., and Komada, Y. (2001). A pivotal role of Rho GTPase in the regulation of morphology and function of dendritic cells. J. Immunol. *167*, 3585-3591.

Kondo, T., Cortese, I., Markovic-Plese, S., Wandinger, K.P., Carter, C., Brown, M., Leitman, S., and Martin, R. (2001). Dendritic cells signal T cells in the absence of exogenous antigen. Nat. Immunol. *2*, 932-938.

Koretzky, G.A., Abtahian, F., and Silverman, M.A. (2006). SLP76 and SLP65: complex regulation of signalling in lymphocytes and beyond. Nat. Rev. Immunol. *6*, 67-78.

Krummel, M.F., and Macara, I. (2006). Maintenance and modulation of T cell polarity. Nat. Immunol. *7*, 1143-1149.

Kupfer, H., Monks, C.R., and Kupfer, A. (1994). Small splenic B cells that bind to antigen-specific T helper (Th) cells and face the site of cytokine production in the Th cells selectively proliferate: immunofluorescence microscopic studies of Th-B antigen-presenting cell interactions. J. Exp. Med. *179*, 1507-1515.

Lämmermann, T., Bader, B.L., Monkley, S.J., Worbs, T., Wedlich-Soldner, R., Hirsch, K., Keller, M., Forster, R., Critchley, D.R., Fassler, R., and Sixt, M. (2008). Rapid leukocyte migration by integrin-independent flowing and squeezing. Nature *453*, 51-55.

Lämmermann, T., Renkawitz, J., Wu, X., Hirsch, K., Brakebusch, C., and Sixt, M. (2009). Cdc42-dependent leading edge coordination is essential for interstitial dendritic cell migration. Blood *113*, 5703-5710.

Lämmermann, T., and Sixt, M. (2009). Mechanical modes of 'amoeboid' cell migration. Curr. Opin. Cell Biol. *21*, 636-644.

Lee, J.H., Katakai, T., Hara, T., Gonda, H., Sugai, M., and Shimizu, A. (2004). Roles of p-ERM and Rho-ROCK signaling in lymphocyte polarity and uropod formation. J. Cell. Biol. *167*, 327-337.

Lee, K.H., Holdorf, A.D., Dustin, M.L., Chan, A.C., Allen, P.M., and Shaw, A.S. (2002). T cell receptor signaling precedes immunological synapse formation. Science *295*, 1539-1542.

Ley, K., Laudanna, C., Cybulsky, M.I., and Nourshargh, S. (2007). Getting to the site of inflammation: the leukocyte adhesion cascade updated. Nat. Rev. Immunol. *7*, 678-689.

Li, Z., Dong, X., Wang, Z., Liu, W., Deng, N., Ding, Y., Tang, L., Hla, T., Zeng, R., Li, L., and Wu, D. (2005). Regulation of PTEN by Rho small GTPases. Nat. Cell. Biol. *7*, 399-404.

Li, Z., Hannigan, M., Mo, Z., Liu, B., Lu, W., Wu, Y., Smrcka, A.V., Wu, G., Li, L., Liu, M., *et al.* (2003). Directional sensing requires G beta gamma-mediated PAK1 and PIX alpha-dependent activation of Cdc42. Cell *114*, 215-227.

Lindquist, R.L., Shakhar, G., Dudziak, D., Wardemann, H., Eisenreich, T., Dustin, M.L., and Nussenzweig, M.C. (2004). Visualizing dendritic cell networks in vivo. Nat. Immunol. *5*, 1243-1250.

Link, A., Vogt, T.K., Favre, S., Britschgi, M.R., Acha-Orbea, H., Hinz, B., Cyster, J.G., and Luther, S.A. (2007). Fibroblastic reticular cells in lymph nodes regulate the homeostasis of naive T cells. Nat. Immunol. *8*, 1255-1265.

MacLennan, I.C. (1994). Germinal centers. Annu. Rev. Immunol. *12*, 117-139.

Madruga, J., Koritschoner, N.P., Diebold, S.S., Kurz, S.M., and Zenke, M. (1999). Polarised expression pattern of focal contact proteins in highly motile antigen presenting dendritic cells. J. Cell. Sci. *112*, 1685-1696.

Mattioli, B., Straface, E., Matarrese, P., Quaranta, M.G., Giordani, L., Malorni, W., and Viora, M. (2008). Leptin as an immunological adjuvant: enhanced migratory and CD8+ T cell stimulatory capacity of human dendritic cells exposed to leptin. Faseb J. *22*, 2012-2022.

Mattioli, B., Straface, E., Quaranta, M.G., Giordani, L., and Viora, M. (2005). Leptin promotes differentiation and survival of human dendritic cells and licenses them for Th1 priming. J. Immunol. *174*, 6820-6828.

Mempel, T.R., Henrickson, S.E., and Von Andrian, U.H. (2004). T-cell priming by dendritic cells in lymph nodes occurs in three distinct phases. Nature *427*, 154-159.

Mempel, T.R., Pittet, M.J., Khazaie, K., Weninger, W., Weissleder, R., von Boehmer, H., and von Andrian, U.H. (2006). Regulatory T cells reversibly suppress cytotoxic T cell function independent of effector differentiation. Immunity *25*, 129-141.

Meraner, P., Horejsi, V., Wolpl, A., Fischer, G.F., Stingl, G., and Maurer, D. (2007). Dendritic cells sensitize TCRs through self-MHC-mediated Src family kinase activation. J. Immunol. *178*, 2262-2271.

Miller, M.J., Hejazi, A.S., Wei, S.H., Cahalan, M.D., and Parker, I. (2004a). T cell repertoire scanning is promoted by dynamic dendritic cell behavior and random T cell motility in the lymph node. Proc. Natl. Acad. Sci. USA *101*, 998-1003.

Miller, M.J., Safrina, O., Parker, I., and Cahalan, M.D. (2004b). Imaging the single cell dynamics of CD4+ T cell activation by dendritic cells in lymph nodes. J. Exp. Med. *200*, 847-856.

Monks, C.R., Freiberg, B.A., Kupfer, H., Sciaky, N., and Kupfer, A. (1998). Three-dimensional segregation of supramolecular activation clusters in T cells. Nature *395*, 82-86.

Negulescu, P.A., Krasieva, T.B., Khan, A., Kerschbaum, H.H., and Cahalan, M.D. (1996). Polarity of T cell shape, motility, and sensitivity to antigen. Immunity *4*, 421-430.

O'Keefe, J.P., and Gajewski, T.F. (2005). Cutting edge: cytotoxic granule polarization and cytolysis can occur without central supramolecular activation cluster formation in CD8+ effector T cells. J. Immunol. *175*, 5581-5585.

Park, J.H., Adoro, S., Lucas, P.J., Sarafova, S.D., Alag, A.S., Doan, L.L., Erman, B., Liu, X., Ellmeier, W., Bosselut, R.*, et al.* (2007). 'Coreceptor tuning': cytokine signals transcriptionally tailor CD8 coreceptor expression to the self-specificity of the TCR. Nat .Immunol. *8*, 1049-1059.

Purtic, B., Pitcher, L.A., van Oers, N.S., and Wulfing, C. (2005). T cell receptor (TCR) clustering in the immunological synapse integrates TCR and costimulatory signaling in selected T cells. Proc. Natl. Acad. Sci. USA *102*, 2904-2909.

Qi, Q., and August, A. (2007). Keeping the (kinase) party going: SLP-76 and ITK dance to the beat. Sci. STKE *2007*, pe39.

Quaranta, M.G., Mattioli, B., Spadaro, F., Straface, E., Giordani, L., Ramoni, C., Malorni, W., and Viora, M. (2003). HIV-1 Nef triggers Vav-mediated signaling pathway leading to functional and morphological differentiation of dendritic cells. FASEB J. *17*, 2025-2036.

Ratner, S., Sherrod, W.S., and Lichlyter, D. (1997). Microtubule retraction into the uropod and its role in T cell polarization and motility. J. Immunol. *159*, 1063-1067.

Reay, P.A., Kantor, R.M., and Davis, M.M. (1994). Use of global amino acid replacements to define the requirements for MHC binding and T cell recognition of moth cytochrome c (93-103). J. Immunol. *152*, 3946-3957.

Revy, P., Sospedra, M., Barbour, B., and Trautmann, A. (2001). Functional antigen-independent synapses formed between T cells and dendritic cells. Nat. Immunol. *2*, 925-931.

Rothoeft, T., Balkow, S., Krummen, M., Beissert, S., Varga, G., Loser, K., Oberbanscheidt, P., van den Boom, F., and Grabbe, S. (2006). Structure and duration of contact between dendritic cells and T cells are controlled by T cell activation state. Eur. J. Immunol. *36*, 3105-3117.

Roy, E., Togbe, D., Holdorf, A.D., Trubetskoy, D., Nabti, S., Kublbeck, G., Klevenz, A., Kopp-Schneider, A., Leithauser, F., Moller, P.*, et al.* (2010). Nck adaptors are positive regulators of the size and sensitivity of the T-cell repertoire. Proc. Natl. Acad. Sci. USA *107*, 15529-15534.

Rudolph, M.G., Stanfield, R.L., and Wilson, I.A. (2006). How TCRs bind MHCs, peptides, and coreceptors. Annu. Rev. Immunol. *24*, 419-466.

Saini, M., Pearson, C., and Seddon, B. (2009). Regulation of T cell-dendritic cell interactions by IL-7 governs T-cell activation and homeostasis. Blood *113*, 5793-5800.

Samaniego, R., Sanchez-Martin, L., Estecha, A., and Sanchez-Mateos, P. (2007). Rho/ROCK and myosin II control the polarized distribution of endocytic clathrin structures at the uropod of moving T lymphocytes. J. Cell. Sci. *120*, 3534-3543.

Samelson, L.E., Patel, M.D., Weissman, A.M., Harford, J.B., and Klausner, R.D. (1986). Antigen activation of murine T cells induces tyrosine phosphorylation of a polypeptide associated with the T cell antigen receptor. Cell *46*, 1083-1090.

Sanchez-Madrid, F., and del Pozo, M.A. (1999). Leukocyte polarization in cell migration and immune interactions. EMBO J. *18*, 501-511.

Sanchez-Madrid, F., Simon, P., Thompson, S., and Springer, T.A. (1983). Mapping of antigenic and functional epitopes on the alpha- and beta-subunits of two related mouse glycoproteins involved in cell interactions, LFA-1 and Mac-1. J. Exp. Med. *158*, 586-602.

Schluns, K.S., Kieper, W.C., Jameson, S.C., and Lefrancois, L. (2000). Interleukin-7 mediates the homeostasis of naive and memory CD8 T cells in vivo. Nat. Immunol. *1*, 426-432.

Scholer, A., Hugues, S., Boissonnas, A., Fetler, L., and Amigorena, S. (2008). Intercellular adhesion molecule-1-dependent stable interactions between T cells and dendritic cells determine CD8+ T cell memory. Immunity *28*, 258-270.

Seddon, B., Tomlinson, P., and Zamoyska, R. (2003). Interleukin 7 and T cell receptor signals regulate homeostasis of CD4 memory cells. Nat. Immunol. *4*, 680-686.

Seder, R.A., Paul, W.E., Davis, M.M., and Fazekas de St Groth, B. (1992). The presence of interleukin 4 during in vitro priming determines the lymphokine-producing potential of CD4+ T cells from T cell receptor transgenic mice. J. Exp. Med. *176*, 1091-1098.

Serrador, J.M., Nieto, M., Alonso-Lebrero, J.L., del Pozo, M.A., Calvo, J., Furthmayr, H., Schwartz-Albiez, R., Lozano, F., Gonzalez-Amaro, R., Sanchez-Mateos, P., and Sanchez-Madrid, F. (1998). CD43 interacts with moesin and ezrin and regulates its redistribution to the uropods of T lymphocytes at the cell-cell contacts. Blood *91*, 4632-4644.

Shulman, Z., Shinder, V., Klein, E., Grabovsky, V., Yeger, O., Geron, E., Montresor, A., Bolomini-Vittori, M., Feigelson, S.W., Kirchhausen, T.*, et al.* (2009). Lymphocyte crawling and transendothelial migration require chemokine triggering of high-affinity LFA-1 integrin. Immunity *30*, 384-396.

Sims, T.N., Soos, T.J., Xenias, H.S., Dubin-Thaler, B., Hofman, J.M., Waite, J.C., Cameron, T.O., Thomas, V.K., Varma, R., Wiggins, C.H.*, et al.* (2007). Opposing effects of PKCtheta and WASp on symmetry breaking and relocation of the immunological synapse. Cell *129*, 773-785.

Skokos, D., Shakhar, G., Varma, R., Waite, J.C., Cameron, T.O., Lindquist, R.L., Schwickert, T., Nussenzweig, M.C., and Dustin, M.L. (2007). Peptide-MHC potency governs dynamic interactions between T cells and dendritic cells in lymph nodes. Nat. Immunol. *8*, 835-844.

Smith-Garvin, J.E., Koretzky, G.A., and Jordan, M.S. (2009). T cell activation. Annu. Rev. Immunol. *27*, 591-619.

Smith, A., Carrasco, Y.R., Stanley, P., Kieffer, N., Batista, F.D., and Hogg, N. (2005). A talin-dependent LFA-1 focal zone is formed by rapidly migrating T lymphocytes. J. Cell. Biol. *170*, 141-151.

Sommers, C.L., Samelson, L.E., and Love, P.E. (2004). LAT: a T lymphocyte adapter protein that couples the antigen receptor to downstream signaling pathways. Bioessays *26*, 61-67.

Sorg, R.V., McLellan, A.D., Hock, B.D., Fearnley, D.B., and Hart, D.N. (1998). Human dendritic cells express functional interleukin-7. Immunobiology *198*, 514-526.

Sprent, J., and Surh, C.D. (2011). Normal T cell homeostasis: the conversion of naive cells into memory-phenotype cells. Nat. Immunol. *12*, 478-484.

Springer, T.A., Dustin, M.L., Kishimoto, T.K., and Marlin, S.D. (1987). The lymphocyte function-associated LFA-1, CD2, and LFA-3 molecules: cell adhesion receptors of the immune system. Annu. Rev. Immunol. *5*, 223-252.

Stachowiak, A.N., and Irvine, D.J. (2008). Inverse opal hydrogel-collagen composite scaffolds as a supportive microenvironment for immune cell migration. J. Biomed. Mater. Res. A *85*, 815-828.

Stefanova, I., Dorfman, J.R., and Germain, R.N. (2002). Self-recognition promotes the foreign antigen sensitivity of naive T lymphocytes. Nature *420*, 429-434.

Steinman, R.M., and Banchereau, J. (2007). Taking dendritic cells into medicine. Nature *449*, 419-426.

Stinchcombe, J.C., Majorovits, E., Bossi, G., Fuller, S., and Griffiths, G.M. (2006). Centrosome polarization delivers secretory granules to the immunological synapse. Nature *443*, 462-465.

Surh, C.D., and Sprent, J. (2005). Regulation of mature T cell homeostasis. Semin. Immunol. *17*, 183-191.

Surh, C.D., and Sprent, J. (2008). Homeostasis of naive and memory T cells. Immunity *29*, 848-862.

Suzuki, J., Yamasaki, S., Wu, J., Koretzky, G.A., and Saito, T. (2007). The actin cloud induced by LFA-1-mediated outside-in signals lowers the threshold for T-cell activation. Blood *109*, 168-175.

Takahashi, T., Kuniyasu, Y., Toda, M., Sakaguchi, N., Itoh, M., Iwata, M., Shimizu, J., and Sakaguchi, S. (1998). Immunologic self-tolerance maintained by CD25+CD4+ naturally anergic and suppressive T cells: induction of autoimmune disease by breaking their anergic/suppressive state. Int. Immunol. *10*, 1969-1980.

Thornton, A.M., and Shevach, E.M. (1998). CD4+CD25+ immunoregulatory T cells suppress polyclonal T cell activation in vitro by inhibiting interleukin 2 production. J. Exp. Med. *188*, 287-296.

Tomassian, T., Humphries, L.A., Liu, S.D., Silva, O., Brooks, D.G., and Miceli, M.C. (2011). Caveolin-1 orchestrates TCR synaptic polarity, signal specificity, and function in CD8 T cells. J. Immunol. *187*, 2993-3002.

Tong, J., Allenspach, E.J., Takahashi, S.M., Mody, P.D., Park, C., Burkhardt, J.K., and Sperling, A.I. (2004). CD43 regulation of T cell activation is not through steric inhibition of T cell-APC interactions but through an intracellular mechanism. J. Exp. Med. *199*, 1277-1283.

Trombetta, E.S., and Mellman, I. (2005). Cell biology of antigen processing in vitro and in vivo. Annu. Rev. Immunol. *23*, 975-1028.

Tseng, S.Y., Waite, J.C., Liu, M., Vardhana, S., and Dustin, M.L. (2008). T cell-dendritic cell immunological synapses contain TCR-dependent CD28-CD80 clusters that recruit protein kinase C theta. J. Immunol. *181*, 4852-4863.

Valitutti, S., Dessing, M., Aktories, K., Gallati, H., and Lanzavecchia, A. (1995). Sustained signaling leading to T cell activation results from prolonged T cell receptor occupancy. Role of T cell actin cytoskeleton. J. Exp. Med. *181*, 577-584.

Vallabhapurapu, S., and Karin, M. (2009). Regulation and function of NF-kappaB transcription factors in the immune system. Annu. Rev. Immunol. *27*, 693-733.

Varma, R., Campi, G., Yokosuka, T., Saito, T., and Dustin, M.L. (2006). T cell receptor-proximal signals are sustained in peripheral microclusters and terminated in the central supramolecular activation cluster. Immunity *25*, 117-127.

Veillette, A., Bookman, M.A., Horak, E.M., and Bolen, J.B. (1988). The CD4 and CD8 T cell surface antigens are associated with the internal membrane tyrosine-protein kinase p56lck. Cell *55*, 301-308.

Vignali, D.A., Collison, L.W., and Workman, C.J. (2008). How regulatory T cells work. Nat. Rev. Immunol. *8*, 523-532.

Viola, A., Schroeder, S., Sakakibara, Y., and Lanzavecchia, A. (1999). T lymphocyte costimulation mediated by reorganization of membrane microdomains. Science *283*, 680-682.

von Freeden-Jeffry, U., Vieira, P., Lucian, L.A., McNeil, T., Burdach, S.E., and Murray, R. (1995). Lymphopenia in interleukin (IL)-7 gene-deleted mice identifies IL-7 as a nonredundant cytokine. J. Exp. Med. *181*, 1519-1526.

Wang, H., Kadlecek, T.A., Au-Yeung, B.B., Goodfellow, H.E., Hsu, L.Y., Freedman, T.S., and Weiss, A. (2010). ZAP-70: an essential kinase in T-cell signaling. Cold Spring Harb. Perspect. Biol. *2*, a002279.

Wolf, K., Muller, R., Borgmann, S., Brocker, E.B., and Friedl, P. (2003). Amoeboid shape change and contact guidance: T-lymphocyte crawling through fibrillar collagen is independent of matrix remodeling by MMPs and other proteases. Blood *102*, 3262-3269.

Woolf, E., Grigorova, I., Sagiv, A., Grabovsky, V., Feigelson, S.W., Shulman, Z., Hartmann, T., Sixt, M., Cyster, J.G., and Alon, R. (2007). Lymph node chemokines promote sustained T lymphocyte motility without triggering stable integrin adhesiveness in the absence of shear forces. Nat. Immunol. *8*, 1076-1085.

Worthylake, R.A., Lemoine, S., Watson, J.M., and Burridge, K. (2001). RhoA is required for monocyte tail retraction during transendothelial migration. J. Cell. Biol. *154*, 147-160.

Wulfing, C., Sjaastad, M.D., and Davis, M.M. (1998). Visualizing the dynamics of T cell activation: intracellular adhesion molecule 1 migrates rapidly to the T cell/B cell interface and acts to sustain calcium levels. Proc. Natl. Acad. Sci. USA *95*, 6302-6307.

Wulfing, C., Sumen, C., Sjaastad, M.D., Wu, L.C., Dustin, M.L., and Davis, M.M. (2002). Costimulation and endogenous MHC ligands contribute to T cell recognition. Nat. Immunol. *3*, 42-47.

Xu, J., Wang, F., Van Keymeulen, A., Herzmark, P., Straight, A., Kelly, K., Takuwa, Y., Sugimoto, N., Mitchison, T., and Bourne, H.R. (2003). Divergent signals and cytoskeletal assemblies regulate self-organizing polarity in neutrophils. Cell *114*, 201-214.

Yokosuka, T., Sakata-Sogawa, K., Kobayashi, W., Hiroshima, M., Hashimoto-Tane, A., Tokunaga, M., Dustin, M.L., and Saito, T. (2005). Newly generated T cell receptor microclusters initiate and sustain T cell activation by recruitment of Zap70 and SLP-76. Nat. Immunol. *6*, 1253-1262.

Zhang, S., Zhang, H., and Zhao, J. (2009). The role of CD4 T cell help for CD8 CTL activation. Biochem. Biophys. Res. Commun. *384*, 405-408.

9 Videos

For the print version videos are available in Quicktime format on CD.

Video 1. Video-assisted fixation of a dynamic T cell / DC contact. The addition of buffered PFA (37°C, 2% v/v final concentration) to the sample at frame 25 (12 min 30 sec) leads to fixation with preserved morphology of both T cell and DC within 30 sec. Note floating objects during the final 3 min. Time-lapse bright-field transmission microscopy. Duration: 10 min.

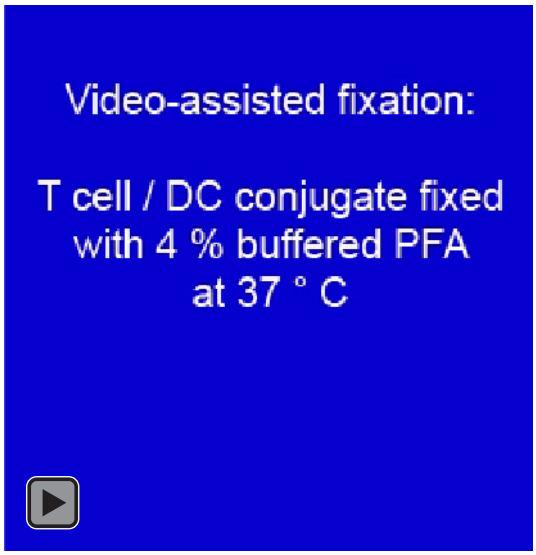

Video 2. Recently activated T cells immigrate into a collagen lattice containing DC in the absence of pOVA. Time-lapse bright-field microscopy. Duration: 2 h. Area: 750 x 500 µm.

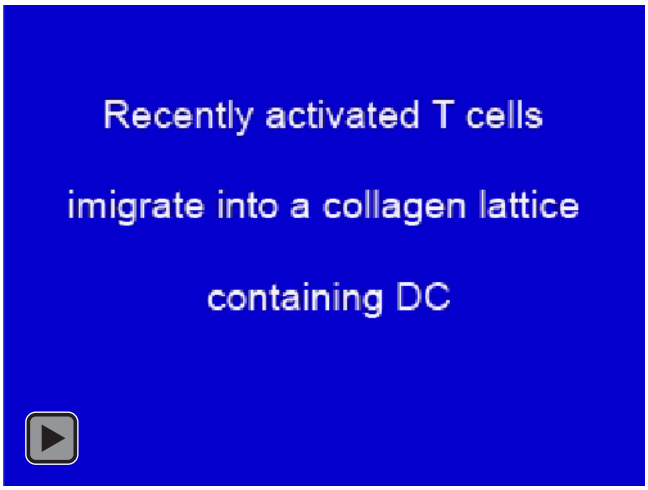

Video 3. Two CFSE-labeled T cells (green) migrating across CMTMR-labeled DC (red) in the absence of pOVA. Both cells and the migratory path of the second cell are highlighted. 4D reconstruction of 50 x 50 x 40 µm volume. Duration: 18 min 30 sec.

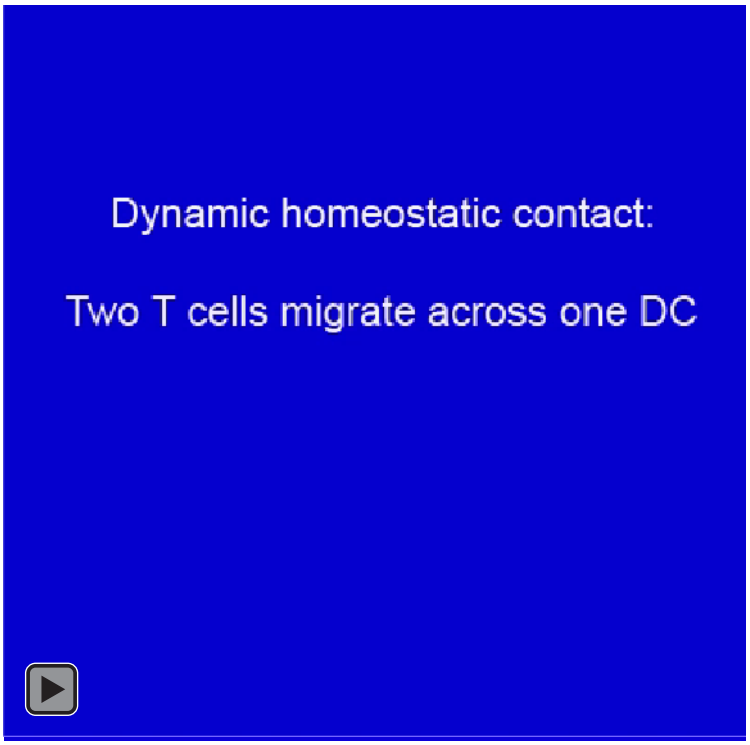

Video 4. Cholera toxin b (CTx b, green) locates to the uropod of T cells (CFSE, red) migrating in 3D collagen. 4D reconstruction of a 70 x 50 x 40 µm volume. Duration: 6 min.

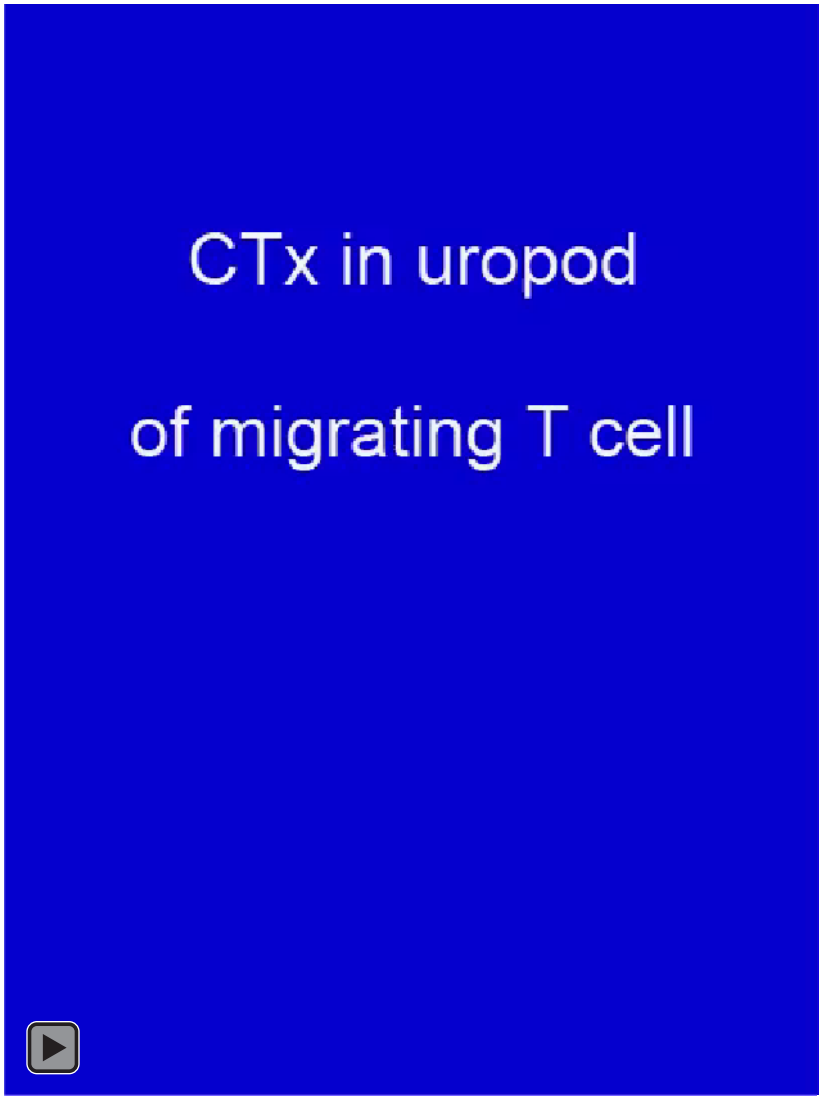

Video 5. CTx b (green) locates to the uropod of T cells (CFSE, red) migrating across a DC (CMTMR, blue). One complete contact with contact acquisition and detachment and one detachment of an already established contact are shown. 4D reconstruction of a 50 x 50 x 40 µm volume. Duration: 6 min 30 sec.

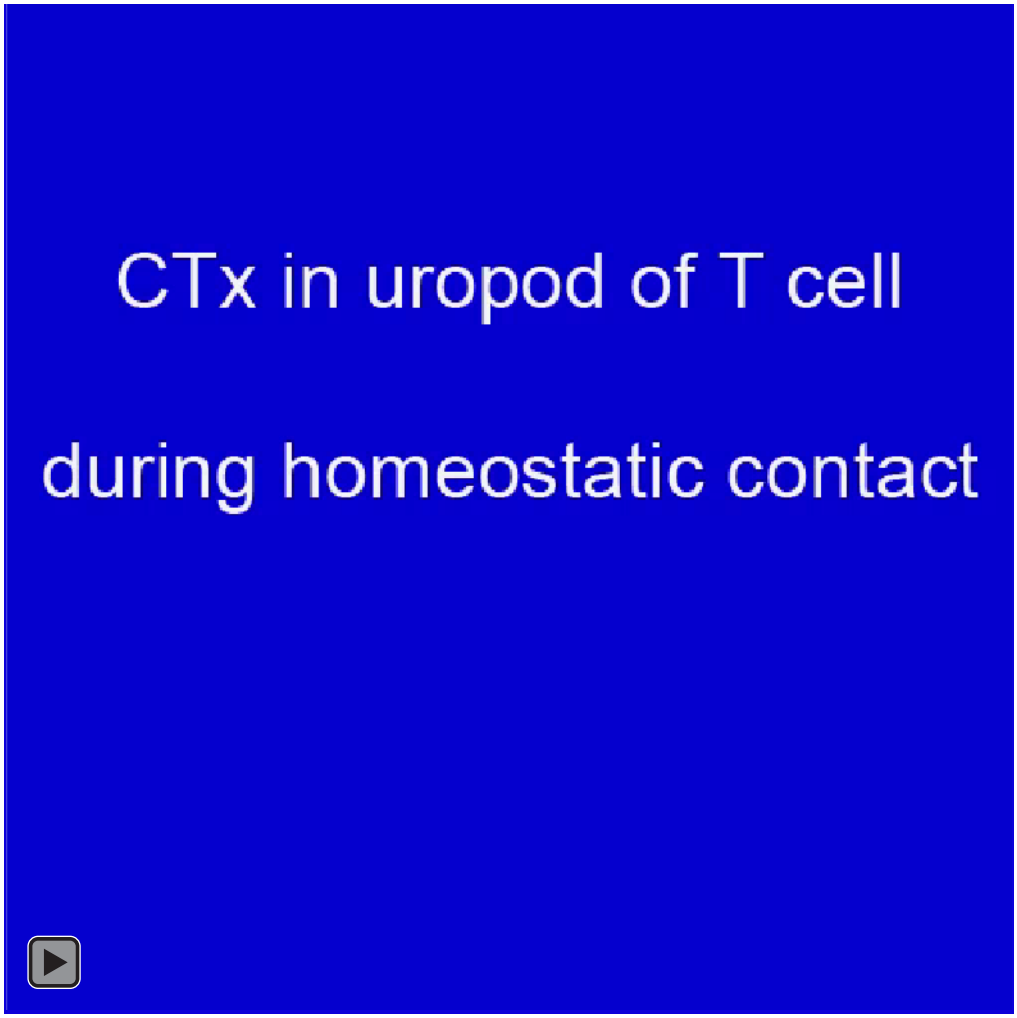

Video 6. pMCC-MHC-GFP (green) expressed and presented by a B10A DC accumulates in the contact plane within minutes after contact acquisition of a 5C.C7 T cell (SNARF; red). 4D reconstruction of a 30 x 30 x 30 µm volume. Duration 15 min.

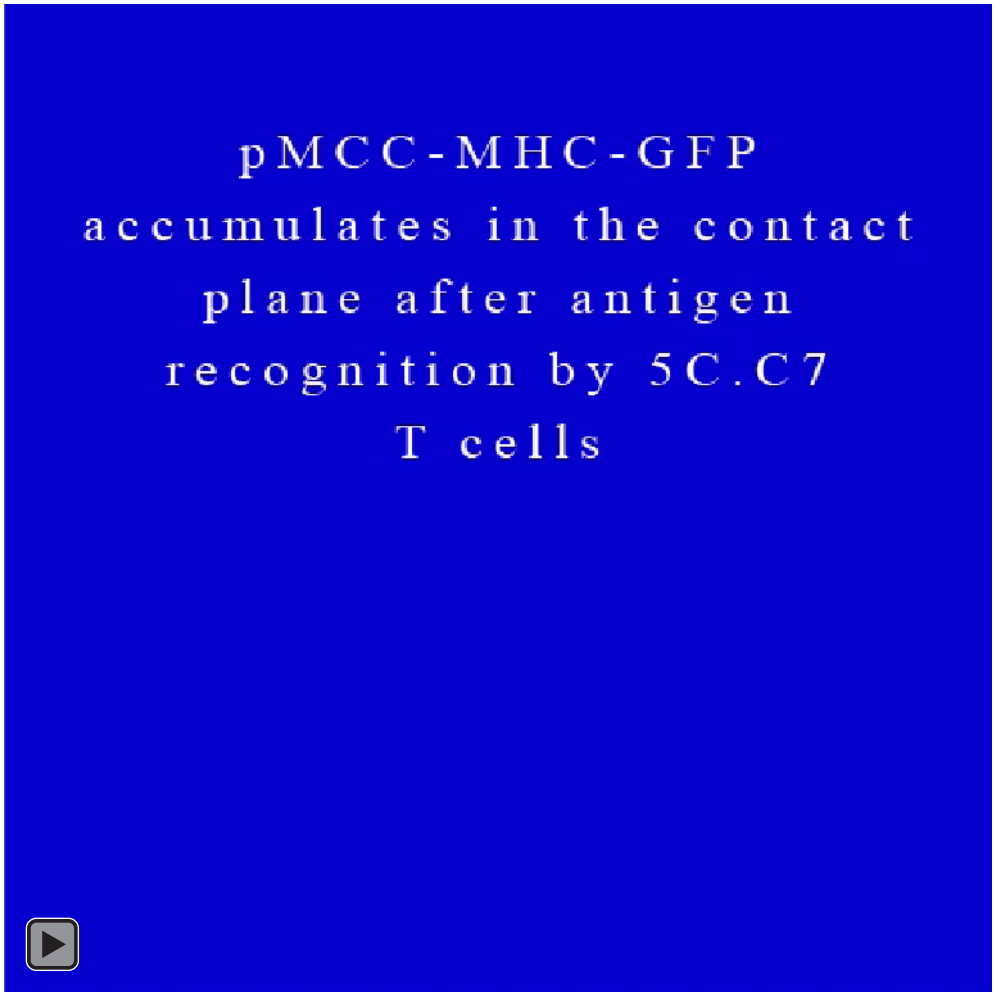

Video 7. CTx b (green) positive intracellular membrane compartments (ER, golgi) relocate to the contact plane between a DO11.10 T cell and a Balb/c DC (CMTMR; red) pulsed with $pOVA_{323-339}$ within minutes after contact acquisition. One additional T cell with CTx b in the centre of the contact plane is bound to the DC throughout the entire recording interval. 4D reconstruction of a 40 x 40 x 30 µm volume. Duration: 19 min.

Video 8. One CFSE labeled DO11.10 T cell (green) acquires contact to the leading edge of a $pOVA_{323-339}$ pulsed DC (CMTMR; red) and slowly moves towards the DC uropod where it integrates into a microcluster of already bound T cells. 4D reconstruction of a 90 x 65 x 50 µm volume. Duration 27 min 30 sec.

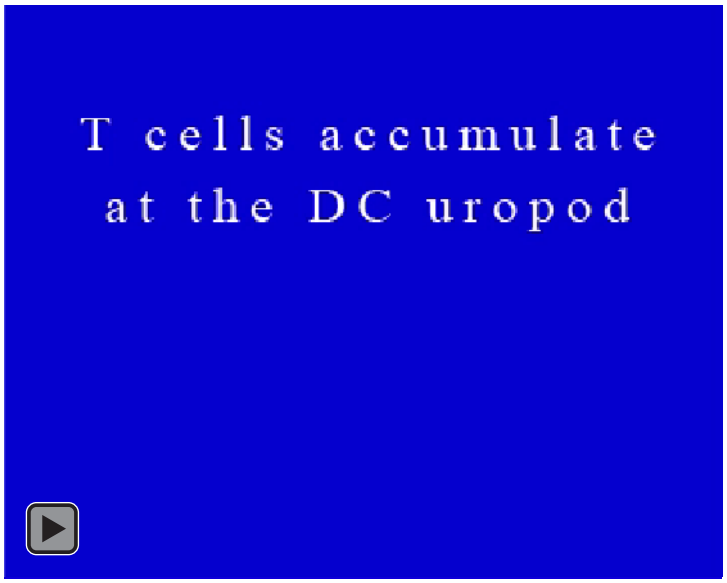

10 Anhang

10.1 Erklärung

Hiermit erkläre ich ehrenwörtlich, dass ich die Dissertation „Dynamic mapping of the immunological synapse in T cell homeostasis and activation“ selbstständig angefertigt und keine anderen als die von mir angegebenen Quellen und Hilfsmittel benutzt habe.

Ich erkläre weiterhin, dass diese Dissertation weder in gleicher Weise noch in anderer Form bereits in einem anderen Prüfungsverfahren vorgelegen hat.
Ich erkläre zudem, vom Fachbereich Humanmedizin der Universität Heidelberg den Grad eines Doktors der Medizin (Dr. med.) verliehen bekommen zu haben.
Ich habe außer den mit dem Zulassungsgesuch urkundlich vorgelegten Graden keine weiteren akademischen Grade erworben oder zu erwerben versucht.

Essen, den

10.2 Eigene Publikationen

Friedl, P., und Storim, J. (2004). Diversity in immune-cell interactions: states and functions of the immunological synapse. Trends Cell Biol. *14*, 557-567.

Storim, J., Brocker, E.B., und Friedl, P. A dynamic immunological synapse mediates homeostatic TCR-dependent and -independent signaling. Eur. J. Immunol. *40*, 2741-2750 (Titelgeschichte).

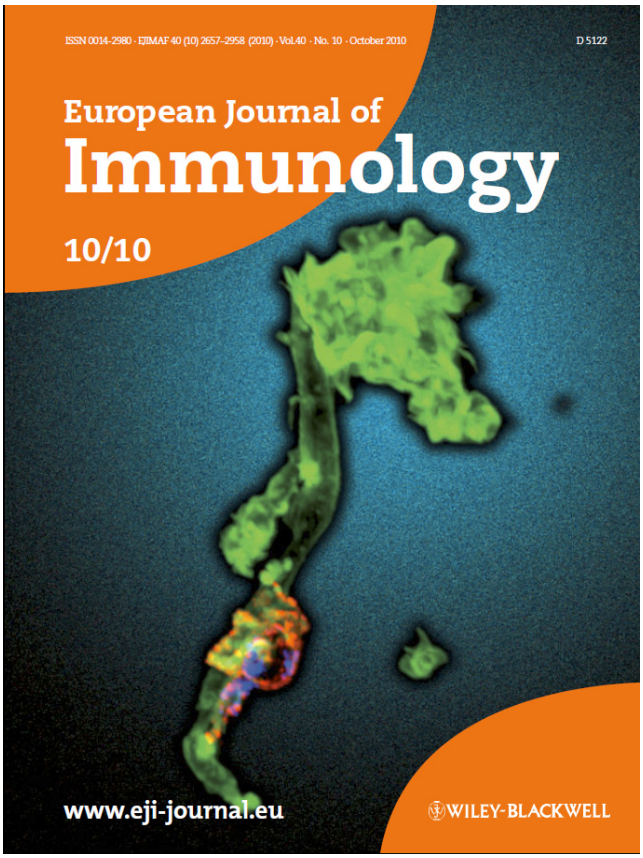

Wesentliche Ergebnisse sowie die hierfür verwendeten Methoden dieser Dissertation wurden in beiden Artikeln publiziert und im Rahmen dieser Dissertation mit Erlaubnis verwendet: Abbildungen 4 bis 17 sowie die Abbildung 22 (inklusive der zugehörigen Legenden), z.T. in modifizierter Form; die Methoden wie sie in den Kapiteln 3.2 sowie 3.5 bis 3.8 beschrieben werden.

Die Daten dieser Dissertation wurden auf folgenden Kongressen präsentiert::

Vortrag beim 2nd joint UK/German adhesion meeting in Berlin, Juli 2002: Storim, J., Kretzschmar, M., Broecker, E. und Friedl, P.; „Molecular topography of a dynamic

immunological synapse”

Vortrag bei der Tagung der Arbeitsgemeinschaft dermatologische Forschung, Februar 2003 in Frankfurt (Main): Storim, J., Kretzschmar, M., Broecker, E. und Friedl, P.; „Molecular topography of a dynamic immunological synapse”

Postervortrag bei der Tagung der Arbeitsgemeinschaft dermatologische Forschung, Februar 2004 in Dresden: Kaemmerer, U., Otto, K., Ossadnik, M., Storim, J., Friedl, P. und

Vortrag beim 57sten Treffen der japanischen Gesellschaft für Zellbiologie, Mai 2004 in Osaka, Japan: Storim, J., Geissler, E., Broecker, E. und Friedl, P.; „Molecular topography of a dynamic immunological synapse”

Workshop im Rahmen eines ECTS Kurses zum Thema Tissue Engineering, Juni 2004 in Würzburg: „Technical aspects of Confocal and Multiphoton-Microscopy”

Vortrag bei der Tagung der Deutschen Gesellschaft für Immunologie, September 2005 in Kiel: Storim, J., Broecker, E. und Friedl, P.; „Reconstructing interaction dynamics of T cells and dendritic cells at high resolution“

Vortrag beim 2nd joint UK/German adhesion meeting in London, Juli 2006: Storim, J. und Friedl, P.; „Organization and function of a dynamic homeostatic synapse"

Vortrag bei der Tagung der Arbeitsgemeinschaft dermatologische Forschung, März 2007 in Freiburg: J. Storim, E. B. Bröcker, P.Friedl; „Organization and function of a dynamic homeostatic synapse between T lymphocytes and dendritic cells"

10.3 Danksagungen

Allen voran danke ich Prof. Peter Friedl für die Überlassung des interessanten Themas, für die enge und gute Betreuung sowie für die großartige Unterstützung während der gesamten Zeit.

Martina Jossberger danke ich für die unschätzbare Hilfe bei der praktischen Durchführung der Experimente und für die gute und freundschaftliche Zusammenarbeit.

Besonderer Dank gilt Frau Prof. Eva B. Bröcker für viele fruchtbare Diskussionen und ihre Unterstützung, ohne die mein fortgesetztes wissenschaftliches Arbeiten neben der klinischen Tätigkeit nicht möglich gewesen wäre.

Prof. Ron Germain danke ich für die Möglichkeit, Experimente für die Doktorarbeit am National Institute of Health durchzuführen. Dr. Katrin Eichelberg hat mich exzellent in die erforderlichen Techniken eingelernt.

Michael Krimpmann danke ich für die Hilfe bei der Programmierung des Excel Makros, mit dessen Hilfe die Analyse von Zell-Zell Kontakten möglich wurde und für seine langjährige Freundschaft.

Kenneth Cooke kann ich nicht genug für die sorgfältige Durchsicht des Textes und die vielen Hinweise danken, die das Englisch der Arbeit deutlich verbessert haben.

Dem IZKF, allen voran Prof. Walter und Prof. Rethwilm, danke ich für die Möglichkeit, im Rahmen des MD/PhD Programms diese Arbeit durchführen zu können.

Abschließend möchte ich mich bei allen Kollegen im Labor für die vielen hilfreichen Diskussionen, die gute Zusammenarbeit und das exzellente Arbeitsklima bedanken.

10.5 Widmung

meinen Eltern